REPUBLIC OF TURKEY
BİNGÖL UNIVERSITY
INSTITUTE OF SCIENCE

SPECTRA OF THE SECONDARY PARTICLES (p, n, d, α) AFTER SPALLATION FOR $_{79}Au^{197}$ AND $_{92}U^{238}$ ELEMENTS

MASTER THESIS

SORAN JALAL QADIR

PHYSICS

THESIS SUPERVISOR
Prof. Dr. İskender DEMİRKOL

BİNGÖL-2018

PREFACE

CONTENTS

LIST OF SYMBOLS

ADS   : Accelerator Driven System

DPT   : State Planning Organization

CERN   : European Nuclear Research Center

CEM   : Cascade Exciton Model

PHT   : Proton Accelerator Plant

MeV   : Mega electron Volt

KeV   : Kilo electron Volt

GeV/c   : Giga electron Volt / Speed of Light

mb   : Millibar

$(d\sigma/dE)$: Energy spectra

E   : Energy

β : Beta

α , ^4He : Alpha

n   : Neutron

p   : Proton

d   : Deuteron

He   : Helium

Z   : Atomic Number

A	: Mass Number
θ	: Angle
µA	: Micro Ampere
ε	: Epsilon
e-	: Electron
e+	: Positron
σ	: Cross section
σR	: Reaction cross section
λC	: Propagation speed
°	: Degree
σa	: Average lifetime
U	: Uranium
Au	: Gold
Th	: Thorium
Kr	: Krypton
$P_\upsilon\,(\varepsilon)$	: number of neutrons and protons
dε	: number of possible excitons at equilibrium
$n_\chi\upsilon$	: number of particles in type and in an exciton state
λc (ε)	: The velocity of a particle (ε) to the continuous zone by channel energy
D_n	: The initial population section in an n-exciton chain
g	: Refers to the single-particle level intensity
IThEC	: International Thorium Energy Committee
JAERI	: Japan Atomic Energy Research

LIST OF FIGURES

LIST OF TABLES

$_{79}$Au^{197} ve $_{92}$U^{238} ELEMENTLERİN SPALLASYON SONRASI OLUŞAN İKİNCİL PARÇACIKLARIN (p, n, d, α) SPEKTRASI

ÖZET

Bu çalışmada p + $_{79}$Au^{197} ve p + $_{92}$U^{238} reaksiyonlari sonrasinda oluşan (n, p, d, α) ikincil parçaciklar için enerji spektrasının hesaplanması denge öncesi hesabı etkisini kapsayan Kaskad Eksiton Modeli ve Intranükleer Kaskad Modeli kullanılarak ALICE / ASH, CEM03 ve PCROSS bilgisayar proğramları ile yapılmıştır. Hızlandırıcıdan elde edilen proton ışınları 20-290 MeV aralığındaki enerjilere sahiptir. Hibrid Model, geometriye bağlı hibrid model ve kaskad aksiton modele dayalı hesaplanan sonuçlar Nükleer Enerji Ajansı data bankasından temin edilen deneysel datalar ile karşılaştırılmıştır. Ayrıca spallation ile ilgili olduğu için hızlandırıcı kaynaklı sistem (ADS) hakkında kısa bir giriş yapma ihtıyacı duyulmuştur.

2018, 124 sayfa

Anahtar Kelimeler: Enerji spektrumu, spallation, enerji, hızlandırıcı, ALICE/ASH, CEM03, PCROSS ve deneysel veri.

SPECTRA OF SECONDARY PARTICLES (p, n, d, α) AFTER SPALLATION FOR $_{79}Au^{197}$ AND $_{92}U^{238}$ ELEMENTS

ABSTRACT

In this study calculation of energy spectra for the secondary particles (n, p, d, α) occurring after spallation in the reactions p + $_{79}Au^{197}$ and p + $_{92}U^{238}$ is performed using Cascade Exciton Model including preequilibrium effect and Intranuclear Cascade Model with CEM03, PCROSS and ALICE/ASH computer program. The proton beams have 20-290 MeV energy ranges which obtained with accelerator. Calculated results based on hybrid model, geometry-dependent hybrid model and cascade-exciton model are compared with the experimental data taken from data bank of Nuclear Energy Agency. Also we need a brief introduction about acceleration driven system (ADS), because (ADS) has an event of spallation.

2018, 124 pages

Keywords: Energy spectra, spallation, energy, accelerator, ALICE/ASH, CEM03, PCROSS and experimental data.

1. INTRODUCTION

The experimental results are exposure to nuclear studies and have a great importance when we want a better understanding in each (reaction, spallation, accelerator, energy spectra). These topics are chaining and are very important in the nuclear physics, because any parts in nuclear have relation with reaction, and spallation is a fundamental of explosion, also this process updated at accelerator, when proton has accelerated in the target element and has reaction occurred. While the reactions of this research have a more calculations, this one is to proof that our aim, because these topics that research they needed a great evidence for verification that events. Understanding any theme in nuclear reaction is not easy, but if we present explanation, we can understand it well, therefore in here it will encourage us to clarify an acceleration driven system (ADS), because that process have lots of reaction events. The conclusions of experimental and theoretical sides of this research need the calculating and explanation with graphing. As well as about the accelerator, the accelerated proton beam inters the target element, causing of scattering of some particles. For these products it needs a best result and use some programs to get many conclusions related to it. After the spallation it has a lot of particles are scattering the target, therefore in here four particles are described such as (proton, neutron, deuteron, alpha). Consequently this used target needs to be heavy elements to scattering the high energy wanted and produce the best spallation process, therefore that research use a two heavy elements such as Uranium (^{238}U) and Gold (^{197}Au). Those energies produce the spallation process conditioned have been kept as high as possible to get the best result in these examinations. In this context, high energy particles emerge from the target element and interact with surrounding elements (internuclear cascade). The accelerators driven system consists of a coupling of a sub-critical nuclear core reactor and a proton beam produced in particle accelerator; these particles injects into a target for the secondary particles production by spallation reactions. The accelerator driven system began as a system and developed in the 1990s and more than one basic-

research program launched. In this context, ADS reactor developed at CERN region and established-In 1945,the European Organization for Nuclear Research known as CERN, when (C. Rubbia) employees CERN came to the forefront, while Carlo Rubbia an Italian particle physicist and inventor who shared the Nobel Prize in Physics in 1984 by (Simon van der Meer) for work leading to the discovery of W and Z particles at CERN. In this study; the cross sections of particles emitted in the accelerated proton bombarded by the light elements, and calculated by a programing system. This process will be an important place to elevation of renewable energy and produced it and in use in our country. In this study, PCROSS, CEM03 and ALLICE/ASH programs are using to theoretically get the results. The theoretical calculated values are achieved by some programs and compared with each other, so as to know how much the difference between the results and this will be presented by explanatory graphs. Experimental and theoretical taken it and the energy used is between at 20 MeV to 290 MeV. In this study, only two light elements are used for the wanted results. Firstly, the information on the spectra the scatter from the four particles and the secondly is about the cross section in CEM03 program when produced and calculated.

2. LITERATURE REVIEWS

(Progress et al. 2002) The European Spallation Source (ESS) is a multi-disciplinary research facility based on what will be the world's most powerful pulsed neutron source (Beers et al. 2014). In (ESS) committee has presented at now under construction in Lund, Sweden in 17 July 2015. At least 17 European countries will act as partners in the construction and operation of ESS at 11 March 2014. The facility is being construction in Lund, while the ESS Data Management and Software Centre (DMSC) will be in Copenhagen, Denmark at 17 July 2015. First neutrons on the target are predictable in 2019, with the user program planned for 2023, and building of entire facility comprehensive by 2025. ESS is the world's next-generation neutron source, and will allow scientists to see and understand basic atomic structures and forces at length and time scales unachievable at other spallation sources.

(Bée 1988) ESS will use spallation, a process in which fragments of material (spall) when ejected from a body due to impact or stress. The future facility as composed of a linear accelerator in which protons accelerated and collide with a rotating, helium-cooled tungsten target at 17 July 2015. By this process, intense pulses of neutrons emitted and led through beamlines to experimental stations, where this book done on dissimilar materials. This will help discover and develop new materials with applications in industrial, pharmaceutical drugs, aerospace, engines, plastics, energy, transportations, transportation, information technology and biotechnology at 2012, 2014, and 2015 (Berggren and Matic 2012). According to its designers, ESS will give neutron beams up to 30 times brighter than any current neutron source; ESS is also designed will be carbon-neutral and expected to reduce CO_2 emissions in the region.

(Medeiros-Romao and Vandeplassche 2012) Accelerator Driven Systems are promising tools for the efficient transmutation of nuclear waste products in dedicated industrial

Installations transmute. The Myrrha project at (Mol, Belgium), located itself on the path towards these applicate ions with a multipurpose and versatile system based on a liquid PbBi (LBE) cooled fast reactor (80 MW), which is may be operated in both critical and subcritical modes. In the after case the core is found by spallation neutrons obtained from a 600 MeV proton beam hitting the LBE coolant/target. The accelerator gain control this beam is a CW superconducting linac which is laid out for the highest achievable reliability. The combination redundant and of a fault tolerant scheme should allow obtaining an MTBF value in excess of 500 hours that required for optimal integrity and successful operation of ADS. Myrrha is probable will be working in 2023. The approaching 4-year period is fully dedicated to R&D; actions, and in the field of accelerator they are entirely focused on the reliability aspects.

(Thorium Energy Conference 2013) Some laboratory experiments and many theoretical studies have shown the theoretical possibility of each as plant. Carlo Rubbia, a nuclear physicist, Nobel laureate, and previous director of CERN, was one of first to consider a design of a subcritical device, the so-called "energy amplifier". In 2005, a number of large-scale projects are going on in Europe and Japan to further develop subcritical device technology. In 2012 CERN scientists and engineers launched the International Thorium Energy Committee (iThEC), an organization devoted to pursuing this goal and which organized the (ThEC13) conference on the subject.

(Mishima et al. 2007) The Research Reactor Institute of Kyoto University started the KART (Kumatori Accelerator-driven Reactor Test facility) project in fiscal year 2002 under the Contract with the Ministry of Education, Nation, Sports, Science and Technology of Japan. Determination of this research project is to show the basic feasibility of accelerator-driven system (ADS), studying influence of incident neutron energy on the effective multiplication factor in a subcritical nuclear fuel system. For this purpose, a variable-energy FFAG (Fixed Field Alternating Gradient) accelerator complex were a constructed and coupled with the Kyoto University Critical Assembly (KUCA). This paper progress the present status of project and some of results from the task performed up to Fiscal Year 2005.

(Team, C. S. N. S. A. 2006) The China Spallation Neutron Source (CSNS) is a newly approved high-power accelerator project based on an H - linear accelerator and a rapid cycling synchrotron. During the past year, a number of major revisions made on the design including the type of front end, the linac frequency, the carriage layout, the ring lattice, also the type of ring components. Now, we discuss the rationale of design reconsiderations, status of R&D efforts, and upgrade considerations.

(Heilbron and Seidel 1989) Lawrence's 60-inch cyclotron, when magnet poles 60 inches (5 feet, 1.5 meters) in diameter, this device in University of California Lawrence Radiation Laboratory, Berkeley, in August, 1939, the most influential accelerator in the global at the time. Glenn T. Seaborg and Edwin M. McMillan (right) used it to find plutonium, neptunium and many other transuranic elements and isotopes, at when they received the 1951 Nobel Prize in chemistry. The cyclotron's massive magnet is at left, also the flat accelerating chamber between its poles in the midpoint. The beamline which analyzed the particles is at right.

(Kumar et al. 2003) in this study they have presented assessment of neutron array, isotopic distribution of created nuclei and heat donations of dissimilar nuclear and atomic processes in collision of proton beam with heavy targets of dissimilar materials, shapes and sizes using current version of Dubna Cascade Code-2001.

(Sandberg 1982) reported that employ of copper multireaction spallation detectors in a particle yield testing at CERN super proton synchrotron to compute the angular and energy spectra of secondary hadrons about a thick copper target bombarded with 225 GeV/c protons.

(Demirkol 2003) The production of neutron is key parameter for the Acceleration Driven System and the selection of target is one from important matters. By to be used Cascade-Exciton Model, in this study the neutron's numbers and energies have been obtained from collisions with p (proton) energetic from 20 MeV to 1500 MeV of heavy elements (Au, Hg, W, Bi, Pb).

3. MATERIAL AND METHOD

3.1. The Acceleration Driven System (ADS)

In book (NEA Nuclear Science Committee 2002) explained the concept of accelerator-driven systems (often called hybrid systems) combines a particle accelerator with a sub-critical core (see Figure 3.1). Most proposals assume proton accelerators, delivering continuous-wave beams with an energy around 1 GeV. The accelerator is either a linear accelerator (linac) or a circular accelerator (cyclotron). High-power accelerators needed under continuous development, and the building of machines with the required specifications, i.e. electrical efficiencies were vicinity is 50% and beam powers up to 10 MW for cyclotrons and up to 100 MW for linacs, now appears by practical.

The protons injected at spallation target to produce source neutrons for driving the subcritical core. The target made of heavy metal in solid or liquid state. Spallation reactions in the target emit a few tens of neutrons per incident proton, which introduced into the sub-critical core to induce further nuclear reactions. Except for the sub-critical state, the core is very like that of a critical reactor. It can design to use either with a thermal or fast neutron spectrum (Takahashi and Rief 1992).

The energy conversion part of an accelerator-driven nuclear power system is like that of a normal power plant. However, in the accelerator-driven system, the electrical energy which recycled to the accelerator reduces the net electrical efficiency of system. For an ADS with a neutron multiplication reason of 0.95, the reduction amounts to about 12%. This means that the accelerator driven system produces about 14% more high-level waste and rejects about 20% more heat to the atmosphere than a normal power plant with the same net electrical output (Bowman et al. 1992).
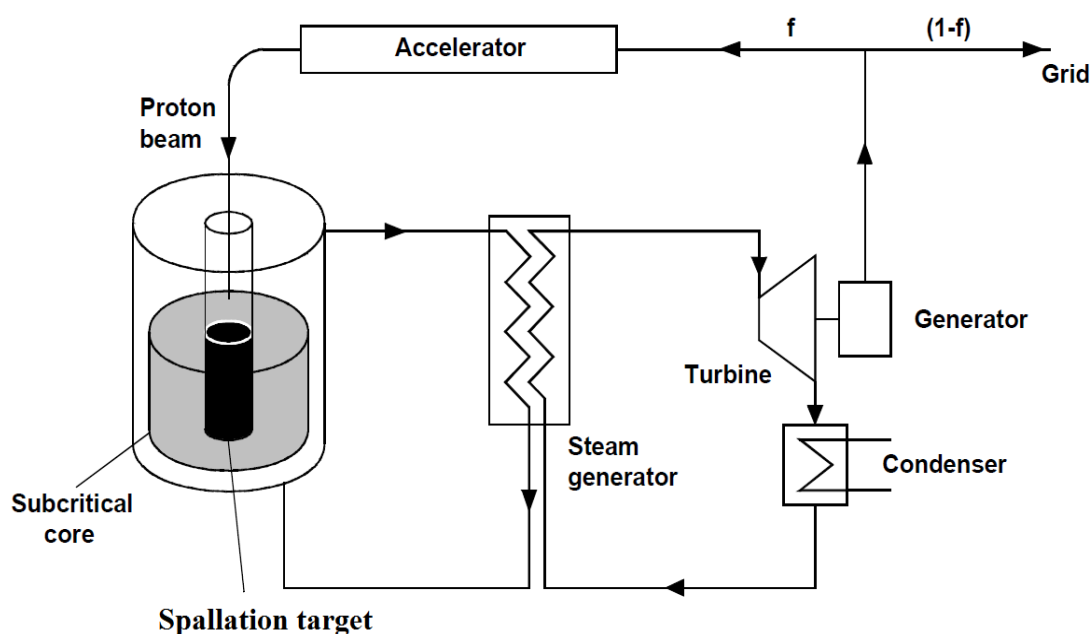
Figure 3.1. Concept of an accelerator-driven system (NEA Nuclear Science Committee 2002)

The principal advantages and disadvantages of accelerator-driven systems as compared with the corresponding critical reactor systems and summarized in (Table 3.1). The comparison applies not only to transmutation applications on which the present study focused, but also to other applications such as the breeding of fissile material (electro breeding), thus development of thorium and ^{233}U fuel cycle, and development of ultra-safe energy producers. For instance, the potential for improving the neutron economy, which related to the neutron abundance of spallation process, is more relevant for breeding than for transmutation applications (NEA Nuclear Science Committee 2002).

In the context of transmutation, the principal non safety-related advantage of ADS is the increased core design and fuel management flexibility resulting from the removal of criticality condition. However, this advantage has weighed against several technical and working disadvantages. For example, the benefit from lengthening the reactor cycle has balanced against the investment in the more powerful accelerator required for coping with the lower end-of-cycle neutron multiplication reason (Maschek et al. 2008).

Table 3.1. Comparison of accelerator-driven sub-critical and critical reactor systems (NEA Nuclear Science Committee 2002)

	Advantages of accelerator-driven systems	**Disadvantages of accelerator-driven systems**
Design and operation	♦ The possibility to use a reactor core at a neutron multiplication reason below 1 opens opportunities for new reactor concepts, including concepts which are otherwise ruled out by an insufficient neutron economy. ♦ In particular, this allows transmutes designed as pure TRU or MA burners and hence fraction of specialized transmutes in the reactor park of minimized. ♦ Proportionality of reactor power to the accelerator current simplifies the reactor control.	♦ Accelerator: Very high reliability required to protect structures from thermal shocks. ♦ Beam window and target subjected to unusual stress, corrosion and irradiation conditions. ♦ Sub-critical core: Increased power peaking effects due to external neutron source. ♦ Compromises between neutron multiplications cause and accelerator power required. ♦ Increased overall complexity of plant. ♦ Reduction in net plant electrical efficiency due to power consumption of accelerator.
Safety	♦ The reactivity margin to prompt criticality it can increased by an extra margin which does not depend on the delayed neutrons. ♦ This enables the safe operation of cores with degraded characteristics as they are typical e.g. for pure MA burners. ♦ Excess reactivity can remove, allowing the design of cores with a reduced potential for reactivity-induced accidents.	♦ New types of reactivity and source transients have being dealt with (external neutron source can vary rapidly and reactivity feedbacks in TRU- and MA-dominated cores are weak).

Note: Issues of particular relevance for transmutation of TRU and minor actinides (MA) underlined.

Important design and material problems arise from installation of a target in the center of a reactor: the interfacing of an accelerator with a reactor rises containment questions, and the target and surrounding structure materials subjected to complex degradation phenomena due to joined thermo-mechanical loads, high-energy particle irradiation and, in contact with liquid heavy metals, corrosion effects which are much more severe than those run into normal reactors. This applies particularly to the beam window which may,

therefore, require frequent replacement. High-power accelerators will have improved with respect to the beam losses which cause radiation damage and activation in the accelerator components and the frequency of beam trips. In ADS, beam trips cause similar temperature and mechanical stress transients as fast control rod insertions (scrams) in critical reactors. Current accelerators feature beam trip frequencies which lay orders of magnitude above the current criteria for such transients. Regarding safety aspects, the prominent feature of ADS is its reduced potential for reactivity-induced accidents. This is particularly relevant for actinide burners which suffer from a general degradation of safety limits of core. From the viewpoint of transmutation, show conclusion from (Table 3.1). This ADS system has interesting design and safety advantages, but that must weighed against non-trivial technical and working disadvantages which will also have economic consequences. The diverse technical aspects of ADS have studied in many OECD Member countries. However, there is still a need for assessing more thoroughly the added value the ADS in the context of complete fuel cycles (Abderrahim et al. 2010).

3.2. Accelerators

A Particle Accelerator is a device which uses electromagnetic fields to propel charged particles or ions to high speeds and contain them in well-defined paths from of beams; now there are more than 30,000 accelerators in operation around the world. There are two basic classes of accelerators: electrostatic and oscillating field accelerators. When electrostatic accelerators are use static electric fields to accelerate particles, Oscillating field accelerators, and uses radio frequency electromagnetic fields to accelerate particles, and avoid the breakdown problem. Accelerators in various forms used in production and preparation of wide range of electronic devices. They include processes such as Ion Implantation, where the high energy beams of electrons subjected on semiconductors to dope them with impurity elements to conduct required amounts of electricity to power up the electronic devices, Ion Implantation for hardening of surfaces. This is mainly concentrated on strengthening the material used for preparation of semiconductors. They are also applied in processes like Electron Beam material processing, where the kinetic energy of electrons converted into heat energy thus enabling fusion of two materials of very thin sized foils or layers in electronic devices (Jayanth 2016).

3.2.1. Low Energy Accelerators

Generally used to produce bundles with energies between 10-100 MeV. And it used in a variety of applications, comprise particle therapy for oncological reasons, radioisotope production for medical diagnostics, ion implanted for industry of semiconductors, furthermore accelerator mass spectrometers used for measurements of rare isotopes such as radiocarbon (Witman 2014).

3.2.2. Medium Energy Accelerators

It is usually used to produce bundles with energies of 100-1000 MeV. In this range of energies, nucleons emit π mesons when they collide with the nucleus. Therefore, these accelerators used to investigate the role of nuclear quartz meson exchange (Krane and Halliday 1988).

3.2.3. High Energy Accelerators

Generally used to produce bundles with energies of 1 GeV (1000 MeV) and higher. Their target is to produce a lot of new particle types from nuclear inspection and check their properties. Thus speaking, accelerators are "ion sources" (Krane and Halliday 1988), which emit ion or electron beams that are commonly used in all accelerators after separating them according to energy levels and are also shown in (Figure 3.2).
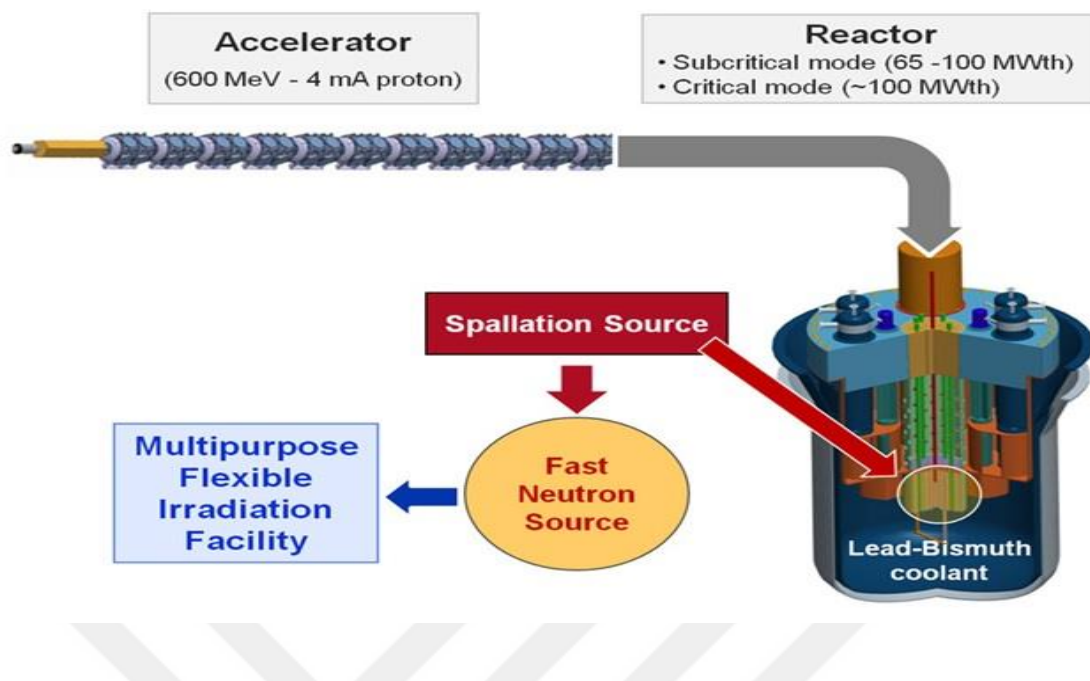
Figure 3.2.   Explained the accelerator in accelerator driven system (ADS) (http://www.accelerators-for-society.org/prospects/index.php?id=10)

nuclear reactors based on a core with fissile fuel configured such that neutrons emitted in the fission process can keep up a chain reaction. In an ADS, by contrast, the neutrons must prove a sustainable fission chain reaction and knocked out of a spallation target by high-energy protons from an accelerator. MYRRHA (Multi-purpose hybrid research reactor for high-tech applications) conceived as an accelerator driven system (ADS) able to use in sub-critical and critical modes. It consists a proton accelerator of 600 MeV, when the spallation target likewise a multiplying nuclei with MOX fuel, while this process cooled by liquid lead-bismuth (Pb-Bi). Image credit: Nuclear Research in SCK-CEN Belgian of Centre in Moll (Sarotto et al. 2013).

3.3. Accelerator Types

3.3.1. Electrostatic Accelerator

An electrostatic nuclear accelerator is one of two main types of particle accelerators, while charged particles accelerated by subjection to a static high voltage potential. When the static high voltage method has compared it, the dynamic fields used in oscillating particle accelerators. Owing to their simpler project, historically these accelerators

developed earlier. These machines operated at lower energy than some larger oscillating field accelerators, and to the extent that the energy system scales with the cost offset machines, in wide-ranging terms these machines are less expensive than higher energy machines, and as such they are much more public. Many universities universal have electrostatic accelerators for research purposes (Janes et al. 1966).

3.3.2. Cyclotron Accelerators

A type of particle accelerator, those accelerators charged subatomic particles, such as protons and electrons, in an externally spiraling path, importantly increasing their energies. Cyclotrons used to get about high-speed particle collisions in other to study subatomic structure. A cyclotron is a type of particle accelerator designed by Ernest O. Lawrence in 1934 in which charged particles accelerate outwards from the center along a spiral path (Nave 2012). It is a particle accelerator that moves charged particles into a circular orbit and a constant magnetic field. See the (Figure 3.3).
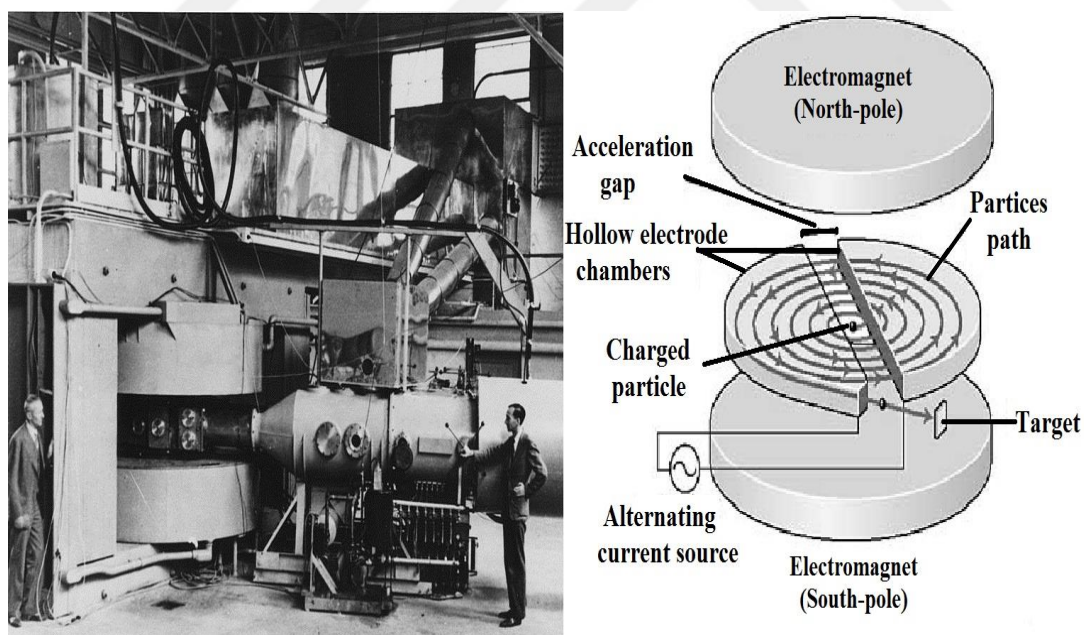
Figure 3.3.   Lawrence's 60-inch cyclotron, with magnet poles 60 inches (5 feet, 1.5 meters) in diameter, at the University of California Lawrence Radiation Laboratory (Heilbron and Seidel 1989)

This figure explained the designer of cyclotron, and type of particle accelerator in which particles spiral inside two shaped the hollow metal electrodes, when placed facing each

other under the effect of a strong vertical magnetic field, achievement energy by a high-frequency voltage applied between these electrodes. Lawrence, along with Richard Livingston, designed the 4.5-inch-wide cyclotron in 1931 to increase the hydrogen ion's energy beyond 0.8 MeV. In 1932, 11 inches of cyclotron and 1.1 MeV of energetic protons obtained. In 1935, a 27-inch cyclotron designed to accelerate the protons to 3.6 MeV. He found 37 inches in 1937, a 60-inch cyclotron in 1939, and awarded the Nobel Prize. In 1944 he designed a 180-inch cyclotron with 100 MeV (Lawrence 1951).

3.3.3. Synchrotron

A synchrotron is a particular type of cyclic particle accelerator, when sloped from the cyclotron, where an accelerating particle beam travels around a fixed locked-loop path. The magnetic field which bends of particle beam and into its closed path increases with time during the accelerating process, existence synchronized to the increasing kinetic energy of particles and shown in (Figure 3.4) (Chao et al. 2013).
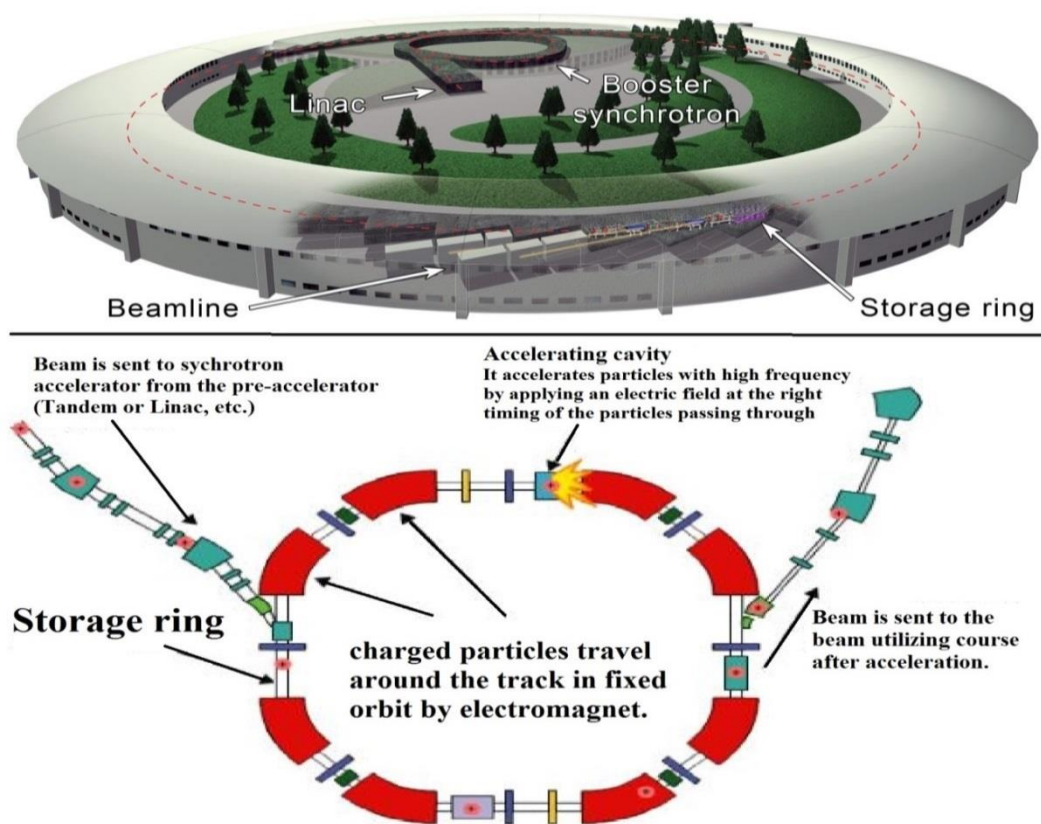
Figure 3.4. Explained the schematic diagram for the synchrotron at two pictures
(http://www.science20.com)

3.3.4. Linear Accelerator

A linear accelerator (LINAC) is the device most commonly used for external beam radiation treatments for diseases with cancer. The linear accelerator used to treat all parts/organs of body. It brings a high-energy x-rays to region of patient's tumor. Linear accelerators (linear accelerators - linac) are computer controlled devices that produce high-energy X-rays and electrons, see (Figure 3.5). Electrons torn off from the metal target under high voltage, such as in an X-ray tube, accelerate within the electromagnetic field to have higher kinetic energy. In this way, the electrons are the range (4-25) MeV targets in the distance target, and X-rays in the range of 4-25 MV energy (Chen and Williams 2011).
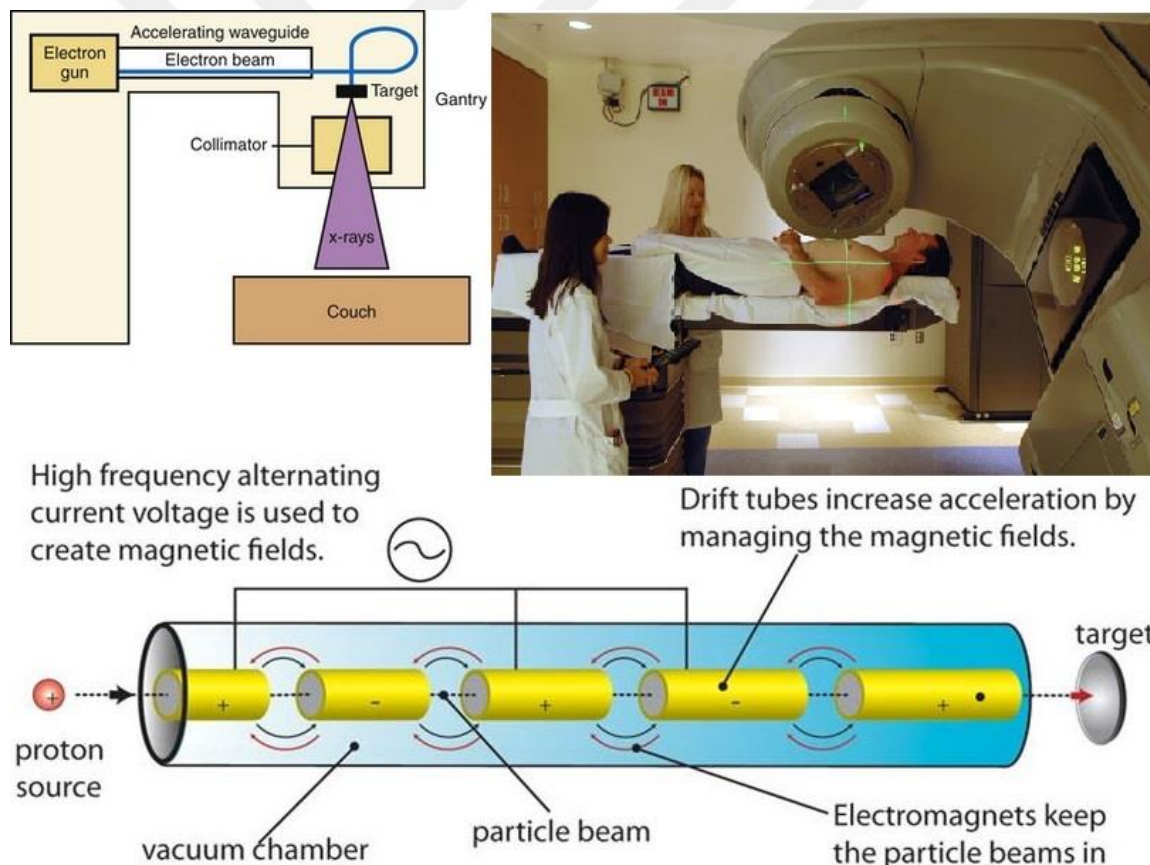
Figure 3.5. Explained the diagram of linear accelerator (Image-Guided Radiation Therapy) (http://clinicalgate.com)

This uses microwave technology to accelerate electrons in a part of accelerator called the "wave guide, when collide with a heavy metal target can produced of high-energy x-ray.

These high energy x-rays formed as they exit the machine to shape form of patient's tumor and the customized beam directed to the patient's tumor. The beam can formed either by blocks and placed in the head of machine or by a multi-leaf collimated incorporated into the head of machine. Patient lies on a movable treatment couch and lasers used to make sure the patient is in the proper place. The beam comes out of a part of accelerator called a gantry, when this device can rotated around the patient. Radiation can carried to the tumor from any angle by rotating the gantry and moving the treatment couch (http://clinicalgate.com).

3.4. Accelerator Source System

The accelerator must give a beam power which is commensurate to the rate of transformations which required it. No existing accelerator can meet such a performance and a dedicated facility must construct. We describe an alternative based on the superconducting cavities (SC) now in standard use at the LEP e+,e- collider which planned to end its operation by year 2000. After this time, with reasonable alterations, the fully operational and tested LEP SC-system offers the formidable opportunity of being redeployed replace, accelerating a great (30 mA) proton current to at least 1 GeV required by the full-scale (1500 MW thermal) EA operated at the conservative multiplication coefficient, k =0.95. Owing to the high-efficiency of SCs, even at such small value — typical for a "repository" — where fraction of electric power for the accelerator is about 10% (Rubbia and Rubio 1996).
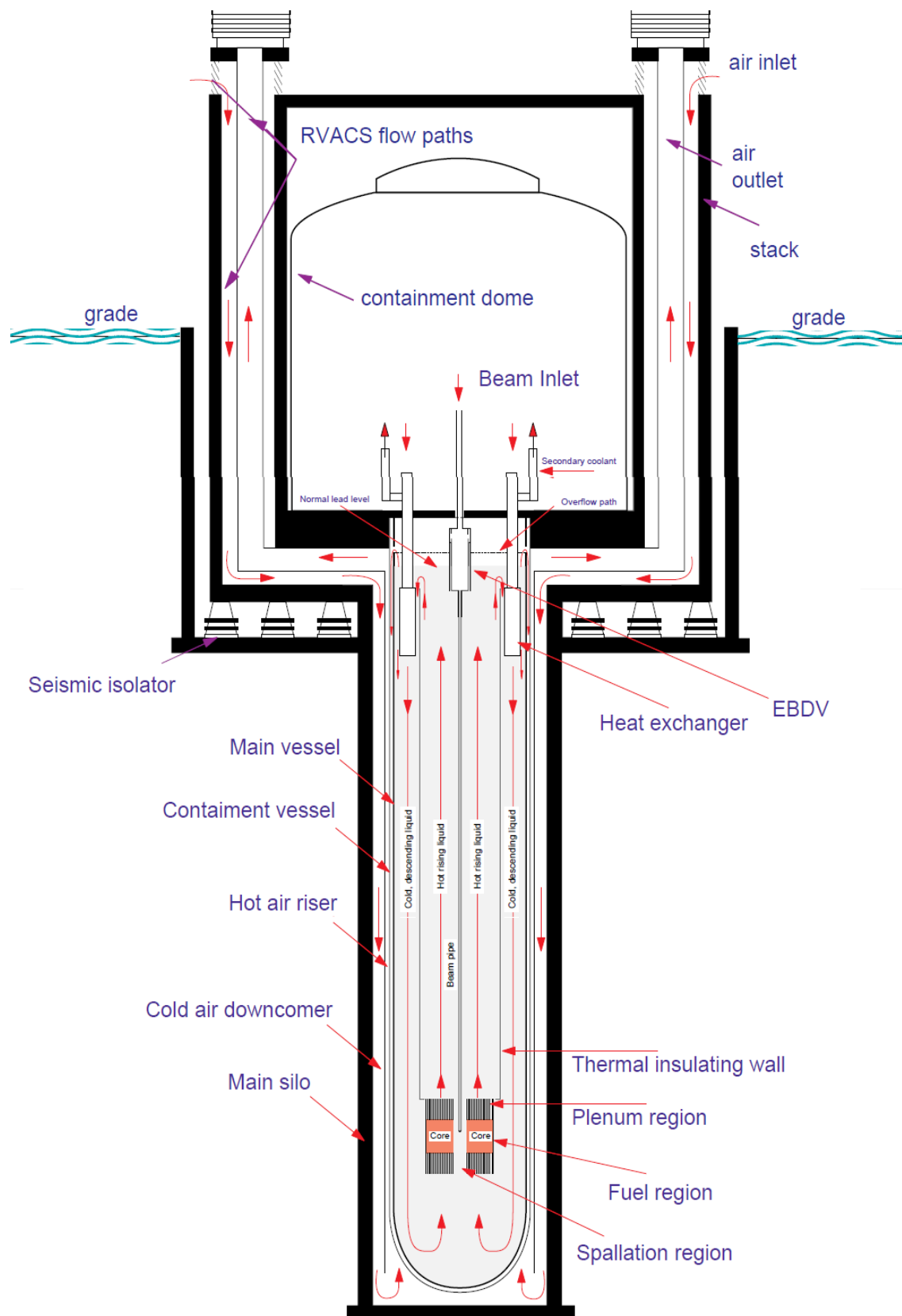
Figure 3.6.   General structure of sub-critical system (Rubbia et al. 1995), the silo is underground; under the grade level (EBDV stands for Emergency Beam Dump Volume)

In (Figure 3.6) has high energy beam of injected through the top and made to interact in the Lead near the core. Although the heat produced caused by nuclear cascade extracted by heat replaces. More the inside of vessel is free of obstructions, in instruction to let a healthy circulation of cooling liquid. Circulation of Lead in vessel and ensured it, also this process was exclusively by natural convection. There are four 375 MW are heat exchangers to transfer the heat from the primary Lead to the intermediate heat transport system. It must be designed in such a way as to introduce a small pressure drop in order not to slow down too much the convective cooling flow. The liquid exiting from the core at about 600/650 °C once cooled to 400 °C by the heat exchangers descends along the periphery and feeds the lower part of core and the target region. A thermally separating wall separates the two flows (Rubbia and Rubio 1996).

3.5. Major Accelerators in the World

There are many applied research in nuclear science and many technical advanced about the accelerators in the world, therefore today has most are making that technologies and produced by research students, or research Universities are the basic of century developments. At (Figure 3.7) is explained the accelerator technologies in world and developed.
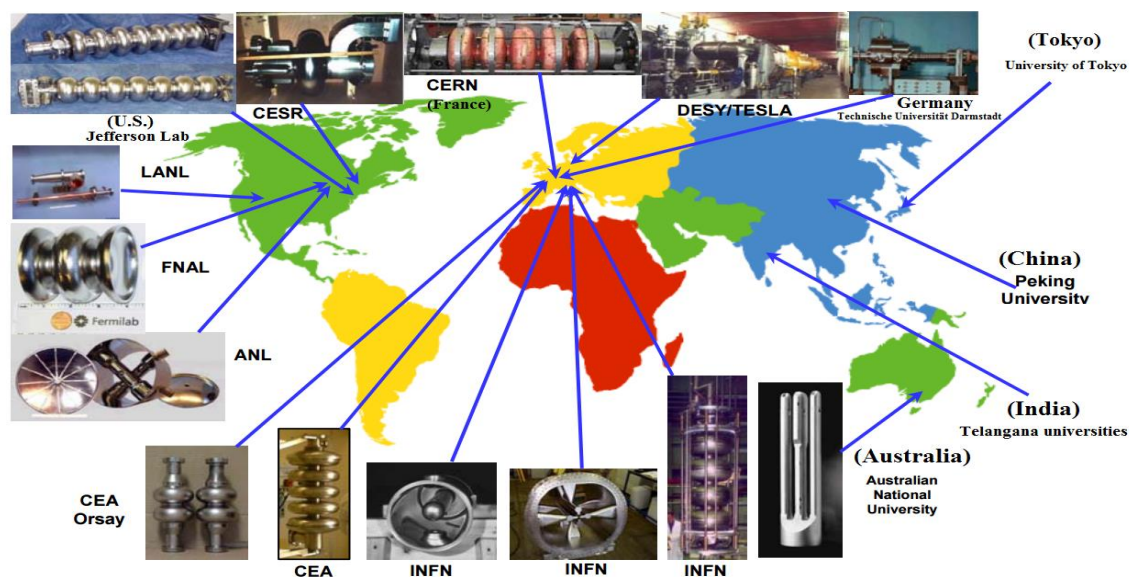
Figure 3.7. Developing Accelerator Technologies in the World
(http://www.nirs.qst.go.jp/ENG/core/ace/index.html)

3.5.1. CERN

CERN is the European Organization for Nuclear Research. The name CERN obtained from the acronym in French advice, there is an European Organization for Nuclear Research, a temporary body founded in 1952 with the mandate of establishing a world-class fundamental physics research organization in Europe. The convention establishing CERN of ratified on 29 September 1954 by 12 countries in Western Europe (Belgium, Greece, Germany, France, Italy, Denmark, Sweden, Netherlands, England, Switzerland, Norway and Yugoslavia) (Tomer 2014).

CERN As seen in (Figure 3.8). The NA61/SHINE facility at European Organization for Nuclear Research, CERN, on the Franco-Swiss border nearness Geneva. The acceleration chain delivers proton and nuclear beams to the T2 target in North Area target cavern at the beginning of H2 beam-line. Then the beams are either directly transported to the detector or used to produce secondary beam. The proton and ion acceleration chains use different particle sources, linear accelerators (LINAC2 and LINAC3) and circular accumulator machines (PSB and LEIR). Theis direction of Proton Synchrotron (PS) and the Super Proton Synchrotron (SPS) (NA61/SHINE facility at the CERN SPS, 2014).
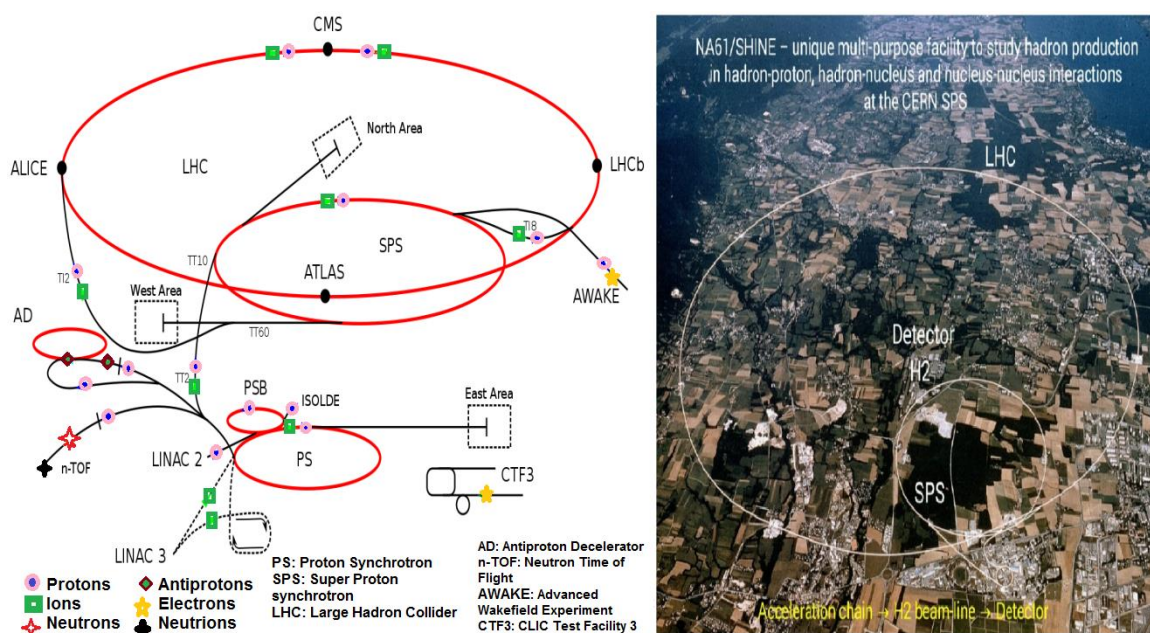
Figure 3.8. European Center for Nuclear Research (CERN) in (Genève, Switzerland) (NA61/SHINE facility at the CERN SPS, 2014)

3.5.2. Fermilab

Fermilab is a particle physics laboratory near at Chicago city in the United States (Figure 3.9). Established in 1967 as the National Accelerator Laboratory, while retitled the Fermi National Accelerator Laboratory in memory of Nobel prize-winning physicist Enrico Fermi in 1974.
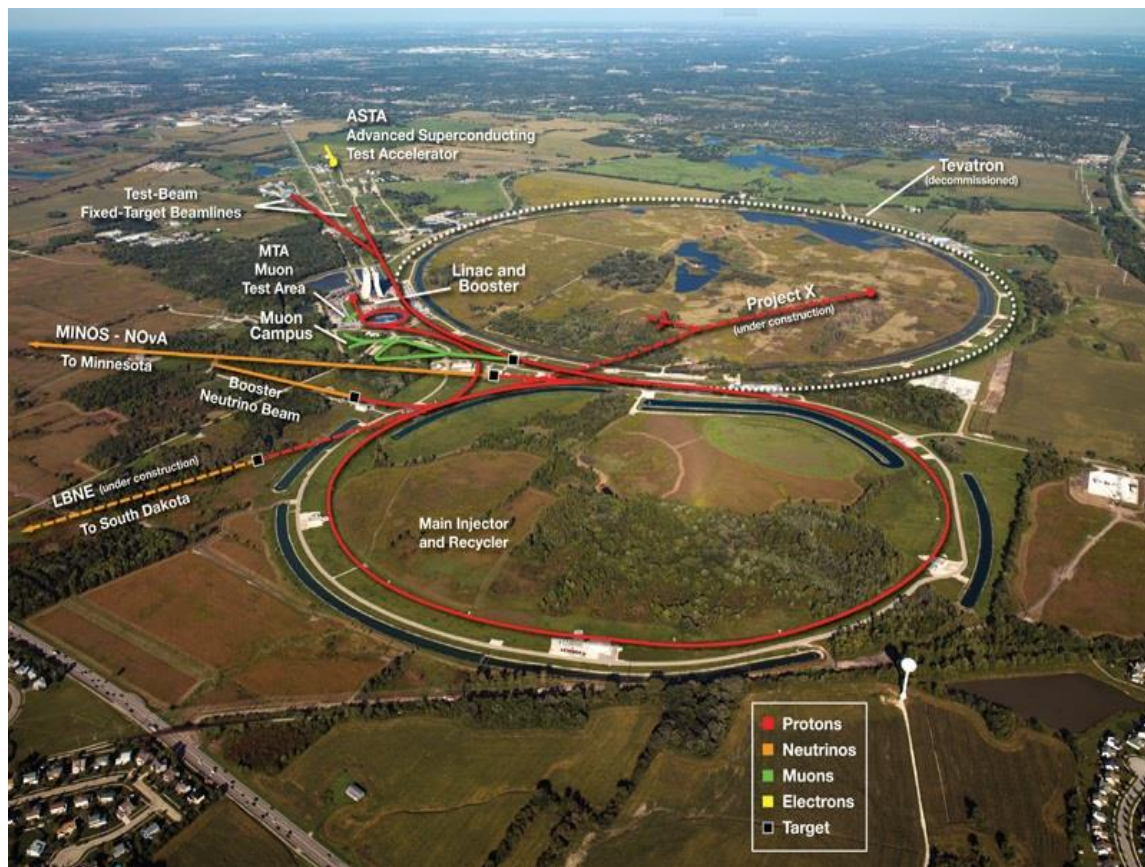
Figure 3.9.   FERMILAB (Tevatron Accelerator) (Cho 2008)

"A Plan for Discovery" evolved from the 2007 report of Fermilab Steering Group. The Steering Group produced response at broad spectrum of U.S. particle and accelerator physics groups are preparation of its report, which equipped advice to Fermilab, the Particle Physics Project Setting priorities Panel, the High Energy Physics counselor Panel and the funding agencies as they considered options for new particle accelerators and experiments in the United States. The some key accidents have occurred in particle physics over the last four years, consisting the successful startup of Large Hadron

Collider, along the timeline for the International Linear Collider, and the end of Tevatron resolutions. These events have evidence Fermilab as it implemented the recommendations of Steering Group and the Particle Physics Project Prioritization Panel and have led to development of "A Plan for Discovery" (Hill et al. 2011).

3.5.3. Desy

DESY is the largest national research laboratory in Germany signed on 18 December 1959 in Hamburg, Germany, while that construction of first particle accelerator, DESY is a German Electron Synchrotron and started in 1960. At that time it was the largest facility of this kind and was able to accelerate electrons to 7.4 GeV. On 1 January 1964 the first electrons accelerated in the synchrotron and the research on elementary particles began. The international attention first focused on DESY in 1966 due to its contribution to validation of quantum electrodynamics, which obtained with results from the accelerator. In the succeeding decade DESY established itself as a center of excellence for the development and operation of high-energy accelerators. The synchrotron radiation, which comes up as a side influence, was first used in 1967 for absorption measurements. For the ascending spectrum there had not been any conventional radiation sources in advance. The European Molecular Biology Laboratory (EMBL) made use of possibilities that arose with the new technology and in 1972 established a permanent branch at DESY with the aim of analyzing the structure of biological molecules by synchrotron radiation. See (Figure 3.10) when the electron-synchrotron in DESY II and the proton-synchrotron at DESY III whole taken into operation in 1987 and 1988 respectively as pre-accelerators for HERA (Heinze et al. 2015).
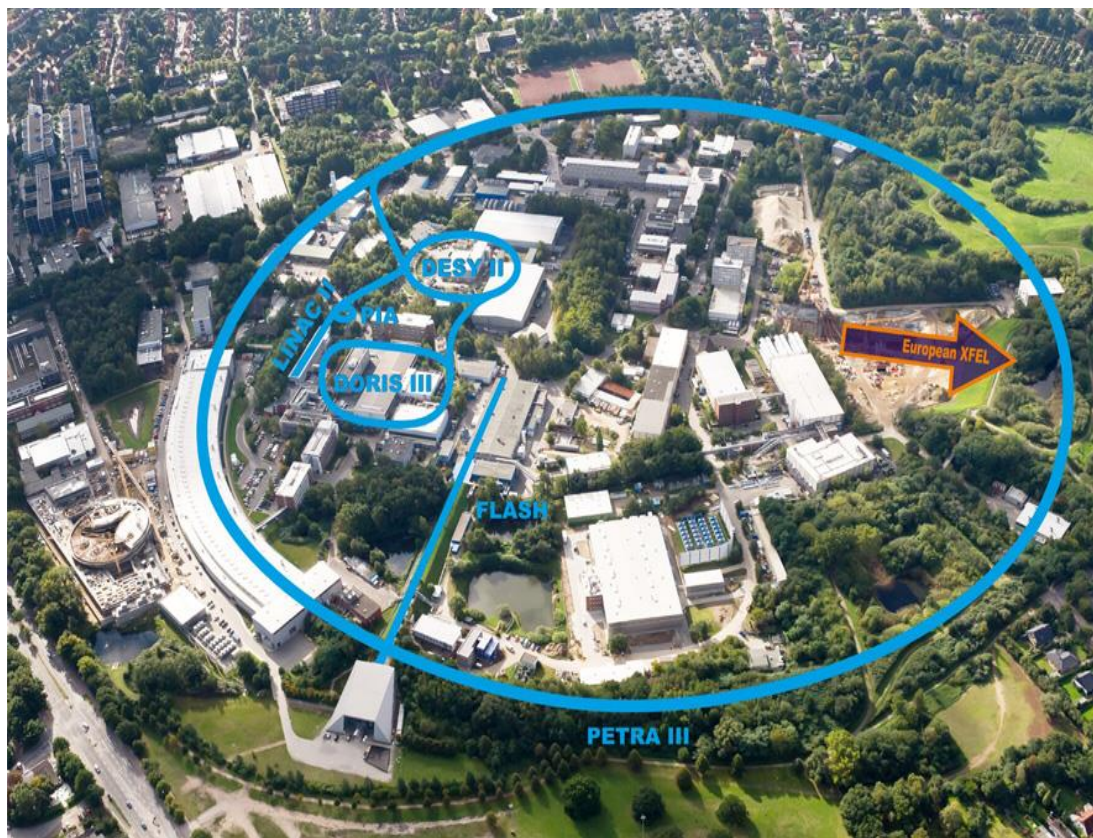
Figure 3.10.   Area of DESY accelerators (Hamburg, Germany) (http://h1.desy.de/)

3.6. Proton Accelerator

When the nucleus in the center of an atom collides with a high-intensity proton beam, the nucleus destroyed and different particles: neutrons, mesons, anti-protons, neutrinos and muon's disintegrated from π-means of generated. These are known as secondary particles and various kinds of research will conducted using these particles. For example, in research on life science, medical stores and nutrition will developed through the study of protein and enzyme functions. While information of genetic mechanisms obtained from the structure of DNA (Deoxyribo-Nucleic Acid) will develop new medicines to treat incurable illnesses. This type of research can lead to resolving such global problems as disease and food shortages.

In the material science, the technology developed by probing the basic mechanism of high-temperature superconductivity will apply to improve linear motor cars. The techniques to make high-performance batteries for electric and low-pollution vehicles

will be found by learning the electrical properties of various materials. Research on advanced nuclear systems is investigating the practical application of safer forms of nuclear knowledge, new energy systems and transmutation of long-lived radioactive nuclides to short-lived unique. Research of nuclear and particle physics aims to clarify elementary particle theory. The results attained will advance the search for the most fundamental principle and the last in matter. As tools for these research activities, building of a linear accelerator and synchrotrons 3 billion (3 GeV) and 50 billion electron volts (50 GeV) planned. In calculation, to make effective use to the secondary particles generated by these accelerators, a life and material science easy, a nuclear and particle physics easily, and an accelerator-driven alteration experimental facility will take form. While construction with slated is start in economic year 2001, with practical tests to get under way in FY2006. See (Figure 3.11) when the basic project and R&D of main components are already in progress (Shimomura 2009).
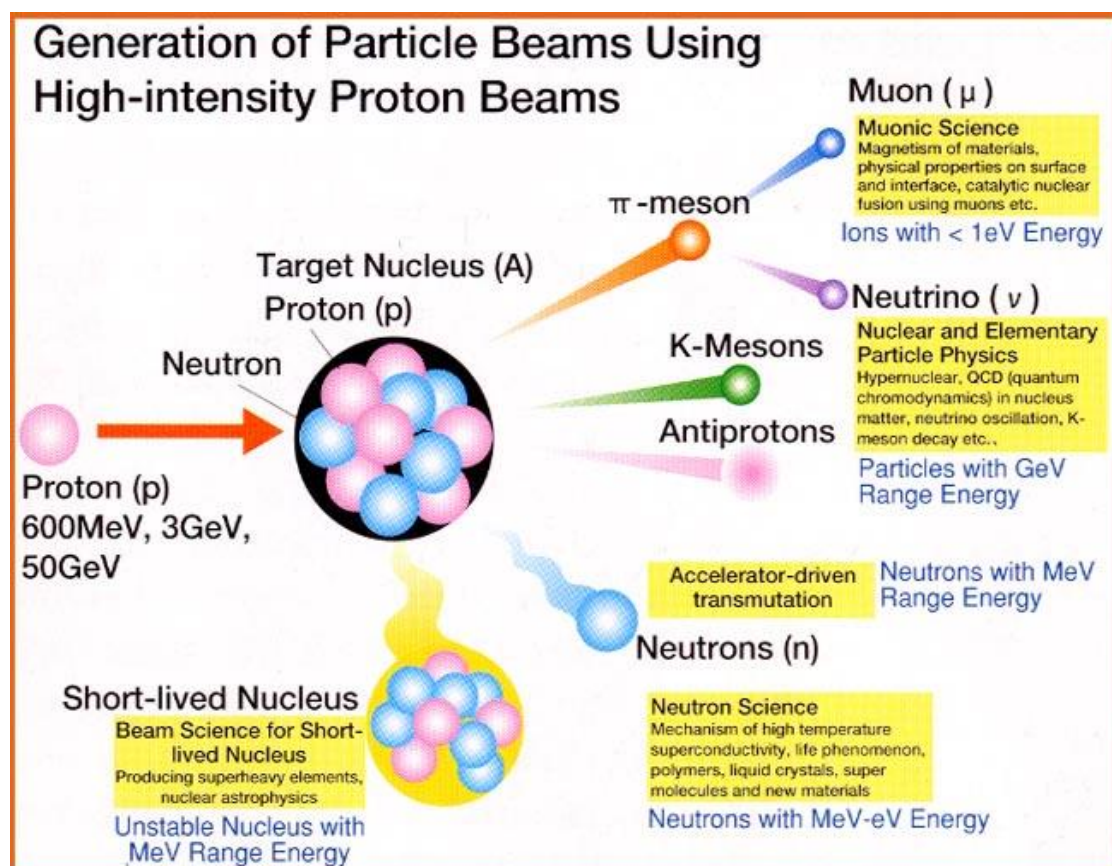
Figure 3.11.   The high-intensity proton accelerator (JAERI 2005)

3.7. The Spallation Process

Nuclear spallation is one of processes by which a particle accelerator likely used to protons, neutrons, or deuteron. Also any elements are target such as uranium, lead or other heavy metal target used it, when these particles are incident in, and 20 to 30 neutrons ejected after each influence. Although this is a far more expensive way of producing neutron beams than by a chain reaction of nuclear fission in a nuclear reactor, although the advantage that the beam can pulsed with relative comfort. Notion of nuclear spallation was first coined by (Nobelist Glenn T. Seaborg) in his doctoral when right researches on the inelastic scattering of neutrons in 1937 (Seaborg 1967).

There is no precise definition of spallation: this terms covers is interaction of high energy hadrons such as (protons, neutrons, pions, etc.) or light nuclei (deuteron, triton, etc.), from a few 10 of MeV to a few GeV, with nuclear targets. It corresponds to the reaction mechanism by which this high energy projectile pulls out of target some nucleons or light nuclei, leaving a waste nucleus (spallation product). Depending on the conditions, the number of sent out light particles, and specifically neutrons, likely quite large. This is of course the feature of outermost importance for the so-called ADS (Kadi and Revol 2001).

At these energies it is no longer correct to think of nuclear reaction as proceeding through establishment of compound nucleus. The first collision between the incident projectile and the target nucleus leads to a series of fast direct reactions (Intra-Nuclear Cascade, ~ 10^{-22} sec) whereby each nucleon or small groups of nucleons ejected from the nucleus. At energies above a few GeV in nucleon, Partition of nucleus can also converse (Pre-Compound Stage, $< 10^{-18}$ sec). After the intra-nuclear cascade phase of reaction, the nucleus is left in the excitation state. Thereafter relaxes its ground state by "evaporating" nucleons, mostly neutrons (Kadi and Revol 2001 September). The spallation process is depicted in (Figure 3.12), showing two stages of process (intra-nuclear cascade and evaporation). For thick targets, high energy secondary particles can undergo further spallation reactions (inter-nuclear cascade) as illustrated in (Figure 3.13).
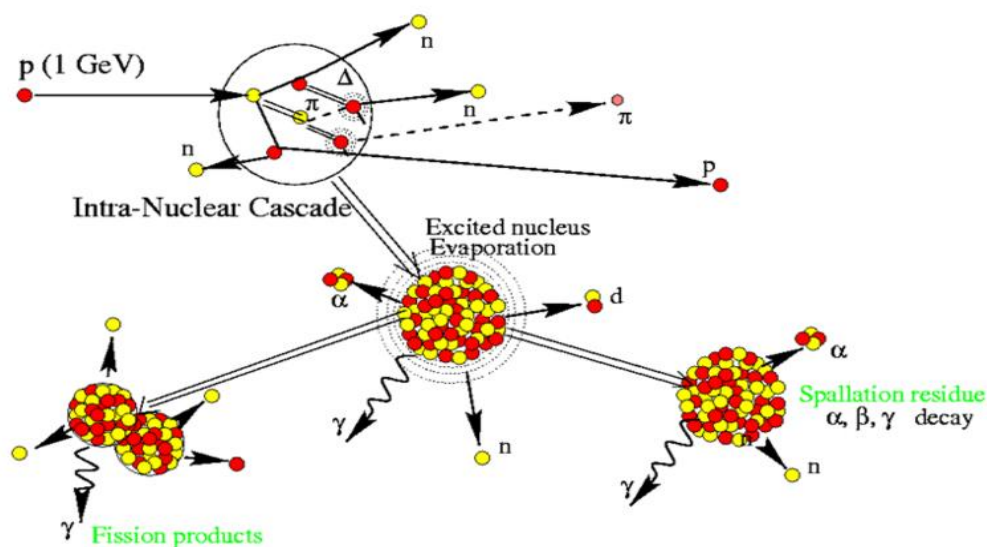
Figure 3.12. The Illustration of spallation process in thick targets, with evaporation competing with high energy fission (David 2015)
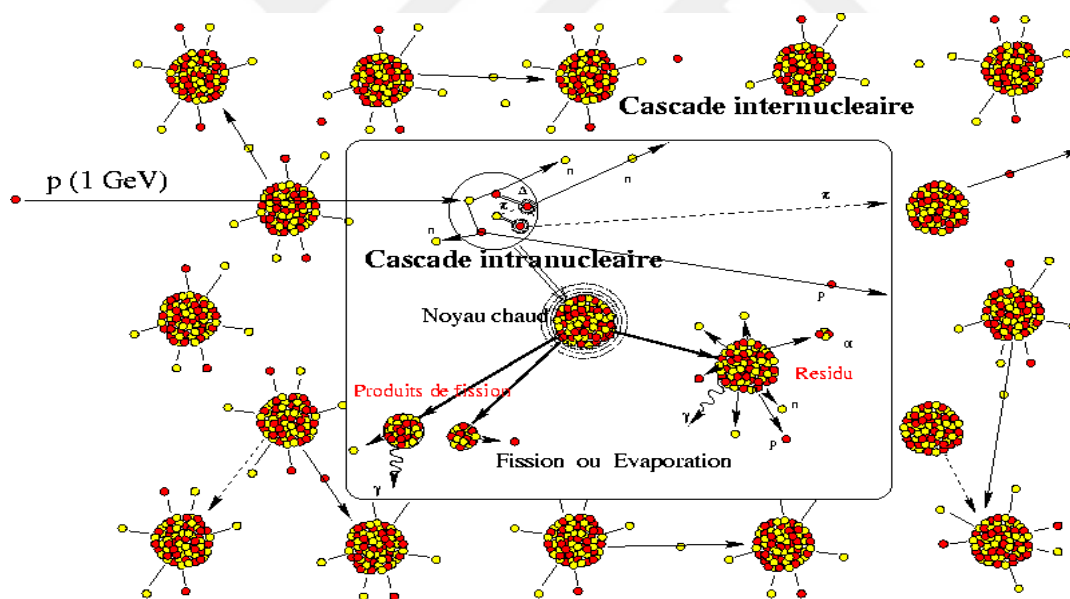
Figure 3.13. Illustration of inter-nuclear cascade in thick targets (Kadi and Revol 2001)

For some target materials, low energy spallation neutrons can enhance neutron production through low energy (n,xn) reactions. For weightier nuclei, high energy fission can compete with evaporation (e.g. tungsten and lead). Some spallation targets such as thorium and depleted uranium can further fission by low energy spallation neutrons (> 1 MeV).

3.8. Fission

When an atom splits into two parts or more, either during a natural decay or when instigated within a lab, it scattered energy, this process is known as fission. It has excessive potential as a source of power, but it also has a number of positivistic, environmental, and political concerns attached to it that can hinder its use. Therefore an atom has protons and neutrons in its center of nucleus. In fission, the nucleus splits, each through radioactive decay or since it has bombarded by other subatomic particles known as neutrinos. The resulting pieces have less rallied mass than the unique nucleus, with the missing mass changed into nuclear energy see (Figure 3.14) (Murray and Holbert 2014).

In 1938, German physicists Otto Hahn and Fritz Strassman bombarded a uranium atom with neutrons in trying to use heavy elements. In a surprising twist, they wound up schism the atom into the elements of barium and krypton, both importantly smaller than the uranium that the pair started out with. Previous duties that by physicists had resulted in only very small slivers being cut off for an atom, so on the pair puzzled by unexpected results (McCracken et al. 2012).
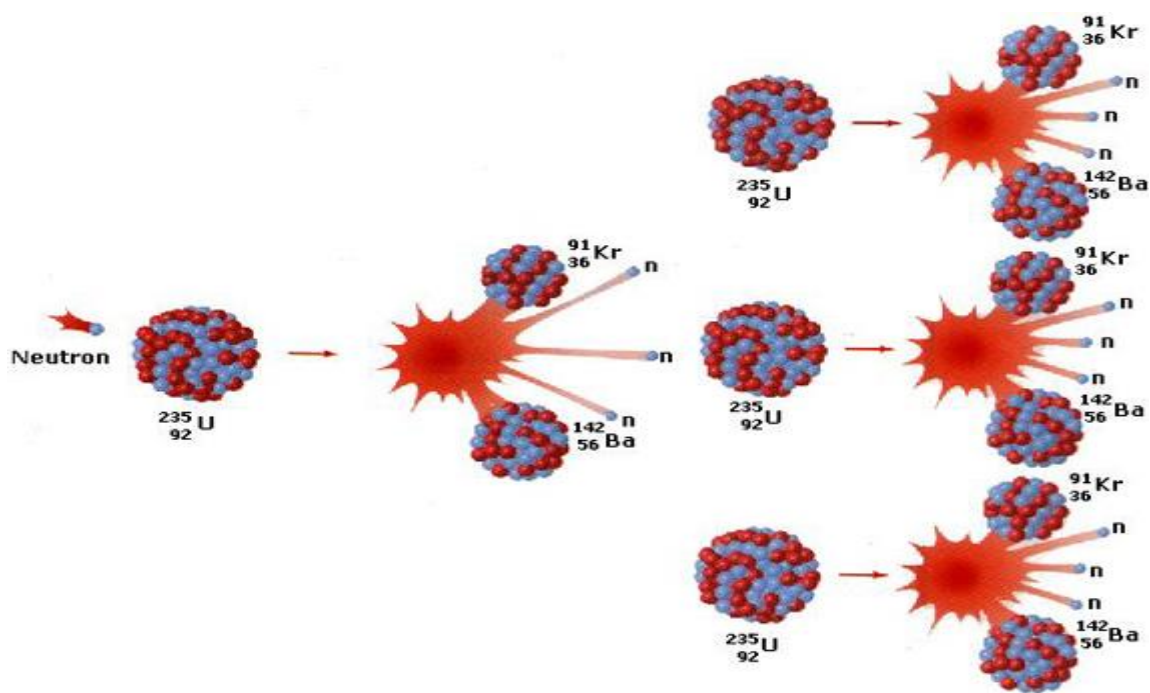
Figure 3.14.   Controlled fission occurs when a neutrino bombards the nucleus of an atom (Uranium) (http://www.tutorvista.com)

This figure explained the bombarding nucleus and nucleus is breaking it into two smaller, or for two similarly sized nuclei. Each newly (krypton and barium) freed neutron can go on to cause two separate reactions, each of which can cause at smallest two more. A single influence can jumpstart a chain reaction, driving the scatter of still more energy. Therefore this figure is representation of a:

$$_{92}U^{235} + {_0}n^1 \rightarrow 3\ {_0}n^1 + {_{36}}Kr^{92} + {_{56}}Ba^{141} + energy$$
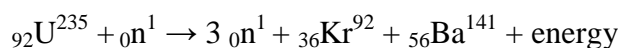
Nuclear Fission is the process of splitting a heavy nucleus to form two new elements with smaller nuclei. One of most significant nuclear reactions is that of uranium (^{235}U) which used in nuclear reactors and atomic weapons. This fission of uranium (^{235}U) is warp and woof when a neutron of enough speed collides with the nucleus of uranium (^{235}U). This collision produces a uranium (^{236}U) which immediately splits into two lighter elements i.e. krypton (^{91}Kr) and barium (^{142}Ba). This event also releases three neutrons and energy. The neutrons produced are ability of product more nuclear fission events if they meet a uranium (^{235}U) nucleus. If a sufficient amount of mass of uranium (^{235}U) is present then the reaction becomes self-sustaining resulting in production of massive measure of energy, thermal, light, ionizing radiation and atomic explosion. Nuclear Fission Equation of uranium (^{235}U) is given below (Smyth and Henry 1945).

3.9. Difference between spallation and fission

Advanced fission reactors and high power accelerator spallation targets subject materials are damaging particle irradiation. Although these technologies derive their utility from different nuclear reactions and divergent applications, they experience many common features. Further, the physical mechanisms of radiation response are cross-cutting. For example, swelling, phase instability, hardening, flow localization, and embrittlement must understand to estimate component lifetimes. Additional commonalities include reliance on the same classes of materials and sometimes on the same alloy for critical components. In addition, databases supporting designs are mainly derived from the same relatively few irradiation facilities and from similar types of experiments. Emphasis at placed on development of fundamental knowledge were support alloy design strategies

for resistance to irradiation and to form a scientific basis to develop better materials (Mansur et al. 2004).

Computational models for spallation and fission reactions used in an accelerator breeding and transmutation code have evaluated by performing calculations for thin targets of Bismuth(Bi), Lead(Pb), Thorium(Th) and Uranium(U) in the energy at when ranged between 50–1000 MeV. Proton and neutron non-elastic and fission cross sections are been derived from the counts of real collisions and fission events in the targets. Several fission models at combination by spallation model and compared with the experimental data due to (Ishimoto et al. 2002). There is a good agreement has obtained for a model with the level density parameters an =A/10 and af/a fitted to the data due to (Il'inov et al.). The mass of a target is dependence of non-elastic cross sections has calculated also with use of best model. A good accepted with the experimental data obtained over a range of nuclear masses (Nakahara and Yasuaki 1983). Although we can provides some difference between the spallation and fission, (Table 3.2) is showing that the Comparison.

Table 3.2. Difference between the spallation and fission (Mansur et al. 2004)

Spallation	Fission
1-Spallation is a process in which fragments of material (spall) ejected from a body due to impact or stress.	Fission occurs when an atom splits into two portions, for either through natural decay or when instigated within a lab, it scattered energy. This process is known as fission.
2- It is not a chain reaction process.	It is a chain reaction process.
3-There is a (20-30) neutron or protons were expelled after each impact.	Only one neutron expelled after each impact.
4-Is a process which the continuous of a flow.	Is a process which the continuous of a pulse operation.

3.10. Pre-Equilibrium Models in Nuclear Reactions

The model proposed by Griffin has used to investigate the approach of a compound nucleus to statistical equilibrium. A set of master equations attribute the equilibration process and utilizing Williams' transition-rate expressions are obtainable. These equations have used to study the occupation probabilities and the instantaneous and time-integrated particle energy spectra at function of time elapsed from the first target-projectile interaction. Differences of results for a sample system formed with three excites at excitation energies of 24 and 96 MeV are obtainable. While a sensitivity of results pre-equilibrium model are changes in the values of model parameters and used inspected it. In addition, particle spectra resulting from closed-form and master-equation calculations are difference, as are the results attained using several about sets of transition-rate expressions for closed-form calculations. The results of using different forms for the state density of system have also been inspected. Finally, a large number of published experimental particle energy spectra have analyzed in terms of pre-equilibrium model. Initial conformations consisting of three particles and holes for nucleon-induced reactions and five particles and holes for α ion induced reactions were generally indicated by these analyses. Furthermore, it is found that pre-equilibrium particle emission probably accounts for tens of percent of total reaction cross section. Results of data analysis are all usually consistent with other recent work on the pre-equilibrium statistical model (Cline and Blann 1971).

The main models that examine pre-equilibrium reactions:

 a) Full Exciton Model.
 b) Hybrid Model.
 c) Geometry Dependent Hybrid Model.
 d) Cascade-Exciton Model.

3.10.1. Full Exciton Model

An approach combining essential features of exciton and intranuclear cascade models is developed. The cascade-exciton model predictions for the energy spectra, angular distributions and double differential cross sections of nucleons and complex particles as well as for the excitation functions are analyzed at incident nucleon energies $T_0 \lesssim 100$

MeV and in a large range of nuclear target masses. We discuss the relative role of different interaction mechanisms and their possible experimental identification (Gudima et al. 1983). Subsequent interactions together form more of a particle-ridge situation. In addition, there are equilibrium processes in the Exciton Model. In this process, we can also calculate the chance of particle emission. This computation method, however, produces direct numerical solutions of paired Pauli Master equations. The basic feature of this model is that a nuclear reaction is a function to time. The following Equation is defined in (Eq 3. 1).

$$\frac{d\sigma}{d\varepsilon} = \sigma R \sum_{n=n_0}^{\bar{n}} \left[\frac{X_\gamma \rho_{n-1} U}{\rho_n(E)} \right] \cdot \left[\frac{\lambda_c(\varepsilon)}{W_C(E) + W + (E)} \right] D_n \qquad (3. 1)$$

When

$$U = E - B_v - \varepsilon \qquad (3. 2)$$

Where the first set of square brackets represents the number of exciting of type (v) which could be emitted with channel energy (ε), and the second set represents the chance that the particle will emitted before any (n) exciting configuration on the average either emits a particle or undergoes an intranuclear (two body) interaction. Here the decay normalization based on any action of all members of n-exciton configuration ensemble, a two-body interaction or particle emission. One can calculate precisely the fraction of ensemble which will emit a particle, and the fraction which will make a two-body transition, and these two fractions sum to unity for the n exciting ensemble (Blann et al. 1976; Gadioli et al. 1973).

3.10.2. Hybrid Model

The hybrid model is a semi-classical approach analogous to the INC, where each particle interacts independently of all others. A result of this is a different normalization than that of exciton model is with:

$$p_v(\varepsilon) = \sum_{\Delta n=+2}^{n} n = n_0 \left[\frac{n_x v N_n(\varepsilon, U)}{N_n(E)} \right] g.d_\varepsilon \left[\frac{\lambda_c(\varepsilon)}{\lambda_c(\varepsilon) + \lambda + (\varepsilon)} \right] D_n \qquad (3.3)$$

Where the second set of square brackets has a denominator consisting of two body transition rate and continuum emission rate of exciton under consideration, and not integrated over all exciting as;

$$\frac{d\sigma(\varepsilon)}{d\varepsilon} = \sigma_R p_v(\varepsilon) \qquad (3.4)$$

The result of this difference for decay normalization is great, for now, e.g., a 2plh configuration could decay by both particles and the hole making a two-body transition (which would give a 3n exciton final configuration), or by one and only one exciting being emitted, or by two and only two excites being emitted (Blann and Vonach 1983; Sierk 1986). With two types of excites (neutrons and protons) the number of exclusive possibilities increases.

It is shown as. P_v (ε) is the number of neutrons and protons, always located between the dε energies ε + dε and ε, n; The number of possible excitons at equilibrium, n_χ v; The number of particles in type and in an excited state, E; Exciton energy of compound system, N (ε, U); Nn (E), where n is the number of exciting properly arranged in such a way as to share among the other n-1 exactions of excited energy =E-Bv-ε when emitted by an exciting ε channel energy; The total number of particles plus n (n =p + h) in the excited energy, $\lambda c(\varepsilon)$; The velocity of a particle (ε) to the continuous zone by channel energy, $\lambda+(\varepsilon)$; The intracellular passage speed when an energetic particle is continuously distributed to the region, Dn; The initial population section in an n-exciton chain, σ_R; Reaction effect section, g; Refers to the single-particle level intensity. The quantity in square brackets in (Eq 3.3) above gives the particle numbers between continuous zone energy ε and ε + dε. The second parenthesized part is the ratio of transition speed to the continuous zone to the total transition speed. This model is also a suitable method in closed type calculations. Therefore, the exciting energies of target nuclei become important as well as the calculation of influence cross section is important. For this

reason, the particle sent in this model may also be complex. Thus, it is possible to find the nucleus publishing account.

3.10.3. Geometry Dependent Hybrit Model

The Geometry Additive Hybrid Model is a variation of exciton equation that works with the kernel and the definition of kernel and kernel scattering. In 1983, the calculations of this model were made by Blann and Vonach,

$$\frac{d\sigma v(\varepsilon)}{d\varepsilon} = \sigma_R p_v(\varepsilon) \tag{3.5}$$

$$p_v(\varepsilon)d\varepsilon = \sum_{\Delta n=+2}^{n} n = n_0 \left[\frac{n_x v N_n(\varepsilon, U)}{N_n(E)} \right] g.d_\varepsilon \left[\frac{\lambda_c(\varepsilon)}{\lambda_c(\varepsilon) + \lambda + (\varepsilon)} \right] D_n \tag{3.6}$$

Here, σ_R in (Eq. 3.5 and Eq. 3.6) is the reaction cross section, n χ v; N is the number of π-type particles (protons or neutrons) in the exciton state, P v (ε) dε; Shows the number of υ type particles (protons or neutrons) that are continuously distributed between the energies ε and ε + dε. Also; A (ε) is the rate at which a particle (ε) propagates to the continuous region with channel energy, while λ + (ε) The intracellular pass-through rate of a ε-energized particle, Dn; The first population section in an n-excited chain, σ_R; Reaction effect section, g; Single-particle level intensity. Thus, the measure in square brackets in (Eq 3.6) gives the number of particles between energy ε and ε + dε; in the second parentheses is the ratio of passage velocity of particles to the reaction zone to the total particle velocity. Furthermore, in this model, the extreme particle-to-state density from the cross-section is important, and particle-nucleation formation is dependent on the nuclear surface. That is why there is a small difference in the energy in the constant region. In addition, it is observed that the angular contribution of absorbed particle and the fraction to be released are separated from the Hybrid Model due to the angular change (Blann and Vonach 1983).

3.10.4. Cascade Exciton Model

The nucleus-nucleon reactions in the central energy region are important because they are useful in studying particle emission previous to equilibrium. The main reason underlying the understanding of nuclear structure and the mechanism of particle ejection is development of pre-equilibrium conception. By examining succession of nuclear reactions at nuclear levels, more than one feature of nuclear reactions can be examined in detail. Cascade Exciton Assumes that modeled reactions take place in three stages: The first stage is the transition to nuclear levels, the second stage refers to the balance phase, and the third phase refers to the balance state. In general, these three stages contribute to the experimentally measured values. Accordingly, for particle spectrum can be writing this equation:

$$\sigma(P)dp = \sigma_{in} [N^{cas} (P) + N^{prq} (P) + N^{eq} (P)]dp \qquad (3.7)$$

Cascade stage of interaction is described by the Dubna version of intranuclear cascade model (Barashenkov 1972; Barashenkov et al. 1969). The inelastic scattering effect section is calculated in the transient model. The Cascade model accounts for the reaction geometry that holds all the information about the kinematic characteristics of fast particles, but ignores interactions between cascade particles. On the other hand; Exciton model treats the excited quartz-particle gas as an excited nucleus that interferes with the interactions of hh, ph and PP (ie, "particle-hole" degrees of freedom are included). The conditions of Cascade model are better fulfilled at higher energies where the kinetic energy of particle exceeds the binding energy of nucleus. It is important to combine these two models to improve the definition of nuclear reaction properties of particles that emerge in a large energy region (Gudima et al. 1983).

3.11. Calculation Method

This research discovered an energy spectra for secondary particles (n, p, d, α) after spallation reaction to ($_{79}Au^{197}$, $_{92}U^{238}$) targets, and provide the energy for incident proton between (20-290) MeV, when firstly reaction for gold target is 20 MeV but for uranium target is 50 MeV. This process applied by some programs, also these programs practicable with a worked on computer device. Such as reactions are practiced by two steps: Firstly needed defined those energy spectra (MeV) and cross section (mb/MeV) for each particles, also this defined must to be any programs such as (CEM03, ALICE/ASH, PCROSS), and this calculations comparing them with results when presented at website internet named (Nuclear Energy Agency) from EXFOR and these results called the (Experimental Data). Likewise secondly, this process must be drawing with a plot by (Grapher7) program, and showing that comparison between those calculations. Although each result must do layout of plot by a graph program, thus this concept showed that results are more clearly. Finally it can be said this research calculates of produced the best results, because the numbers of calculation are near to each other, so that results are correct.

3.11.1. CEM03 Computer Program

CEM03 calculates total reaction and fission cross-sections, nuclear fissilities, excitation functions, nuclide distributions (yields) of all produced isotopes separately as well as their A- and Z-distributions, energy and angular spectra, double-differential cross-sections, mean multiplication, i.e. the number of ejectiles per inelastic interaction of projectile with the target, ejectile yields and their mean energies for n, p, d, t, ^{3}He, α, Pion$^+$, Pion$^-$, and Pion^0. In addition, (CEM03) give in its output separately the yields of Forward (F) and Backward (B) produced isotopes, their mean kinetic energies, A and Z-distributions of mean emission angle, their parallel velocities, and the F/B ratio of all products in the laboratory system, distributions of mean angle between two fission fragments, of neutron multiplicity, of excitation energy, of momentum and angular momentum, and of mass and charge numbers of residual nuclei after the INC and preequilibrium stages of reactions, as well as for fission nuclei before and after fission.

CEM03 calculates reactions induced by nucleons, pions, bremsstrahlung and monochromatic photons on not too light targets at incident energies from ~10 MeV (~30 MeV, in the case of gamma) up to several GeV. This Manual describes the basic assumptions of improved CEM as realized in the code CEM03, essential technical details of code such as description of input and output files, and gives the user with necessary information for practical use and for possible change of CEM03 output, if required (Mashnik and Sierk 2012).

3.11.2. ALICE/ASH Computer Program

The ALICE/ASH program is a slightly modified and improved version of ALICE91 program. This program cannot use for energies up to 290 MeV. While ALICE/ASH program is used for finding as energy spectra of resulting products, angular distribution of secondary particles, exciton function, cross section calculations, and publishing spectrum. Several types of calculations and combinations can performed including a standard Weisskopf-Ewing evaporation with multiple particle emission, S-wave approximation to provide an upper limit to enhancement of gamma-ray de-excitation due to momentum effects, and an evaporation calculation that can include fission competition is caused the Bohr-Wheeler approach. ALICE/ASH91 calculates precompound decay via Hybrid and GDH models with multiple precompound decay algorithms, double differential spectra and single, and reaction product cross sections (Blann 1991).

3.11.3. PCROSS Computer Program

A new PC code PCROSS for neutron induced reaction calculations up to 25 MeV incidents of developed, where the latest theoretical development in the model as employed. A combination of exciton model and multistep direct reaction model parametrization was used to describe the high energy part of spectra. In the PCROSS code several models for level density calculations are available. The code includes a subroutine to generate the input data. In the existing paper some calculation results for (n.n′) and (n,p) emission spectra in the range of 5 to 25 MeV and for (n,p) and (n,2n′) excitation functions up to 20 MeV are shown. Therefore in this program it has a good description of experimental data achieved (Capote et al. 1991).

4. FINDING AND DISCUSSION

4.1. p+$_{92}$U^{238} Reaction

Uranium is a chemical element with symbol U and atomic number 92. It is a silvery white metallic in the actinide series of periodic table. A uranium atom requires 92 protons and 92 electrons. When ^{238}U is the most common isotope of uranium found in nature, making up over 99% of it. Unlike ^{235}U it is non-fissile, which means it cannot tolerate a chain reaction. Though, it is fissionable by quick neutrons, and is fertile, meaning it can being a transmuted to fissile ^{239}Pu, although melting point of uranium is equal to 1132°C (Katz et al. 1986). ^{238}U cannot support a chain reaction because inelastic scattering reduces neutron energy below the range where fast fission of one or more next-generation nuclei is probable. Doppler broadening of ^{238}U neutron absorption resonances, more absorption as fuel temperature increases, is also an important negative feedback mechanism for reactor control. (Mc Clain et al. 2005)

4.1.1. Neutron Energy Spectra (dσ/dE) for p + $_{92}$U^{238} Reaction at E$_p$=50 MeV

Figure 4.1. Shows a comparison of ALICE, CEM03 and Experimental data results for the energy spectra ($\frac{d\sigma}{dE}$) of neutrons when $_{92}$U^{238} element is bombarded by protons at 50 MeV. The figure shows the many difference energy spectra at each program. When ALICE data's is more than each CEM03 and Experimental data, and Experimental data is more than the CEM03.

Table 4.1. Show the numerical results of $\frac{d\sigma}{dE}$ both for ALICE, CEM03 and Experimental data's. As can be seen in the table, the maximum $\frac{d\sigma}{dE}$ at ALICE/ASH =3591 mb/MeV while E_n =0.5 MeV, maximum $\frac{d\sigma}{dE}$ at Experimental data =2591 mb/MeV while E_n =0.7 MeV, and CEM03 =4.7559 mb/MeV while E_n =0.7 MeV.

Table 4.1. Neutron energy spectra for p + $_{92}U^{238}$ reaction, E_p=50 MeV, Calculations have been made by ALICE, CEM03 programs and experimental data taken from EXFOR

ALICE /ASH		CEM03		Experimental Data (Khlopin 1973)	
E_n (MeV)	dσ/dE (mb/MeV)	E_n (MeV)	dσ/dE (mb/MeV)	E_n (MeV)	dσ/dE (mb/MeV)
0.5	3591	0.7	4.7559	0.7	2591
1.5	2361	0.9	4.3301	1.9	2161
2.5	1196	1.1	3.8891	2.1	926
3.5	608.5	1.3	3.4333	3.3	502
4.5	335	1.5	3.0193	4	236
5.5	202.2	1.7	2.6428	5.7	190
6.5	135	1.9	2.2682	5.9	102
7.5	98.64	2.1	2.0403	6.1	77
8.5	77.47	2.3	1.7797	7.3	77.47
9.5	64.31	2.5	1.6357	8.5	52
10.5	55.43	2.7	1.3558	9.7	41
11.5	48.87	2.9	1.183	10.5	37
12.5	43.62	3.1	1.0642	11.5	33.5
13.5	39.23	3.3	0.96169	12.5	22
14.5	35.54	3.5	0.79898	13.5	18
15.5	32.44	3.7	0.69711	14.1	15.52
16.5	29.84	3.9	0.62563	15.3	12.21
17.5	27.64	4.1	0.58301	16.3	11.87
18.5	25.73	4.3	0.54822	17.2	8.64
19.5	24.04	4.5	0.45674	18.6	6.22
20.5	22.53	4.7	0.4613	19.5	5.12
21.5	21.17	4.9	0.40755	20.5	4.81
22.5	19.98	5.1	0.32542	21.5	3.13
23.5	18.92	5.3	0.26228	22.5	2.11
24.5	18	5.5	0.23564	23.5	1.22
25.5	17.16	5.7	0.23733	24.5	1.1
26.5	16.4	5.9	0.22072	25.5	0.96
27.5	15.7	6.1	0.18593	26.5	0.9107
28.5	15.03	6.3	0.17115	27.5	0.8294
29.5	14.42	6.5	0.16769	28.5	0.7937
30.5	13.86	6.7	0.17152	29.5	0.725
32.5	12.76	7.1	0.13574	31.5	0.603
34.5	11.78	7.5	0.11292	33.5	0.4908
36.5	10.7	7.9	0.088849	35.5	0.2888
38.5	9.698	8.3	0.075772	37.5	0.1856
40.5	8.446	8.7	0.069027	39.5	0.0879
42.5	7.164			41.5	0.075033

44.5	5.525			43.5	0.063726
46.5	3.653			45.5	0.056838
48.5	1.392			47.5	0.041121
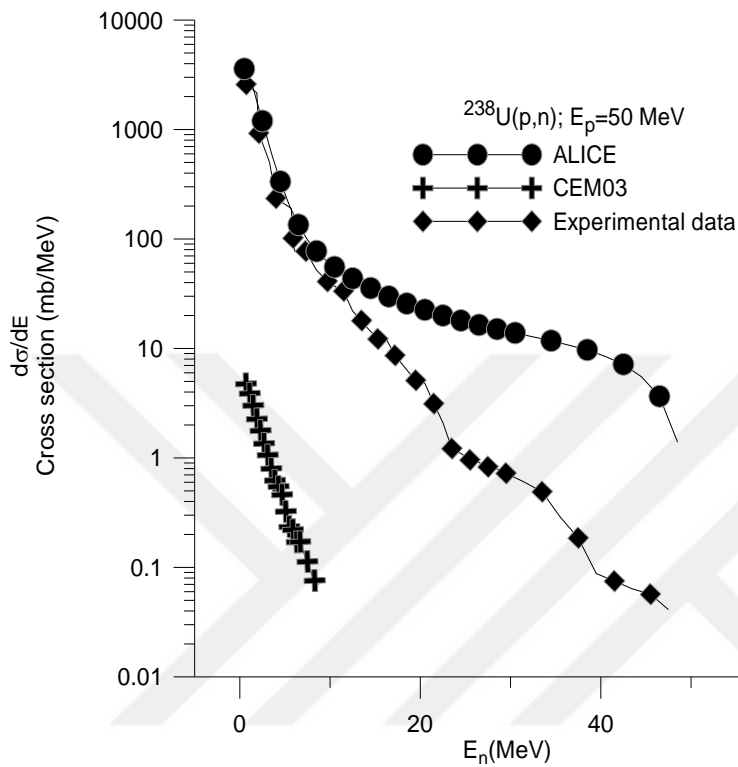
Figure 4.1. Energy spectra $d\sigma/dE$ of neutrons when bombarded $_{92}U^{238}$ element by protons with 50 MeV energy

4.1.2. Proton Energy Spectra (dσ/dE) for p + $_{92}U^{238}$ Reaction at E_p=50 MeV

Figure 4.2. Shows a comparison of ALICE and CEM03 results for the energy spectra $(\frac{d\sigma}{dE})$ of protons when $_{92}U^{238}$ element is bombarded by protons at 50 MeV. The figure shows the less difference energy spectra at both programs. Because the difference between ALICE and CEM03 data is very low and they are close to each other, we can say the data collected by both programs are consistent to each other.

Table 4.2. Show the numerical results of $\frac{d\sigma}{dE}$ both for ALICE and CEM03 programs. As can be seen in the table, the maximum $\frac{d\sigma}{dE}$ at CEM03 is equal to 21.93 mb/MeV while E_p =21 MeV. The maximum $\frac{d\sigma}{dE}$ at ALICE is equal to 20.96 mb/MeV while E_p =20.5 MeV.

Table 4.2. Proton energy spectra for p + $_{92}$U^{238} reaction, E$_p$=50 MeV, Calculations have been made by ALICE and CEM03 programs

ALICE /ASH		CEM03	
E$_p$ (MeV)	dσ/dE (mb/MeV)	E$_p$ (MeV)	dσ/dE (mb/MeV)
6.5	0.02803	6	0.2089
7.5	0.1615	8	0.2089
8.5	0.6329	9	4.595
9.5	1.811	10	8.772
10.5	3.951	11	13.78
11.5	6.906	12	16.29
12.5	10.22	13	15.04
13.5	13.39	14	14.41
14.5	16.01	15	19.63
15.5	17.93	16	20.89
16.5	19.23	17	18.8
17.5	20.09	18	19.01
18.5	20.61	19	15.46
19.5	20.89	20	20.05
20.5	20.96	21	21.93
21.5	20.91	22	16.92
22.5	20.79	24	19.63
23.5	20.6	26	16.6
24.5	20.37	28	19.01
25.5	20.08	30	14.83
26.5	19.77	32	15.66
27.5	19.41	34	12.95
28.5	19.06	36	13.47
29.5	18.73	38	13.99
30.5	18.35	40	9.399
31.5	17.92	42	9.503
32.5	17.48	44	8.145
33.5	17.04	46	5.744
34.5	16.48	48	3.551
35.5	15.9	50	1.253
40.5	12.37		

45.5	6.498		
47.5	3.152		
48.5	1.221		
49.5	0.000024		
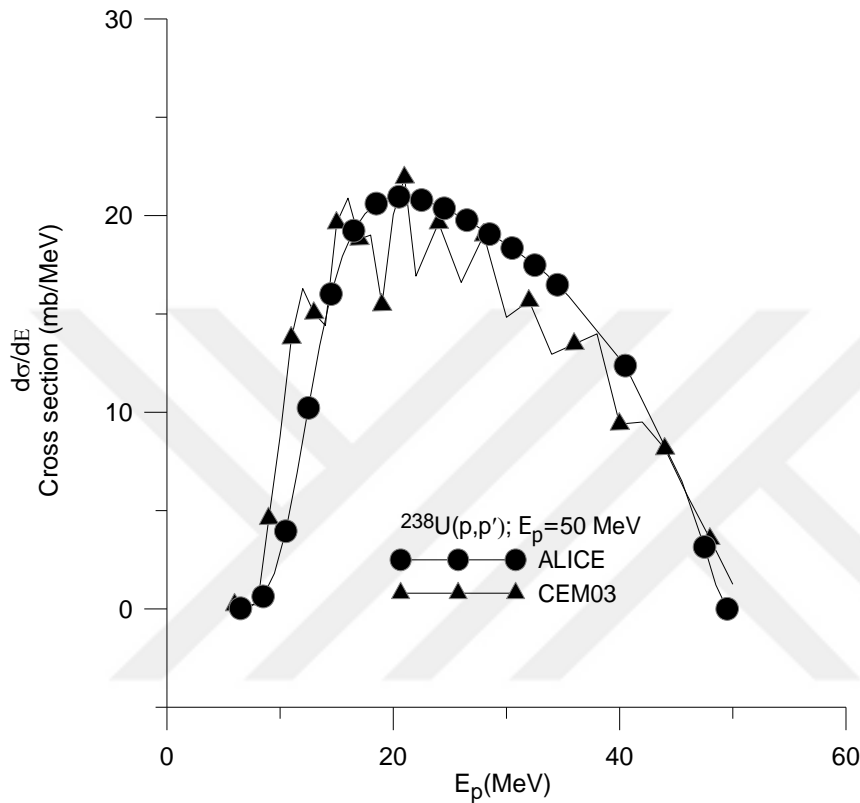
Figure 4.2. Energy spectra $\frac{d\sigma}{dE}$ of protons when bombarded $_{92}U^{238}$ element by protons with 50 MeV energy

4.1.3. Deuteron Energy Spectra (dσ/dE) for p + $_{92}U^{238}$ Reaction at E_p=50 MeV

Figure 4.3. Shows a comparison of ALICE and CEM03 results for the energy spectra ($\frac{d\sigma}{dE}$) of deuterons when $_{92}U^{238}$ element is bombarded by protons at 50 MeV. The figure shows the many difference energy spectra at both programs, therefore CEM03 data's is a more than the ALICE just two points is less and one points is communion between there.

Table 4.3. Shows the numerical results of $\frac{d\sigma}{dE}$ both are ALICE and CEM03 programs. As can be seen in the table, the maximum $\frac{d\sigma}{dE}$ at CEM03 =5.639 mb/MeV while E_d =16 MeV. The maximum $\frac{d\sigma}{dE}$ at ALICE =2.377 mb/MeV while E_d =40.5 MeV.

Table 4.3. Deuteron energy spectra for p + $_{92}U^{238}$ reaction, E_p=50 MeV, Calculations have been made by ALICE and CEM03 programs

ALICE/ASH		CEM03	
E_d (MeV)	dσ/dE (mb/MeV)	E_d (MeV)	dσ/dE (mb/MeV)
6.5	0.0001696	5	0.6266
7.5	0.001741	8	0.2089
8.5	0.01114	9	0.8354
9.5	0.05024	10	0.6266
10.5	0.1637	11	0.6266
11.5	0.3812	12	3.551
12.5	0.6622	13	2.924
13.5	0.942	14	4.595
14.5	1.185	15	5.013
15.5	1.382	16	5.639
16.5	1.532	17	2.924
17.5	1.642	18	5.43
18.5	1.718	19	3.342
19.5	1.765	20	4.177
20.5	1.794	21	2.506
21.5	1.816	22	2.924
22.5	1.839	24	3.968
23.5	1.851	26	2.611
24.5	1.854	28	2.402
25.5	1.85	30	2.611
26.5	1.839	32	1.775
27.5	1.823	34	1.775
28.5	1.805	36	1.253
29.5	1.784	38	1.149
30.5	1.762	40	1.358
31.5	1.744	42	1.775
32.5	1.733	44	1.671
33.5	1.737	46	0.6266
34.5	1.766		
35.5	1.826		
36.5	1.922		
37.5	2.047		

38.5	2.184		
39.5	2.304		
40.5	2.377		
41.5	2.234		
42.5	1.873		
43.5	1.45		
45.5	0.5333		
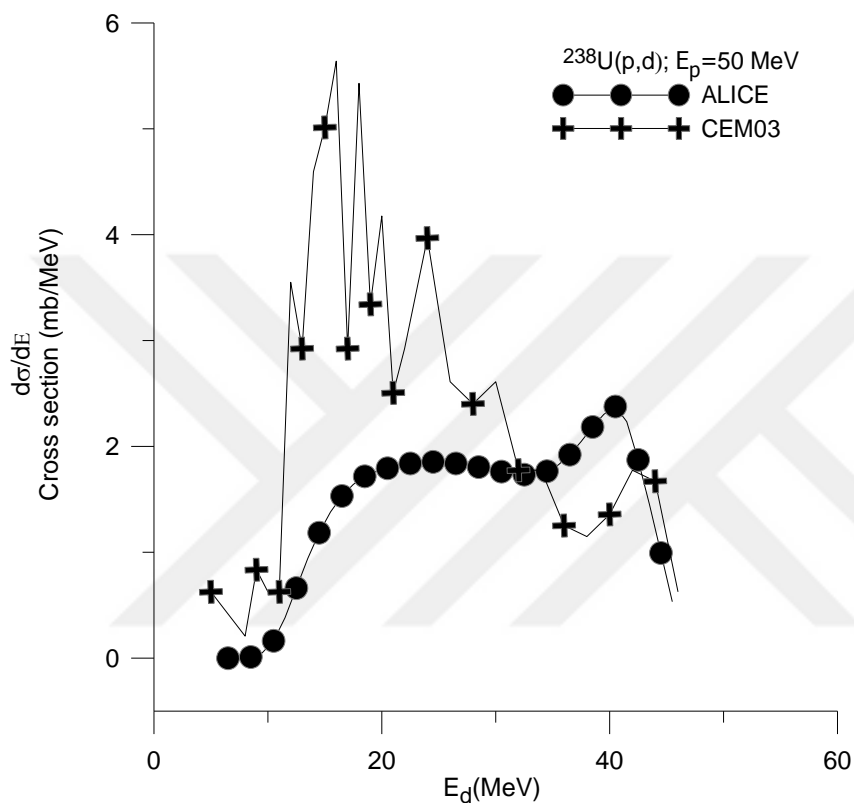
Figure 4.3. Energy spectra $\frac{d\sigma}{dE}$ of deuteron when bombarded $_{92}U^{238}$ element by protons with 50 MeV energy

4.1.4. Alpha Energy Spectra (dσ/dE) for p + $_{92}U^{238}$ Reaction at E_p=50 MeV

Figure 4.4. Shows a comparison of ALICE, CEM03 and Experimental data results for the energy spectra ($\frac{d\sigma}{dE}$) of alphas when $_{92}U^{238}$ element is bombarded by protons at 50 MeV. The figure shows the many difference energy spectra at each program. When ALICE data's is less than each CEM03 and Experimental data, therefore CEM03 and Experimental data shows a biggest data in figure than the ALICE.

Table 4.4. Shows the numerical results of $\frac{d\sigma}{dE}$ both for ALICE, CEM03 and Experimental data's. As can be seen in the table, the maximum $\frac{d\sigma}{dE}$ at Experimental data =1.866 mb/MeV while $E_{4_{He}}$ =26 MeV, maximum $\frac{d\sigma}{dE}$ at CEM03 =1.775 mb/MeV while $E_{4_{He}}$ =30 MeV, and ALICE/ASH =1.114 while $E_{4_{He}}$ =27.5 MeV.

Table 4.4. Alpha energy spectra for p + $_{92}U^{238}$ reaction, E_p=50 MeV, Calculations have been made by ALICE, CEM03 programs and experimental data taken from EXFOR

ALICE/ASH		CEM03		Experimental Data (Conf.nucl.data 2007)	
E_α (MeV)	dσ/dE (mb/MeV)	E_α (MeV)	dσ/dE (mb/MeV)	E_α (MeV)	dσ/dE (mb/MeV)
15.5	0.007955	11	0.2089	9	0.4089
16.5	0.01767	13	0.2089	9.5	0.406
17.5	0.03452	18	0.2089	10	0.56
18.5	0.06234	21	0.6266	15	0.7266
19.5	0.1092	22	0.4177	22	0.8177
20.5	0.1909	24	1.253	24	1.853
21.5	0.3291	26	1.566	26	1.866
22.5	0.5298	28	1.773	28	1.8
23.5	0.754	30	1.775	30	1.82
24.5	0.941	32	0.9399	32	0.88
25.5	1.06	34	0.8354	34	0.82
26.5	1.112	36	0.731	36	0.79
27.5	1.114	38	1.044	38	1.003
28.5	1.098	40	0.3133	40	0.45
29.5	1.061	42	0.2089	42	0.4
30.5	1.01	46	0.3133	46	0.37
32.5	0.8845	50	0.2089	47	0.28
34.5	0.751	56	0.1044	47.5	0.2003
36.5	0.6236				
38.5	0.5083				
40.5	0.4175				
42.5	0.3409				
44.5	0.274				
46.5	0.2158				
50.5	0.123				
54.5	0.06303				
58.5	0.01725				

Figure 4.4. Energy spectra $^{d\sigma}/_{dE}$ of alpha when bombarded $_{92}U^{238}$ element by protons with 50 MeV energy

4.1.5. Neutron Energy Spectra (dσ/dE) for p + $_{92}U^{238}$ Reaction at E_p=110 MeV

Figure 4.5. Shows a comparison of ALICE and CEM03 results for the energy spectra $(\frac{d\sigma}{dE})$ of neutrons when $_{92}U^{238}$ element is bombarded by protons at 110 MeV. The figure shows the less difference energy spectra at both programs. Because the difference between ALICE and CEM03 data is very low and they are close to each other, we can say the data collected by both programs are consistent to each other.

Table 4.5. Shows the numerical results of $\frac{d\sigma}{dE}$ both are ALICE and CEM03 programs. As can be seen in the table, the maximum $\frac{d\sigma}{dE}$ at CEM03 =3867 mb/MeV while E_n =2 MeV. The maximum $\frac{d\sigma}{dE}$ at ALICE =3653 mb/MeV while E_n =0.5 MeV.

Table 4.5. Neutron energy spectra for p + $_{92}U^{238}$ reaction, E_p=110 MeV, Calculations have been made by ALICE and CEM03 programs

ALICE/ASH		CEM03	
E_n (MeV)	$d\sigma/dE$ (mb/MeV)	E_n (MeV)	$d\sigma/dE$ (mb/MeV)
0.5	3653	1	3467
1.5	2850	2	3867
2.5	1688	3	2910
3.5	981.8	4	1977
4.5	600.5	5	1250
5.5	385.6	6	798.1
6.5	260	7	514.7
7.5	182.4	8	333.7
8.5	132.9	9	232.8
9.5	100.9	10	162.6
10.5	79.66	11	127.8
11.5	64.83	12	96.58
12.5	54	13	82
13.5	45.86	14	67.42
14.5	39.68	15	55.07
15.5	34.97	16	52.44
16.5	31.35	17	46.77
17.5	28.53	18	42.92
18.5	26.26	19	38.47
19.5	24.4	20	39.48
20.5	22.84	21	33
21.5	21.53	22	32.39
22.5	20.43	24	31.69
23.5	19.5	26	27.64
24.5	18.7	28	27.13
25.5	18.01	30	21.66
26.5	17.38	32	23.08
27.5	16.81	34	19.84
28.5	16.29	36	17.41
29.5	15.81	38	17.31
30.5	15.37	40	16.7
31.5	14.97	42	13.16
32.5	14.6	44	12.55
33.5	14.25	46	13.57
34.5	13.92	48	11.14
35.5	13.61	50	11.54
36.5	13.32	52	10.93
37.5	13.05	54	9.516

38.5	12.79	56	10.02
39.5	12.56	58	8.099
40.5	12.33	60	9.516
41.5	12.12	62	7.694
42.5	11.92	64	5.871
43.5	11.73	66	4.96
44.5	11.56	68	7.592
45.5	11.39	70	6.378
46.5	11.23	72	5.871
47.5	11.09	74	5.669
48.5	10.95	76	5.77
49.5	10.83	78	5.062
50.5	10.71	80	4.454
60.5	9.901	82	4.657
70.5	9.549	84	4.657
80.5	8.557	86	3.543
90.5	6.08	88	3.847
91.5	5.674	90	3.847
92.5	5.264	94	2.936
93.5	4.73	96	3.239
94.5	4.178	98	3.746
95.5	3.511	100	2.025
96.5	2.772	102	2.203
97.5	1.918	104	3.644
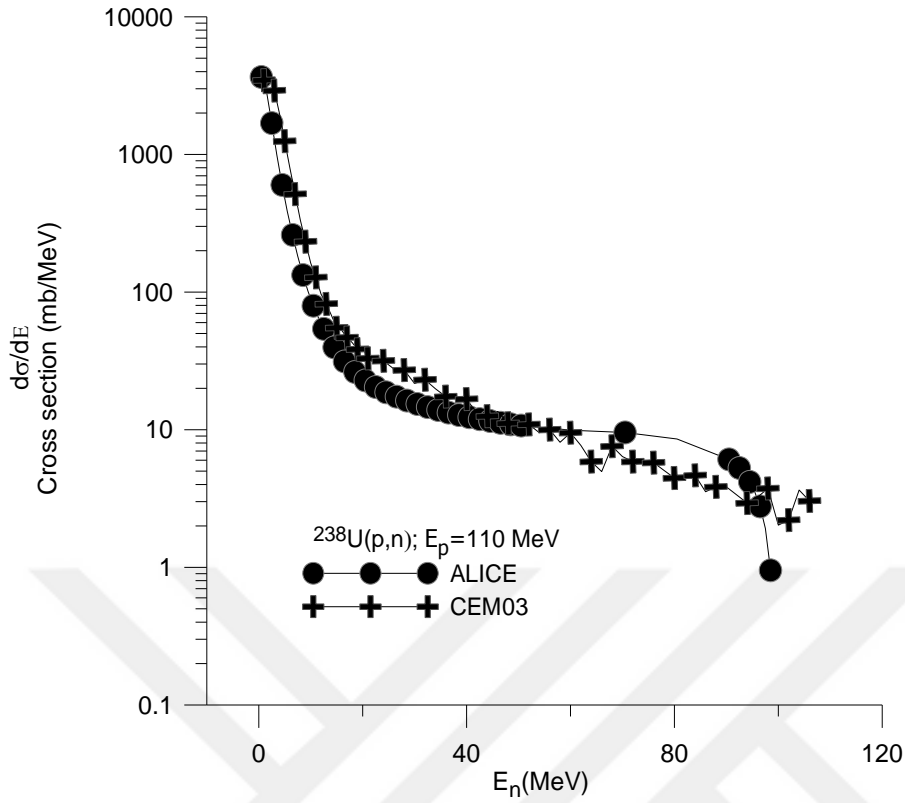
Figure 4.5. Energy spectra $^{d\sigma}/_{dE}$ of neutrons when bombarded $_{92}U^{238}$ element by protons with 110 MeV energy

4.1.6. Proton Energy Spectra (dσ/dE) for p + $_{92}U^{238}$ Reaction at E_p=110 MeV

Figure 4.6. Shows a comparison of ALICE and CEM03 results for the energy spectra ($\frac{d\sigma}{dE}$) of protons when $_{92}U^{238}$ element is bombarded by protons at 110 MeV. The figure shows divided by three parts, firstly both data's are near, and secondly CEM03 more than the ALICE, but thirdly ALICE data's is more than the CEM03.

Table 4.6. Show the numerical results of $\frac{d\sigma}{dE}$ both for ALICE and CEM03 programs. As can be seen in the table, the maximum $\frac{d\sigma}{dE}$ at CEM03 =27.54 mb/MeV while E_p=22 MeV. The maximum $\frac{d\sigma}{dE}$ at ALICE =20.85 mb/MeV while E_p=23.5 MeV.

Table 4.6. Proton energy spectra for p + $_{92}U^{238}$ reaction, at E_p=110 MeV, Calculations have been made by ALICE, CEM03 programs

ALICE/ASH		CEM03	
E_p (MeV)	dσ/dE (mb/MeV)	E_p (MeV)	dσ/dE (mb/MeV)
6.5	0.04369	6	0.8099
7.5	0.2176	7	0.8099
8.5	0.7514	8	0.8099
9.5	1.956	9	4.859
10.5	4.007	10	12.55
11.5	6.746	11	15.18
12.5	9.788	12	17.82
13.5	12.71	13	15.59
14.5	15.17	14	18.83
15.5	17.02	15	24.5
16.5	18.34	16	20.65
17.5	19.28	17	22.27
18.5	19.93	18	23.49
19.5	20.36	19	25.92
20.5	20.62	20	20.65
21.5	20.75	21	25.51
23.5	20.85	22	27.54
24.5	20.82	24	21.06
25.5	20.73	26	21.36
26.5	20.6	28	20.75
27.5	20.46	30	19.64
28.5	20.32	32	18.63
30.5	20.06	34	20.35
31.5	19.91	36	15.49
32.5	19.73	38	18.12
33.5	19.54	40	16.2
34.5	19.35	42	14.27
35.5	19.19	44	11.64
36.5	19.04	46	15.29
37.5	18.92	48	13.16
38.5	18.79	50	11.95
39.5	18.65	52	11.14
40.5	18.51	54	11.34
41.5	18.35	56	11.03
42.5	18.21	58	11.74
43.5	18.07	60	9.415
44.5	17.95	62	10.02
45.5	17.85	64	10.22

46.5	17.75	66	9.01
47.5	17.65	68	7.289
48.5	17.55	70	7.086
49.5	17.45	72	8.807
50.5	17.37	74	9.82
51.5	17.29	76	8.099
52.5	17.22	78	6.479
53.5	17.16	80	6.884
54.5	17.1	82	7.491
55.5	17.04	84	5.973
56.5	16.98	86	7.997
57.5	16.93	88	6.479
58.5	16.88	90	5.77
59.5	16.85	92	7.188
60.5	16.82	94	7.289
70.5	16.63	96	5.467
80.5	14.91	98	6.175
90.5	10.24	100	4.859
91.5	9.505	102	4.859
92.5	8.674	104	3.138
93.5	7.701	106	3.239
94.5	6.647	108	1.215
95.5	5.441		
96.5	4.055		
97.5	2.466		
98.5	0.7215		
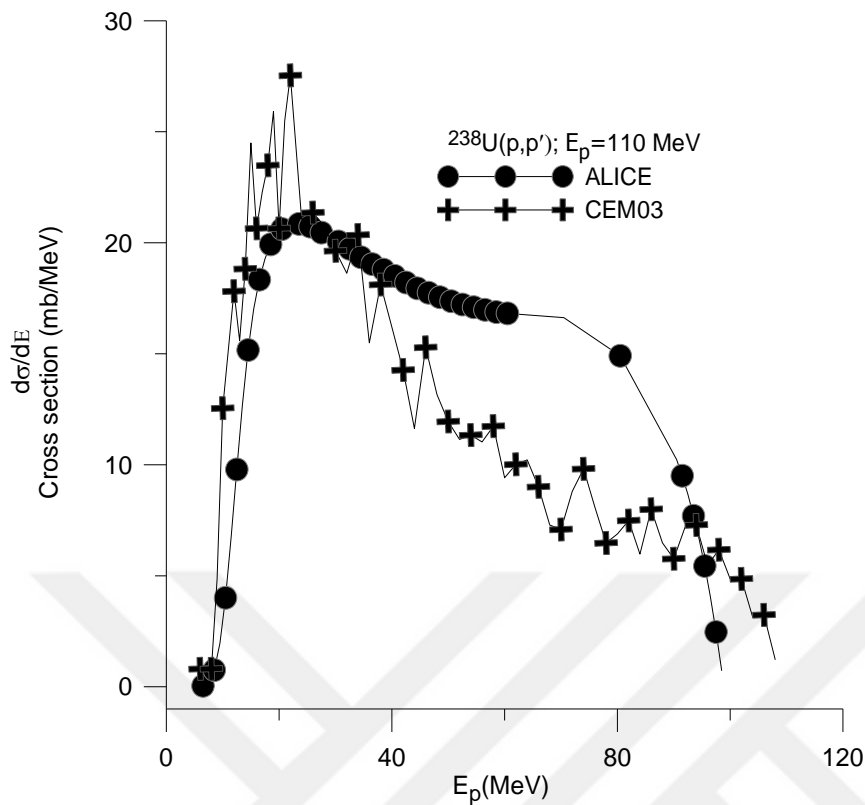
Figure 4.6. Energy spectra $^{d\sigma}/_{dE}$ of protons when bombarded $_{92}U^{238}$ element by protons with 110 MeV energy

4.1.7. Deuteron Energy Spectra (dσ/dE) for p + $_{92}U^{238}$ Reaction at E_p=110 MeV

Figure 4.7. Shows a comparison of ALICE and CEM03 results for the energy spectra $(\frac{d\sigma}{dE})$ of deuterons when $_{92}U^{238}$ element is bombarded by protons at 110 MeV. The figure shows the many difference energy spectra at both programs; firstly CEM03 data's is a more than the ALICE but after this turned is inversely.

Table 4.7. Shows the numerical results of $\frac{d\sigma}{dE}$ both for ALICE and CEM03 programs. As can be seen in the table, the maximum $\frac{d\sigma}{dE}$ at CEM03 =5.467 mb/MeV while E_d =20 MeV. The maximum $\frac{d\sigma}{dE}$ at ALICE =2.956 mb/MeV while E_d =90.5 MeV.

Table 4.7. Deuteron energy spectra for $p + {}_{92}U^{238}$ reaction, at E_p=110 MeV, Calculations have been made by ALICE and CEM03 programs

ALICE/ASH		CEM03	
E_d (MeV)	$d\sigma/dE$ (mb/MeV)	E_d (MeV)	$d\sigma/dE$ (mb/MeV)
6.5	0.001317	2	0.4049
8.5	0.08224	4	0.2025
10.5	0.8317	6	0.6074
12.5	2.16	8	0.4049
14.5	2.563	10	1.417
16.5	2.336	12	4.049
18.5	1.997	14	2.835
20.5	1.729	16	4.657
22.5	1.582	18	4.252
24.5	1.508	20	5.467
26.5	1.462	22	4.657
28.5	1.423	26	4.758
30.5	1.382	30	2.632
32.5	1.338	34	3.239
34.5	1.289	38	1.923
36.5	1.238	42	2.328
38.5	1.188	46	1.215
40.5	1.14	50	0.6074
42.5	1.094	54	1.316
44.5	1.054	58	0.4049
46.5	1.02	62	0.4049
48.5	0.9912	66	0.9111
50.5	0.9699	70	0.2025
60.5	0.9443	72	0.7086
70.5	0.9492	74	0.3037
80.5	0.9566	76	0.3037
90.5	2.956	80	0.2025
91.5	2.8	82	0.1012
92.5	2.402	84	0.1012
93.5	1.891	86	0.1012
94.5	1.338	96	0.3037
95.5	0.8079	98	0.1012
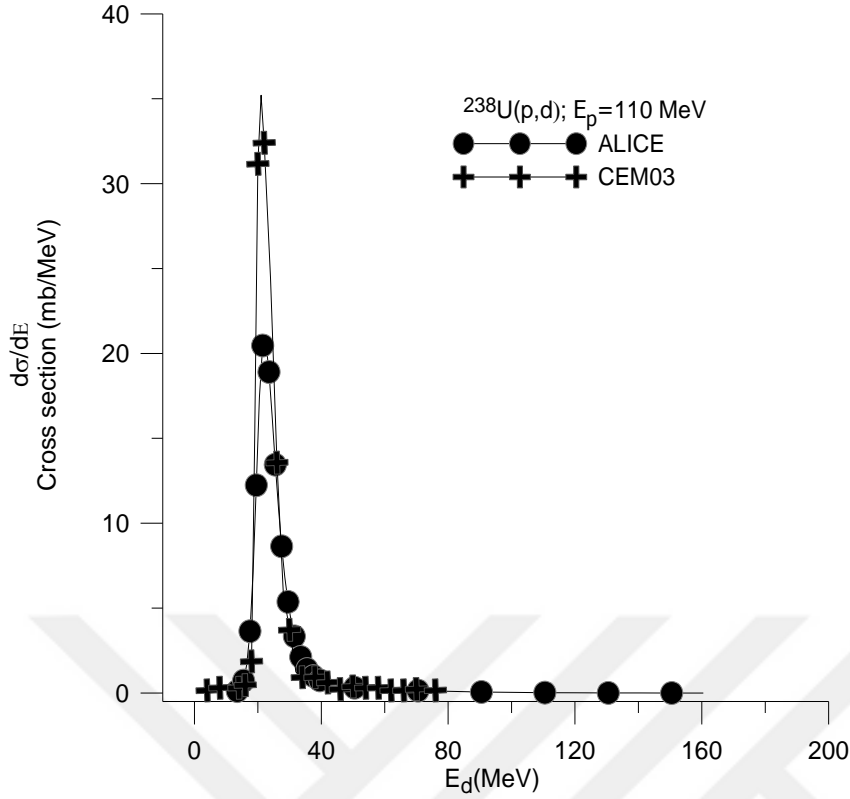
Figure 4.7. Energy spectra $d\sigma/dE$ of deuterons when bombarded $_{92}U^{238}$ element by protons with 110 MeV energy

4.1.8. Alpha Energy Spectra (dσ/dE) for p + $_{92}U^{238}$ Reaction at E_p=110 MeV

Figure 4.8. Shows a comparison of ALICE and CEM03 results for the energy spectra $(\frac{d\sigma}{dE})$ of alphas when $_{92}U^{238}$ element is bombarded by protons at 110 MeV. The figure shows less difference energy spectra at both programs, therefor energy cross sections at ALICE is more in $E_{4_{He}}$ =18.5 MeV unless to $E_{4_{He}}$ =60.5 MeV, and each other energies are less than the CEM03.

Table 4.8. Shows the numerical results of $\frac{d\sigma}{dE}$ are for ALICE and CEM03 programs. As can be seen in the table, the maximum $\frac{d\sigma}{dE}$ at ALICE/ASH =3.519 mb/MeV while $E_{4_{He}}$=25.5 MeV. The maximum $\frac{d\sigma}{dE}$ at CEM03 =2.025 mb/MeV while $E_{4_{He}}$=32 MeV.

Table 4.8. Alpha energy spectra for $p + {}_{92}U^{238}$ reaction, at E_p=110 MeV, Calculations have been made by ALICE and CEM03 programs

ALICE/ASH		CEM03	
E_α (MeV)	dσ/dE (mb/MeV)	E_α (MeV)	dσ/dE (mb/MeV)
15.5	0.02054	4	0.2025
16.5	0.05148	7	0.2025
17.5	0.1142	8	0.2025
18.5	0.2331	9	0.2025
19.5	0.4506	10	0.6074
20.5	0.8306	12	0.4049
21.5	1.43	13	0.2025
22.5	2.199	14	0.2025
23.5	2.919	16	0.2025
24.5	3.371	17	0.2025
25.5	3.519	20	0.6074
26.5	3.445	21	1.215
27.5	3.248	22	1.822
28.5	3.016	24	1.417
29.5	2.767	26	1.62
30.5	2.521	28	1.114
31.5	2.287	30	1.417
32.5	2.071	32	2.025
33.5	1.875	34	1.518
35.5	1.541	36	0.8099
36.5	1.4	38	0.8099
37.5	1.273	40	0.9111
38.5	1.16	50	0.1012
39.5	1.065	60	0.1012
40.5	0.9856	70	0.2025
50.5	0.4452	76	0.1012
60.5	0.2475	80	0.2025
70.5	0.1237	82	0.2025
80.5	0.0553	84	0.1012
90.5	0.02266		
100.5	0.00662		
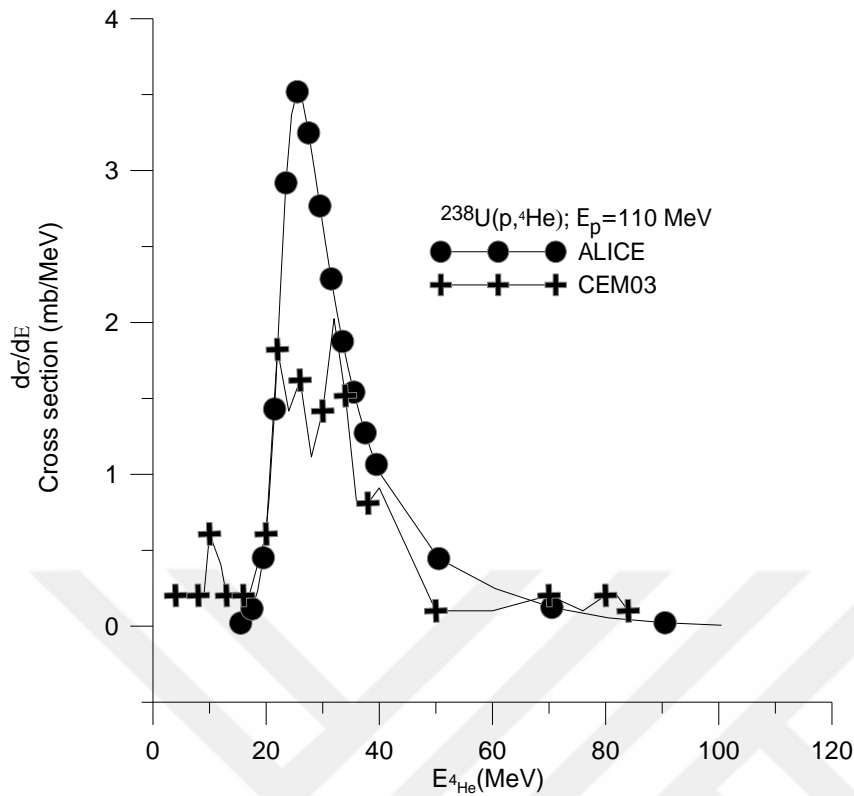
Figure 4.8. Energy spectra $d\sigma/dE$ of alphas when bombarded $_{92}U^{238}$ element by protons with 110 MeV energy

4.1.9. Neutron Energy Spectra (dσ/dE) for p + $_{92}U^{238}$ Reaction at E_p=190 MeV

Figure 4.9. Shows a comparison of ALICE and CEM03 results for the energy spectra $(\frac{d\sigma}{dE})$ of neutrons when $_{92}U^{238}$ element is bombarded by protons at 190 MeV. The figure shows the many difference energy spectra at both programs, therefore CEM03 at E_n=1 MeV unless E_n=78 MeV has more energies cross section than the ALICE but another is less.

Table 4.9. Shows the numerical results of $\frac{d\sigma}{dE}$ both are ALICE and CEM03 programs. As can be seen in the table, the maximum $\frac{d\sigma}{dE}$ at CEM03 =4086 mb/MeV while E_n =2 MeV. The maximum $\frac{d\sigma}{dE}$ at ALICE =2732 mb/MeV while E_n =0.5 MeV.

Table 4.9. Neutron energy spectra for p + $_{92}U^{238}$ reaction, E_p=190 MeV, Calculations have been made by ALICE and CEM03 programs

ALICE/ASH		CEM03	
E_n (MeV)	$d\sigma/dE$ (mb/MeV)	E_n (MeV)	$d\sigma/dE$ (mb/MeV)
0.5	2732	1	3396
1.5	2482	2	4086
2.5	1690	3	3250
3.5	1116	4	2322
4.5	761.8	5	1590
5.5	532.2	6	1074
6.5	378.6	7	748.3
7.5	271	8	509.8
8.5	195.1	9	364.2
9.5	142.4	10	275.6
10.5	105.6	11	199.1
11.5	79.5	12	172.7
12.5	60.57	13	136
13.5	46.78	14	118.3
14.5	36.79	15	91.19
15.5	29.59	16	82.84
16.5	24.41	17	88.78
17.5	20.66	18	73.55
18.5	17.92	19	63.15
19.5	15.89	20	62.96
20.5	14.37	21	54.42
21.5	13.25	22	50.89
22.5	12.41	24	48.01
23.5	11.79	26	41.14
24.5	11.33	28	36.12
25.5	10.97	30	30.92
26.5	10.67	32	25.26
27.5	10.43	34	26.93
28.5	10.22	36	22.19
29.5	10.04	38	22.01
30.5	9.883	40	19.04
31.5	9.742	42	20.52
32.5	9.611	44	19.13
33.5	9.487	46	14.58
34.5	9.367	48	14.49
35.5	9.25	50	13.28
36.5	9.137	52	10.59
37.5	9.029	54	12.26

|			
38.5	8.925	56	11.33
39.5	8.826	58	10.59
40.5	8.728	60	9.101
41.5	8.633	62	10.12
42.5	8.539	64	10.4
43.5	8.445	66	9.194
44.5	8.354	68	6.408
45.5	8.265	70	7.986
46.5	8.178	72	7.986
47.5	8.093	76	7.522
48.5	8.011	78	6.222
49.5	7.93	80	5.943
50.5	7.851	84	5.015
60.5	7.143	86	6.036
70.5	6.579	90	4.55
80.5	6.14	92	4.736
90.5	5.815	94	5.293
100.5	5.631	98	4.643
110.5	5.511	100	5.293
120.5	5.444	102	4.179
130.5	5.42	106	2.6
140.5	5.432	110	3.993
150.5	5.228	112	3.343
160.5	4.272	118	3.25
170.5	1.917	120	3.993
171.5	1.468	130	3.455
172.5	0.9296	140	2.823
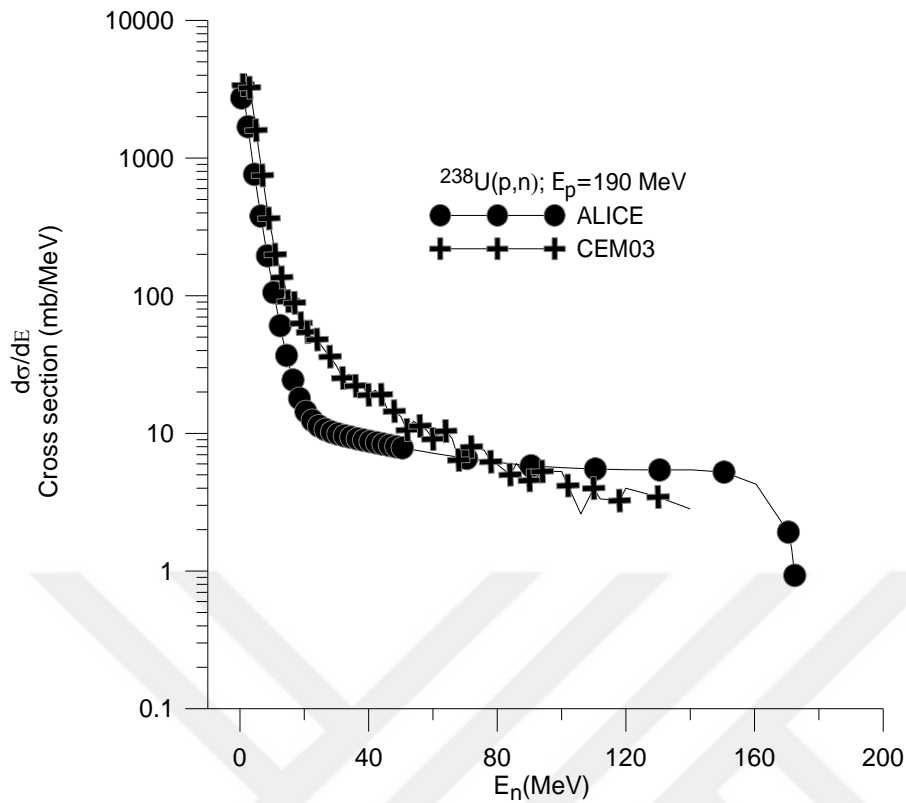
Figure 4.9. Energy spectra $\frac{d\sigma}{dE}$ of neutron when bombarded $_{92}U^{238}$ element by protons with 190 MeV energy

4.1.10. Proton Energy Spectra (dσ/dE) for p + $_{92}U^{238}$ Reaction at E_p=190 MeV

Figure 4.10. Shows a comparison of ALICE and CEM03 results for the energy spectra $(\frac{d\sigma}{dE})$ of protons when $_{92}U^{238}$ element is bombarded by protons at 190 MeV. The figure shows divided by three parts, firstly both data's are near, and secondly CEM03 more than the ALICE, but thirdly ALICE data's is more than the CEM03.

Table 4.10. Shows the numerical results of $\frac{d\sigma}{dE}$ both are ALICE and CEM03 programs. As can be seen in the table, the maximum $\frac{d\sigma}{dE}$ at CEM03 =26.93 mb/MeV while E_p=16 MeV. The maximum $\frac{d\sigma}{dE}$ at ALICE =13.42 mb/MeV while E_p=40.5 MeV.

Table 4.10. Proton energy spectra for p + $_{92}U^{238}$ reaction, E_p=190 MeV, Calculations have been made by ALICE and CEM03 programs

ALICE/ASH		CEM03	
E_p (MeV)	dσ/dE (mb/MeV)	E_p (MeV)	dσ/dE (mb/MeV)
6.5	0.04908	3	0.3715
7.5	0.2544	4	0.7429
8.5	0.8683	5	1.857
9.5	2.148	6	1.672
10.5	4.09	7	1.857
11.5	6.341	8	1.486
12.5	8.48	9	7.058
13.5	10.21	10	16.72
14.5	11.4	11	22.29
15.5	12.08	12	25.07
16.5	12.43	13	26.75
17.5	12.6	14	26.56
18.5	12.69	15	23.4
19.5	12.74	16	26.93
20.5	12.78	17	25.63
30.5	13.4	18	25.44
40.5	13.42	20	20.8
50.5	12.95	22	21.73
60.5	12.35	24	20.71
70.5	11.76	26	20.52
80.5	11.26	28	18.39
90.5	10.85	30	16.25
100.5	10.59	32	14.86
110.5	10.43	34	16.62
120.5	10.34	36	13.56
130.5	10.32	38	12.17
140.5	10.36	40	14.21
150.5	9.879	42	8.822
160.5	7.893	44	12.72
170.5	3.124	46	9.286
171.5	2.223	48	9.937
172.5	1.157	50	9.194
173.5	0.06012	60	6.965
		70	7.429
		80	4.736
		90	4.829
		100	5.2
		110	4.272
		120	5.572
		130	3.993

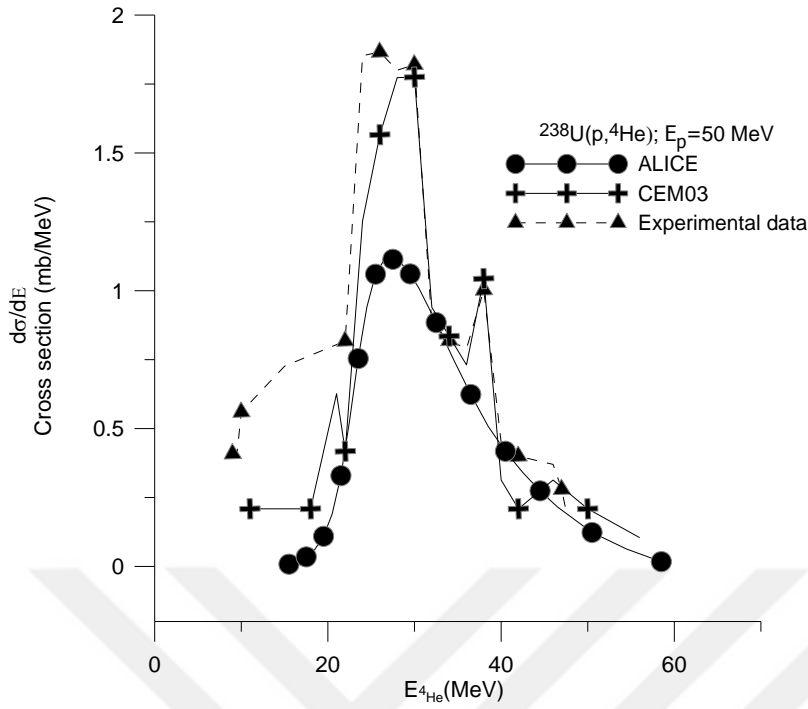|		140	4.216
		150	4.29
		160	3.9
		170	4.03
		180	3.715
		190	1.95
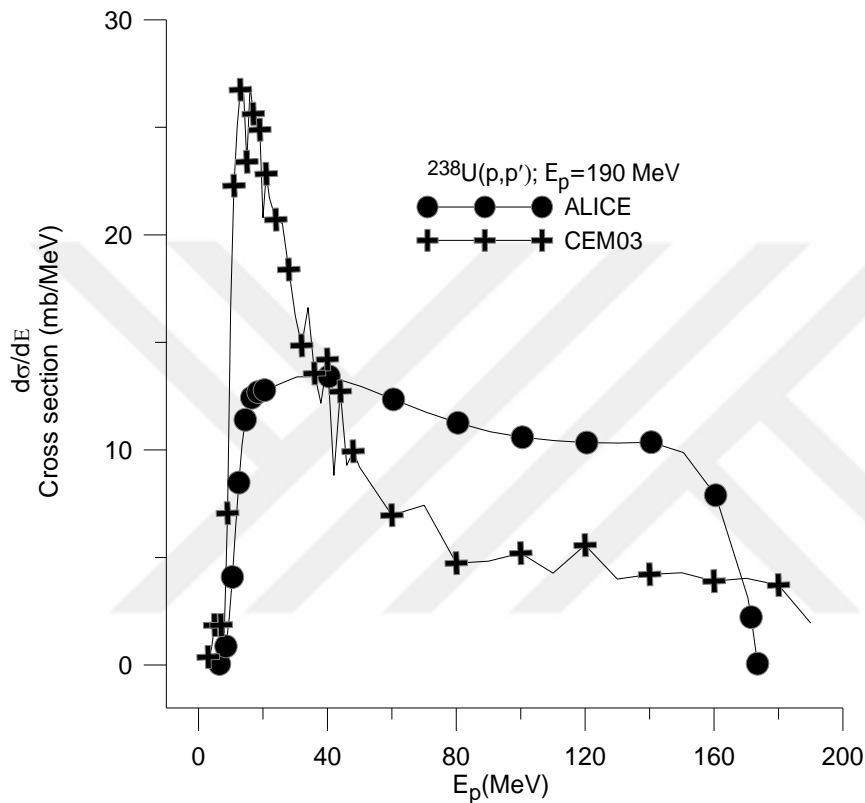
Figure 4.10. Energy spectra $d\sigma/dE$ of protons when bombarded $_{92}U^{238}$ element by protons with 190 MeV energy

4.1.11. Deuteron Energy Spectra (dσ/dE) for p + $_{92}U^{238}$ Reaction at E_p=190 MeV

Figure 4.11. Shows a comparison of ALICE and CEM03 results for the energy spectra $(\frac{d\sigma}{dE})$ of deuterons when $_{92}U^{238}$ element is bombarded by protons at 190 MeV. The figure shows the many difference energy spectra at both programs, therefore CEM03 at E_d=2 MeV unless E_d=70 MeV has more energies cross section than the ALICE and another is less.

Table 4.11. Shows the numerical results of $\frac{d\sigma}{dE}$ both are ALICE and CEM03 programs. As can be seen in the table, the maximum $\frac{d\sigma}{dE}$ at CEM03 =10.4 mb/MeV while E_d =18 MeV. The maximum $\frac{d\sigma}{dE}$ at ALICE =3.997 mb/MeV while E_d =13.5 MeV.

Table 4.11. Deuteron energy spectra for p + $_{92}U^{238}$ reaction, E_p=190 MeV, Calculations have been made by ALICE and CEM03 programs

ALICE/ASH		CEM03	
E_d (MeV)	$d\sigma/dE$ (mb/MeV)	E_d (MeV)	$d\sigma/dE$ (mb/MeV)
6.5	0.002556	2	0.1857
7.5	0.02774	3	0.3715
8.5	0.1637	4	0.5572
9.5	0.6157	5	0.1857
10.5	1.577	6	1.672
11.5	2.812	7	1.672
12.5	3.708	8	1.114
13.5	3.997	9	3.715
14.5	3.819	10	5.2
15.5	3.393	11	4.272
16.5	2.884	12	9.101
17.5	2.389	13	9.472
18.5	1.953	14	7.615
19.5	1.592	15	7.986
20.5	1.304	16	8.729
21.5	1.084	17	10.03
22.5	0.9252	18	10.4
23.5	0.8088	19	8.544
24.5	0.7246	20	6.315
25.5	0.6639	21	6.315
26.5	0.6199	22	7.801
27.5	0.5873	26	7.336
29.5	0.5426	28	5.386
30.5	0.5257	30	5.758
40.5	0.3888	32	4.365
50.5	0.2919	34	2.972

|			
60.5	0.2823	36	3.807
70.5	0.2997	40	2.972
80.5	0.3109	44	2.043
90.5	0.3174	46	1.764
100.5	0.3203	50	1.764
110.5	0.3208	60	0.8358
120.5	0.3192	70	0.4643
130.5	0.3162	80	0.2786
140.5	0.312	90	0.09286
150.5	0.307	94	0.09286
160.5	1.128	98	0.09286
161.5	1.526	106	0.09286
165.5	2.716	112	0.09286
169.5	1.191	130	0.03715
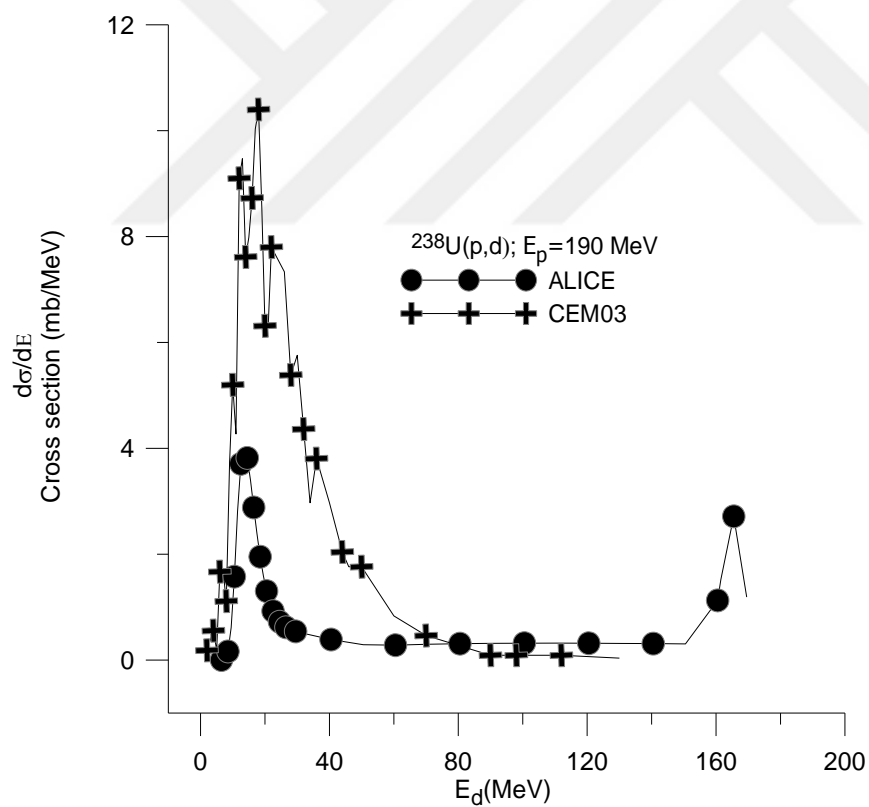
Figure 4.11. Energy spectra $\frac{d\sigma}{dE}$ of deuteron when bombarded $_{92}U^{238}$ element by protons with 190 MeV energy

4.1.12. Alpha Energy Spectra (dσ/dE) for p + $_{92}U^{238}$ Reaction at E_p=190 MeV

Figure 4.12. Shows a comparison of ALICE and CEM03 results for the energy spectra ($\frac{d\sigma}{dE}$) of alphas when $_{92}U^{238}$ element is bombarded by protons at 190 MeV. The figure shows less difference energy spectra at both programs, therefore CEM03 at $E_{4_{He}}$=6 MeV unless $E_{4_{He}}$=18 MeV and $E_{4_{He}}$= 26, 30, 34, 36, 38 MeV unless to final has more energies cross section than the ALICE and another is less.

Table 4.12. Shows the numerical results of $\frac{d\sigma}{dE}$ both are ALICE and CEM03 programs. As can be seen in the table, the maximum $\frac{d\sigma}{dE}$ at CEM03 =6.222 mb/MeV while $E_{4_{He}}$=26 MeV. The maximum $\frac{d\sigma}{dE}$ at ALICE/ASH =5.852 mb/MeV while $E_{4_{He}}$=24.5 MeV.

Table 4.12. Alpha energy spectra for p + $_{92}U^{238}$ reaction, E_p=190 MeV, Calculations have been made by ALICE and CEM03 programs

ALICE/ASH		CEM03	
E_α (MeV)	dσ/dE (mb/MeV)	E_α (MeV)	dσ/dE (mb/MeV)
15.5	0.01768	6	0.1857
16.5	0.05383	7	0.1857
17.5	0.1426	8	0.3715
18.5	0.3393	9	0.5572
19.5	0.7391	10	0.9286
20.5	1.477	11	0.5572
21.5	2.651	12	0.5572
22.5	4.098	13	0.5572
23.5	5.308	14	0.5572
24.5	5.852	15	0.9286
25.5	5.748	16	0.7429
26.5	5.252	17	0.5572
27.5	4.612	18	1.114
28.5	3.982	19	0.5572
29.5	3.417	20	0.5572
30.5	2.936	21	1.486
31.5	2.538	22	3.157

|			
32.5	2.214	24	4.365
33.5	1.951	26	6.222
34.5	1.736	28	3.622
35.5	1.558	30	3.065
36.5	1.409	32	1.95
37.5	1.282	34	2.879
38.5	1.175	36	2.972
39.5	1.089	38	1.672
40.5	1.018	40	1.022
50.5	0.5265	42	1.95
60.5	0.3367	44	1.3
70.5	0.1965	46	1.114
80.5	0.1107	48	0.9286
90.5	0.06298	50	0.8358
100.5	0.0337	52	0.7429
110.5	0.01725	58	0.2786
120.5	0.00847	60	0.4643
130.5	0.003988	66	0.4643
140.5	0.001788	70	0.19686
150.5	0.0007496	80	0.1857
160.5	0.0002838	92	0.1857
170.5	0.000009013	98	0.09286
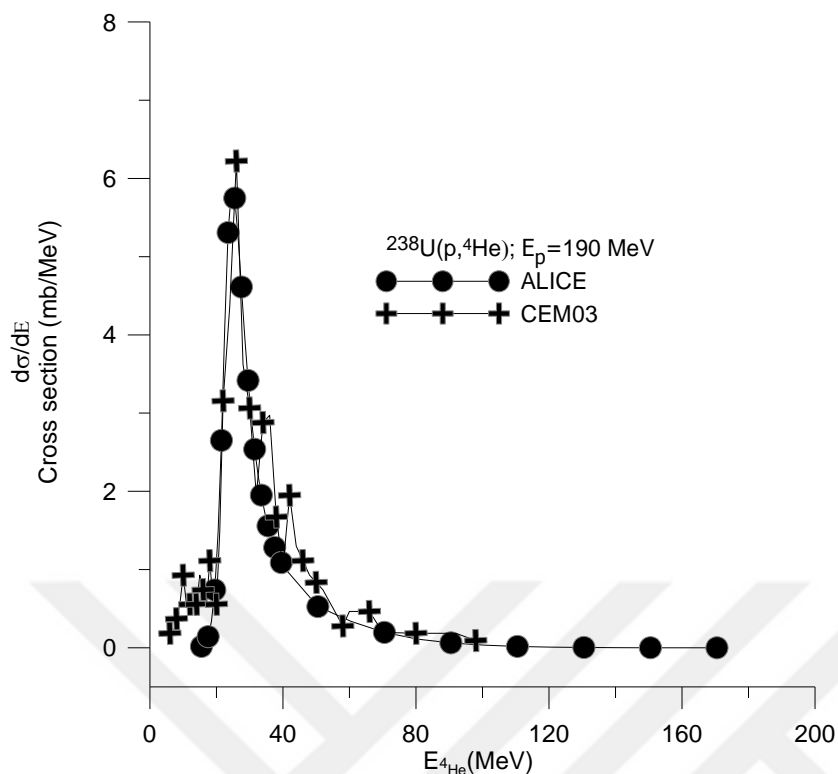
Figure 4.12. Energy spectra $^{d\sigma}/_{dE}$ of alphas when bombarded $_{92}U^{238}$ element by protons with 190 MeV energy

4.1.13. Neutron Energy Spectra (dσ/dE) for p + $_{92}U^{238}$ Reaction at E_p=290 MeV

Figure 4.13. Shows a comparison of ALICE, CEM03 and Experimental data results for the energy spectra ($\frac{d\sigma}{dE}$) of neutrons when $_{92}U^{238}$ element is bombarded by protons at 290 MeV. The figure shows the many difference energy spectra at each program. Consequently this figure shows the difference energy spectra at three data's, therefore CEM03 at E_n =1 MeV unless E_n =190 MeV is more energies cross section than the two data's, and ALICE is more than the Experimental data at E_n =0.5 MeV unless E_n =277.5 MeV.

Table 4.13. Show the numerical results of $\frac{d\sigma}{dE}$ both for ALICE, CEM03 and Experimental data's. As can be seen in the table, the maximum $\frac{d\sigma}{dE}$ at CEM03 =4331 mb/MeV while E_n=2 MeV, maximum $\frac{d\sigma}{dE}$ at ALICE/ASH =1662 mb/MeV while E_n=1.5 MeV, and Experimental data =418.4 while E_n=0.925 MeV.

Table 4.13. Neutron energy spectra for p + $_{92}U^{238}$ reaction, E_p=290 MeV, Calculations have been made by ALICE, CEM03 and Experimental Data from EXFOR

ALICE/ASH		CEM03		Experimental Data (IEEE 1983)	
E_n (MeV)	dσ/dE (mb/MeV)	E_n (MeV)	dσ/dE (mb/MeV)	E_n (MeV)	dσ/dE (mb/MeV)
0.5	1550	1	3442	0.47	248.1
1.5	1662	2	4331	0.49	179.3
2.5	1311	3	3522	0.525	268.7
3.5	976.7	4	2573	0.575	267.4
4.5	733.5	5	1855	0.625	285.3
5.5	552.2	6	1319	0.675	274.7
6.5	415.7	7	911.2	0.725	244.1
7.5	309.9	8	666	0.775	246.9
8.5	229.2	9	502.8	0.825	328.3
9.5	169.7	10	372	0.875	327.6
10.5	126.3	11	286.8	0.925	418.4
11.5	94.29	12	225.3	0.975	368.9
12.5	70.42	13	190.7	1.075	328.1
13.5	52.67	14	158.3	1.15	347.6
14.5	39.63	15	135.4	1.25	384.2
15.5	30.12	16	114.1	1.35	313.9
16.5	23.22	17	96.24	1.45	317.3
17.5	18.2	18	97.83	1.55	332.3
18.5	14.52	19	79.58	1.65	319.5
19.5	11.82	20	72.31	1.75	316.1
20.5	9.84	21	65.58	1.85	308.9
21.5	8.398	22	71.78	1.95	342.5
22.5	7.357	24	55.83	2.1	293.9
23.5	6.611	26	52.55	2.3	347.7
24.5	6.077	28	44.75	2.5	373.3
25.5	5.691	30	39.97	2.7	311
26.5	5.409	32	35.45	2.9	307.6
27.5	5.2	34	34.47	3.1	265
28.5	5.044	36	28.09	3.3	217.3
29.5	4.927	38	27.74	3.5	191
30.5	4.838	40	24.99	3.7	181.9
31.5	4.769	42	20.91	3.9	155.8
33.5	4.669	44	20.2	4.1	150.4
35.5	4.593	46	18.88	4.3	150.9
37.5	4.53	48	20.38	4.5	133.1
39.5	4.477	50	15.86	4.7	135.2
40.5	4.452	52	16.93	4.9	119.5
42.5	4.403	54	14.53	5.25	96.69
43.5	4.378	56	12.58	5.75	89.45

45.5	4.328	58	11.96	6.25	63.96
47.5	4.28	60	12.67	6.75	52.83
49.5	4.232	62	13.2	7.25	41.25
50.5	4.209	64	11.43	7.75	37.28
52.5	4.16	66	11.43	8.25	31.26
54.5	4.112	68	9.305	8.75	23.92
56.5	4.064	70	9.482	9.25	22.35
58.5	4.016	72	8.684	9.75	18.84
60.5	3.968	74	8.153	10.75	15.56
62.5	3.921	76	8.064	11.5	11.81
64.5	3.873	78	7.001	12.5	10.09
66.5	3.826	80	6.115	13.5	8.128
68.5	3.779	82	7.089	14.5	7.79
70.5	3.733	84	7.267	15.5	6.695
72.5	3.687	86	6.735	16.5	7.383
74.5	3.642	88	6.558	17.5	5.931
76.5	3.597	90	6.469	18.5	6.083
78.5	3.553	92	6.558	19.5	5.191
80.5	3.509	94	6.646	21	5.232
82.5	3.466	96	5.937	23	4.664
84.5	3.424	98	6.558	25	3.998
86.5	3.382	100	6.469	27	3.72
88.5	3.341	102	6.469	29	3.176
90.5	3.306	104	4.874	31	3.378
110.5	3.018	106	3.988	33	3.082
130.5	2.783	108	4.697	35	3.137
140.5	2.687	110	4.254	37	3.006
150.5	2.607	112	5.051	39	2.922
160.5	2.54	114	4.076	41	2.704
170.5	2.485	116	3.633	43	2.581
180.5	2.443	118	4.519	45	2.633
190.5	2.411	120	3.899	47	2.517
200.5	2.388	130	3.775	49	2.377
		240	1.382	135	1.264
		250	1.489	145	1.314
		260	1.595	155	1.403
		270	1.648	165	1.559
		280	1.577	175	1.815
		290	1.506	185	2.397
				195	3.39
				210	5.033
				230	4.19
				250	0.7764
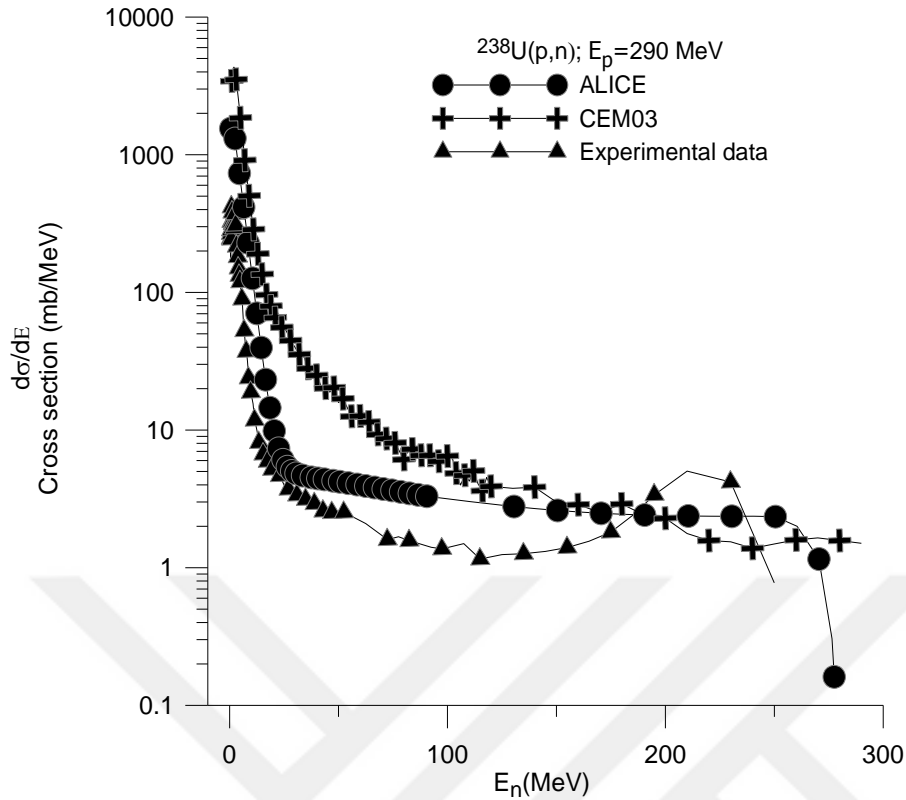
Figure 4.13. Energy spectra $\mathrm{d}\sigma/\mathrm{d}E$ of neutrons when bombarded $_{92}\mathrm{U}^{238}$ element by protons with 290 MeV energy

4.1.14. Proton Energy Spectra (dσ/dE) for p + $_{92}\mathrm{U}^{238}$ Reaction at E_p=290 MeV

Figure 4.14. Shows a comparison of ALICE and CEM03 results for the energy spectra $(\frac{d\sigma}{dE})$ of protons when $_{92}\mathrm{U}^{238}$ element is bombarded by protons at 290 MeV. Consequently this figure shows the difference energy spectra at two programs, therefore CEM03 at E_p=3 MeV unless E_p=66 MeV and E_p =(72, 78, 84) MeV has more than the ALICE energies cross section and another energies are less.

Table 4.14. Show the numerical results of $\frac{d\sigma}{dE}$ both for ALICE and CEM03 programs. As can be seen in the table, the maximum $\frac{d\sigma}{dE}$ at CEM03 =31.02 mb/MeV while E_p=12 MeV. The maximum $\frac{d\sigma}{dE}$ at ALICE =9.891 mb/MeV while E_p=14.5 MeV.

Table 4.14. Proton energy spectra for p + $_{92}U^{238}$ reaction, E_p=290 MeV, Calculations have been made by ALICE and CEM03 programs

ALICE/ASH		CEM03	
E_p (MeV)	dσ/dE (mb/MeV)	E_p (MeV)	dσ/dE (mb/MeV)
6.5	0.04819	3	0.5317
7.5	0.2624	4	1.595
8.5	0.9183	5	2.481
9.5	2.282	6	4.431
10.5	4.285	7	4.608
11.5	6.449	8	3.899
12.5	8.264	9	8.507
13.5	9.433	10	22.15
14.5	9.891	11	25.17
15.5	9.785	12	31.02
16.5	9.363	13	29.24
17.5	8.829	14	29.78
18.5	8.301	15	25.34
19.5	7.828	16	26.23
20.5	7.433	17	30.13
25.5	6.609	18	24.64
30.5	6.678	19	27.47
35.5	6.857	20	24.1
40.5	7.036	21	25.17
45.5	7.102	22	23.93
50.5	7.121	24	23.57
55.5	7.097	26	21.09
60.5	7.025	28	20.91
65.5	6.946	30	17.37
70.5	6.832	32	18.61
75.5	6.72	34	16.04
80.5	6.594	36	14
85.5	6.466	38	15.06
90.5	6.341	40	15.69
95.5	6.228	42	11.96
100.5	6.119	44	11.34
105.5	6.012	46	10.55
110.5	5.909	48	10.63
115.5	5.811	50	10.01
120.5	5.718	52	9.305
125.5	5.63	54	8.773
130.5	5.548	56	7.355
135.5	5.471	58	6.38
140.5	5.4	60	10.28
145.5	5.334	62	8.95

|			
150.5	5.274	64	8.507
155.5	5.219	66	7.621
160.5	5.169	68	6.203
165.5	5.125	70	5.937
170.5	5.085	72	7.355
175.5	5.05	74	5.849
180.5	5.019	76	5.937
185.5	4.992	78	6.646
190.5	4.97	80	5.76
195.5	4.951	82	4.874
200.5	4.935	84	6.824
205.5	4.923	86	5.14
210.5	4.914	88	5.228
215.5	4.907	90	4.874
220.5	4.903	92	4.342
225.5	4.902	94	6.115
230.5	4.902	96	4.342
235.5	4.904	98	5.14
240.5	4.908	100	4.963
245.5	4.914	102	4.342
250.5	4.848	104	5.14
255.5	4.564	106	4.608
260.5	4.055	108	3.456
265.5	3.307	110	5.051
270.5	2.226	112	3.279
275.5	0.7683	114	4.785
276.5	0.4747	116	3.633
277.5	0.1809	118	3.722
		120	3.988
		130	4.342
		140	3.793
		150	3.243
		160	3.403
		170	3.314
		180	3.031
		190	2.871
		200	3.084
		210	2.907
		220	2.623
		230	2.534
		240	2.818
		260	2.659
		280	1.985
		290	1.187
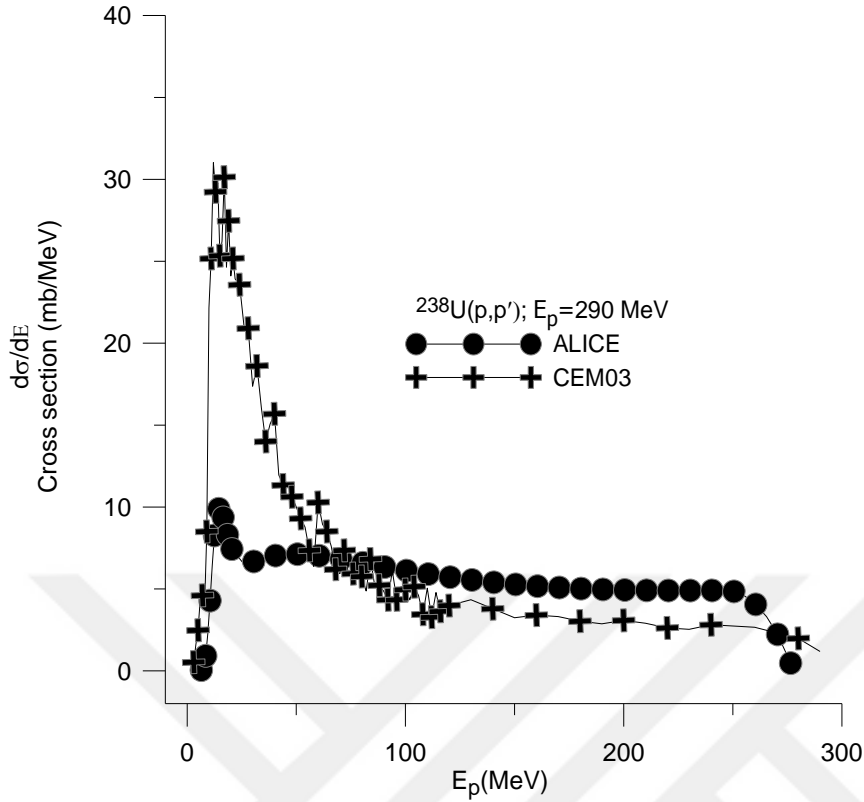
Figure 4.14. Energy spectra $^{d\sigma}/_{dE}$ of protons when bombarded $_{92}U^{238}$ element by protons with 290 MeV energy

4.1.15. Deuteron Energy Spectra (dσ/dE) for p + $_{92}U^{238}$ Reaction at E_p=290 MeV

Figure 4.15. Shows a comparison of ALICE and CEM03 results for the energy spectra ($\frac{d\sigma}{dE}$) of deuterons when $_{92}U^{238}$ element is bombarded by protons at 290 MeV. The figure shows the many difference energy spectra at both programs, therefore CEM03 at E_d=2 MeV unless E_d=130 MeV has more than the ALICE energies cross section and another energies are less.

Table 4.15. Show the numerical results of $\frac{d\sigma}{dE}$ both for ALICE and CEM03 programs. As can be seen in the table, the maximum $\frac{d\sigma}{dE}$ at CEM03 =15.06 mb/MeV while E_d =18 MeV, and maximum $\frac{d\sigma}{dE}$ at ALICE =6.028 mb/MeV while E_d =13.5 MeV.

Table 4.15. Deuteron energy spectra for p + $_{92}U^{238}$ reaction, E_p=290 MeV, Calculations have been made by ALICE and CEM03 programs

ALICE/ASH		CEM03	
E_d (MeV)	dσ/dE (mb/MeV)	E_d (MeV)	dσ/dE (mb/MeV)
6.5	0.003319	2	0.3545
7.5	0.0373	3	1.063
8.5	0.2266	4	1.241
9.5	0.873	5	2.659
10.5	2.283	6	2.659
11.5	4.139	7	3.19
12.5	5.533	8	3.367
13.5	6.028	9	5.671
14.5	5.801	10	6.912
15.5	5.169	11	10.1
16.5	4.383	12	12.94
17.5	3.596	13	11.34
18.5	2.885	14	14.71
19.5	2.28	15	14
20.5	1.784	16	12.58
21.5	1.391	18	15.06
22.5	1.087	20	9.216
23.5	0.8543	22	10.46
24.5	0.6786	24	9.659
25.5	0.5468	26	7.444
26.5	0.4484	28	7.355
27.5	0.375	30	6.292
28.5	0.32	32	7.089
29.5	0.2785	34	6.824
30.5	0.2469	36	5.671
31.5	0.2222	38	5.494
32.5	0.2025	40	4.874
33.5	0.1864	42	2.924
34.5	0.1728	44	3.102
35.5	0.1611	46	2.924
36.5	0.1506	48	2.215
37.5	0.1411	50	1.95
38.5	0.1323	52	2.304
39.5	0.1241	54	1.684
40.5	0.1163	56	1.595
50.5	0.06046	58	1.506
60.5	0.04924	60	0.8862
70.5	0.05359	62	1.329
80.5	0.05689	64	1.418
90.5	0.05934	66	0.4431

100.5	0.06112	68	0.5317
110.5	0.06236	70	0.5317
120.5	0.06317	72	0.3545
130.5	0.0636	74	0.7089
140.5	0.06372	76	0.5317
150.5	0.0636	78	0.5317
160.5	0.06327	80	0.4431
170.5	0.06278	82	0.2659
180.5	0.06216	84	0.5317
190.5	0.06143	86	0.2659
200.5	0.06062	88	0.1772
210.5	0.05976	90	0.1772
220.5	0.05884	92	0.4431
230.5	0.0579	94	0.1772
240.5	0.05693	96	0.08862
254.5	0.0556	98	0.3545
255.5	0.05562	100	0.08862
260.5	0.0909	110	0.08862
270.5	1.96	114	0.08862
274.5	0.7657	116	0.08862
		118	0.1772
		120	0.08862
		130	0.07089
		140	0.05317
		150	0.07089
		160	0.01772
		170	0.03545
		200	0.01772
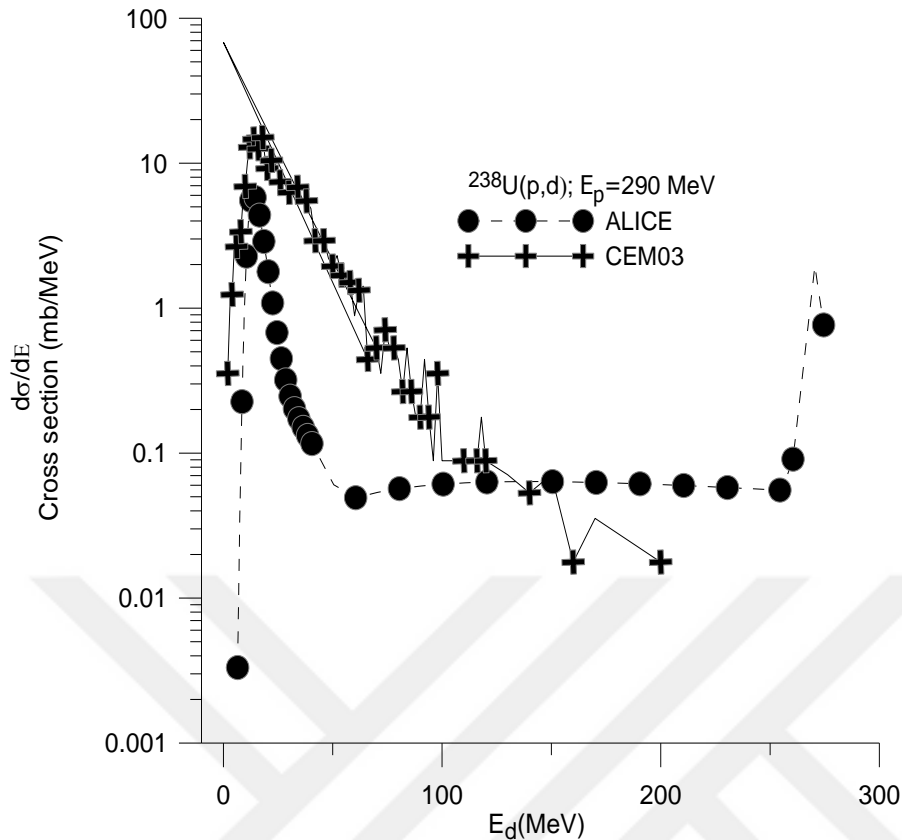
Figure 4.15. Energy spectra $\mathrm{d}\sigma/\mathrm{d}E$ of deuterons when bombarded $_{92}U^{238}$ element by protons with 290 MeV energy

4.1.16. Alpha Energy Spectra (dσ/dE) for p + $_{92}U^{238}$ Reaction at E_p=290 MeV

Figure 4.16. Shows a comparison of ALICE, CEM03 and Experimental data results for the energy spectra ($\frac{d\sigma}{dE}$) of alphas when $_{92}U^{238}$ element is bombarded by protons at 290 MeV. The figure shows the many difference energy spectra at each program. Consequently this figure shows the difference energy spectra at programs, therefore CEM03 at $E_{4_{He}}$=3 MeV unless $E_{4_{He}}$=19 MeV and $E_{4_{He}}$=32, 36, 40, 60, 90 MeV are more than the ALICE and Experimental energies cross section, and ALICE energies cross section is more than the Experimental data's.

Table 4.16. Show the numerical results of $\frac{d\sigma}{dE}$ both for ALICE, CEM03 and Experimental data's. As can be seen in the table, the maximum $\frac{d\sigma}{dE}$ at CEM03 =8.95 mb/MeV while

$E_{4_{He}}$=24 MeV, maximum $\frac{d\sigma}{dE}$ at ALICE/ASH =8.147 mb/MeV while $E_{4_{He}}$=24.5 MeV, and

Experimental data =1.1092 while $E_{4_{He}}$=70 MeV.

Table 4.16. Alpha energy spectra for p + $_{92}U^{238}$ reaction, E_p=290 MeV, Calculations have been made by ALICE, CEM03 and Experimental data at EXFOR

ALICE/ASH		CEM03		Experimental Data (IEEE 1983)	
E_α (MeV)	$d\sigma/dE$ (mb/MeV)	E_α (MeV)	$d\sigma/dE$ (mb/MeV)	E_α (MeV)	$d\sigma/dE$ (mb/MeV)
15.5	0.01414	3	0.5317	70	1.1092
16.5	0.04897	4	0.1772	72.5	1.1036
17.5	0.1441	5	0.1772	74.3	0.962
18.5	0.3731	6	0.5317	77.5	0.89566
19.5	0.8701	7	0.8862	80.3	0.79143
20.5	1.837	8	0.1772	82.5	0.78733
21.5	3.439	9	1.063	84	0.76337
22.5	5.494	10	0.8862	87	0.70955
23.5	7.283	11	1.772	89.2	0.67586
24.5	8.147	12	1.063	92.5	0.5231
25.5	8.045	13	1.595	96.7	0.46888
26.5	7.321	14	1.595	98.3	0.40558
27.5	6.334	15	1.418	100.2	0.3624
28.5	5.318	16	2.304	105	0.25934
29.5	4.388	17	1.063	107.5	0.22634
30.5	3.588	18	1.418	110.4	0.20347
31.5	2.927	19	1.595	115.3	0.15072
32.5	2.394	20	1.241	120.2	0.11809
33.5	1.97	21	4.608	122.5	0.10112
34.5	1.636	22	5.317	128	0.08318
35.5	1.374	24	8.95	133	0.07089
36.5	1.168	26	6.203	141	0.07871
37.5	1.005	28	3.899	148	0.06663
38.5	0.8778	30	1.772	152.5	0.05462
39.5	0.78	32	2.747	158	0.05276
40.5	0.7037	34	1.595	166.5	0.04097
50.5	0.3379	36	1.506	168.5	0.04926
60.5	0.2375	38	0.6203	172	0.03764
70.5	0.1497	40	0.7089	174.5	0.0361

80.5	0.09143	42	0.5317	176.5	0.03264
100.5	0.03276	46	0.6203	180	0.02925
110.5	0.01839	48	0.4431	182.5	0.0273
130.5	0.005374	52	0.3545	185	0.01069
150.5	0.001475	56	0.1772		
170.5	0.0003879	60	0.4431		
190.5	0.000000098	64	0.1772		
250.5	0.000001002	90	0.2659		
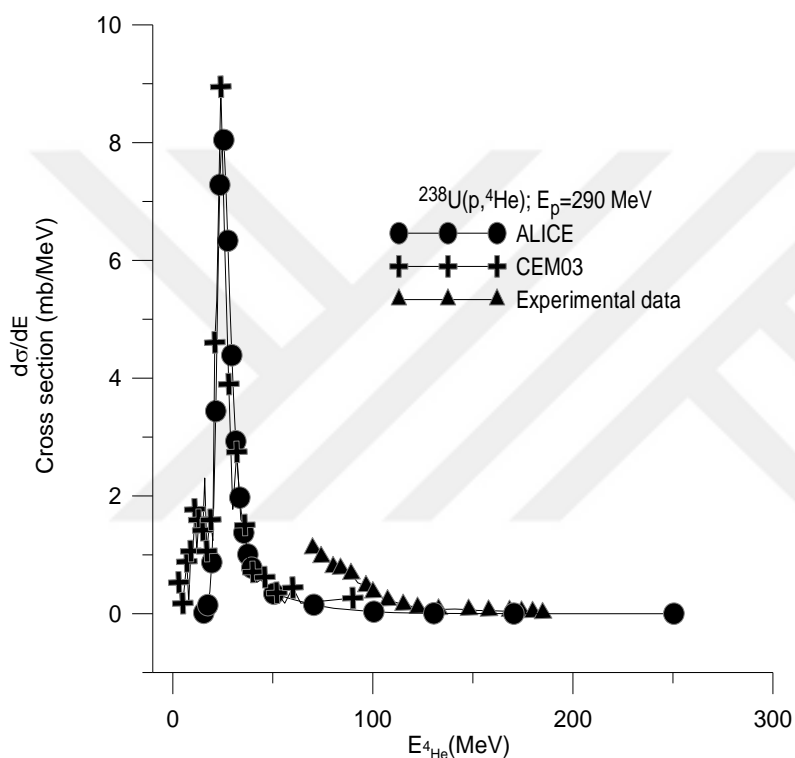
Figure 4.16. Energy spectra $\frac{d\sigma}{dE}$ of alphas when bombarded $_{92}U^{238}$ element by protons with 290 MeV energy

4.2.   p + $_{79}Au^{197}$ Reaction

Gold is a chemical element with symbol Au and atomic number 79. In its purest form, it is a bright, somewhat reddish yellow, dense, soft, flexible, and supple metal. Chemically, gold is a transition metal and a group 11 element, although melting point of gold =1,064 °C and boiling point=2,700 °C. Gold ($_{79}Au^{197}$) has one stable isotope, and 18 radioisotopes, when ^{195}Au being the most stable with a half-life of 186 days. Gold is

presently considered the heaviest monoisotopic element (bismuth formerly held that dissimilarity, but bismuth-209 has been found to be slightly radioactive). (Parsons 2014)

4.2.1. Neutron Energy Spectra (dσ/dE) for p + $_{79}$Au^{197} Reaction at E$_p$=20 MeV

Figure 4.17. Shows a comparison of ALICE, CEM03 and Experimental data results for the energy spectra ($\frac{d\sigma}{dE}$) of neutrons when $_{79}$Au^{197} element is bombarded by protons at 20 MeV. The figure shows the less difference energy spectra at each data's. Because the difference between ALICE and CEM03 data is very low and they are close to each other, we can say the data collected by both programs are consistent to each other.

Table 4.17. Show the numerical results of $\frac{d\sigma}{dE}$ both for ALICE, CEM03 and Experimental data. As can be seen in the table, the maximum $\frac{d\sigma}{dE}$ at Experimental data =1980 mb/MeV while E_n=1.01 MeV, maximum $\frac{d\sigma}{dE}$ at ALICE/ASH =1434 mb/MeV while E_n=0.5 MeV, and CEM03 =1084 while E_n=1 MeV.

Table 4.17. Neutron energy spectra for p + $_{79}$Au^{197} reaction, E$_p$=20 MeV, Calculations have been made by ALICE, CEM03, PCROSS and Experimental Data from EXFOR

ALICE/ASH		CEM03		PCROSS		Experimental Data (Yadernaya 1980)	
E$_n$ (MeV)	dσ/dE (mb/MeV)	E$_n$ (MeV)	dσ/dE (mb/MeV)	E$_n$ (MeV)	dσ/dE (mb/MeV)	E$_n$ (MeV)	dσ/dE (mb/MeV)
0.5	1434	1	1084	0.5	726.091	1.01	1980
1.5	790.1	2	902.2	0.65	701.081	2.9	560
2.5	346.2	3	399.2	0.8	695.277	4.99	103
3.5	148.8	4	162.2	0.95	667.617	6.48	42
4.5	68.79	5	68.69	1.1	647.986	8.27	20
5.5	36.71	6	37.12	1.25	615.559	9.94	15.4
6.5	23.17	7	21.49	1.4	588.771	12.12	11.5
7.5	16.76	8	12.13	1.55	554.347	15.14	7.4
8.5	13.15	9	14.32	1.7	524.755	17.83	7
9.5	10.68	10	12.57	1.85	490.688	9.5	10.68

|							
10.5	8.768	11	11.4	2	461.011	10.5	8.768
11.5	7.177	12	10.38	2.15	428.823	11.5	7.177
12.5	5.832	13	8.769	2.3	400.66	12.5	5.832
13.5	4.681	14	6.577	2.45	371.209	13.5	4.681
14.5	3.67	15	6.577	2.75	319.109	14.5	3.67
15.5	2.735	16	4.677	2.9	296.099	15.5	2.735
16.5	1.829	17	3.946	3.05	272.987	16.5	1.829
17.5	0.9322	18	3.508	3.35	232.809	17.5	0.9322
		19	1.315	3.65	198.252		
				4.25	143.955		
				5.15	91.091		
				6.05	60.7633		
				7.25	39.2972		
				8.15	30.5956		
				9.05	25.0655		
				10.25	20.0374		
				11.15	17.1931		
				12.05	14.7177		
				13.25	11.8709		
				14.05	12.4495		
				15.25	16.1802		
				16.05	8.40633		
				17.25	2.78113		
				18.05	15.5797		
				19.25	23.3449		
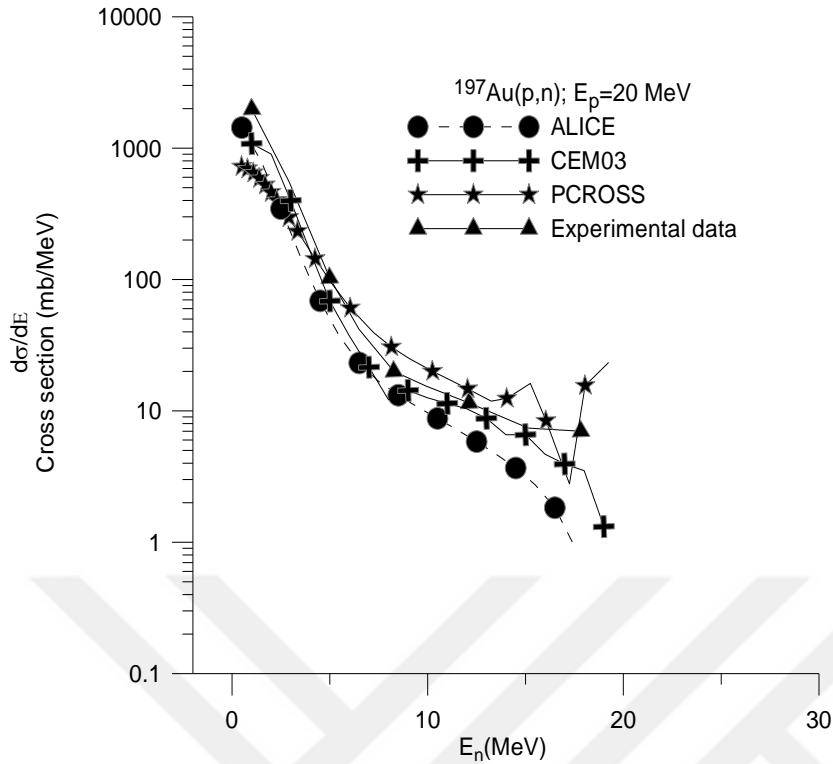
Figure 4.17. Energy spectra $\frac{d\sigma}{dE}$ of neutrons when bombarded $_{79}Au^{197}$ element by protons with 20 MeV energy

4.2.2. Proton Energy Spectra (dσ/dE) for p + $_{79}Au^{197}$ Reaction at E_p=20 MeV

Figure 4.18. Shows a comparison of ALICE, CEM03 and PCROSS results for the energy spectra ($\frac{d\sigma}{dE}$) of protons when $_{79}Au^{197}$ element is bombarded by protons at 20 MeV. Consequently this figure shows the difference energy spectra at programs, therefore PCROSS at E_p=1.9 MeV unless E_p=9.95 MeV has more than the CEM03 and ALICE energies cross section and CEM03 is more than the ALICE just one point by way E_p=8 MeV.

Table 4.18. Show the numerical results of $\frac{d\sigma}{dE}$ each ALICE, CEM03 and PCROSS programs. As can be seen in the table, the maximum $\frac{d\sigma}{dE}$ at PCROSS =33.4716 mb/MeV while E_p=3.65 MeV. The maximum $\frac{d\sigma}{dE}$ at CEM03 =8.916 mb/MeV while E_p=12 MeV. And maximum $\frac{d\sigma}{dE}$ at ALICE/ASH =3.433 mb/MeV while E_p=13.5 MeV.

Table 4.18. Proton energy spectra for p + $_{79}$Au^{197} reaction, E_p=20 MeV, Calculations have been made by ALICE, CEM03 and PCROSS programs

ALICE/ASH		CEM03		PCROSS	
E_p (MeV)	$d\sigma/dE$ (mb/MeV)	E_p (MeV)	$d\sigma/dE$ (mb/MeV)	E_p (MeV)	$d\sigma/dE$ (mb/MeV)
0.5	0	8	0.2923	1.9153	0
1.5	0	9	3.8	2	3.55194
2.5	0	10	5.262	2.15	9.94363
3.5	0	11	7.016	2.9	29.0767
4.5	0	12	8.916	3.95	32.6407
5.5	0.01547	13	6.577	4.25	30.9839
6.5	0.07269	14	8.185	4.85	26.3916
7.5	0.2467	15	5.846	5.15	23.8954
8.5	0.6501	16	6.869	5.75	19.1842
9.5	1.337	17	7.746	6.05	17.1143
10.5	2.159	18	3.654	6.95	12.0556
11.5	2.854	19	2.046	7.25	10.7525
12.5	3.282	20	0.7308	7.85	8.72108
13.5	3.433			8.15	7.95391
14.5	3.355			8.75	6.79522
15.5	3.08			9.05	6.3361
16.5	2.639			9.95	5.41561
17.5	2.025			10.25	5.15755
18.5	1.284			10.85	4.69356
19.5	0.4023			12.05	3.89041
				13.25	3.1363
				14.05	2.61564
				15.25	1.76683
				16.45	0.801096
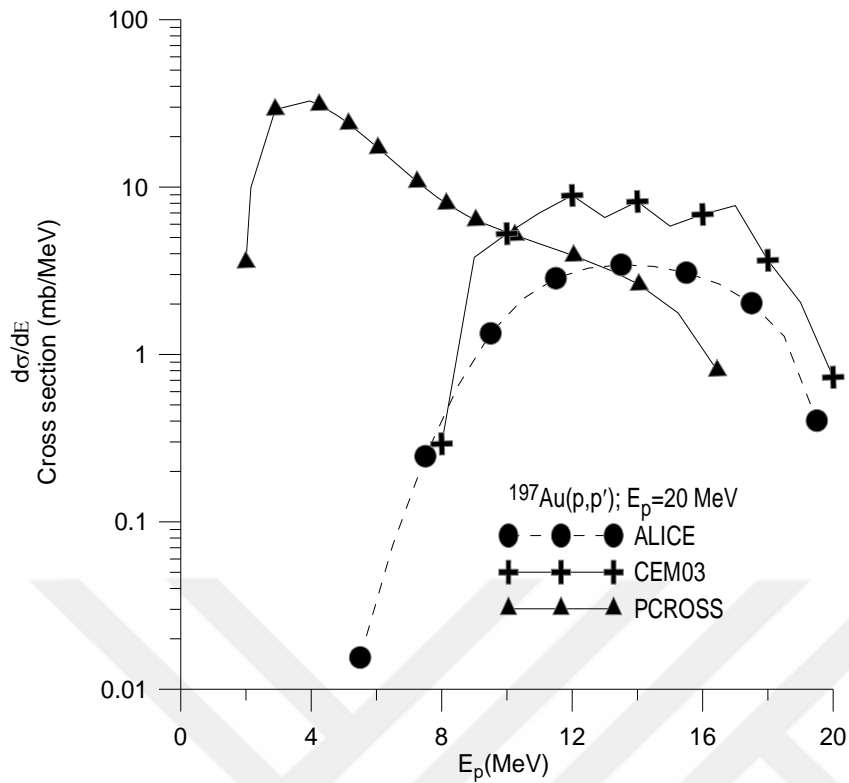
Figure 4.18. Energy spectra $^{d\sigma}/_{dE}$ of protons when bombarded $_{79}Au^{197}$ element by protons with 20 MeV energy

4.2.3. Deuteron Energy Spectra (dσ/dE) for p + $_{79}Au^{197}$ Reaction at E_p=20 MeV

Figure 4.19. Shows a comparison of ALICE and CEM03 results for the energy spectra ($\frac{d\sigma}{dE}$) of deuterons when $_{79}Au^{197}$ element is bombarded by protons at 20 MeV. The figure shows the many difference energy spectra at both programs, therefore CEM03 at E_d=13 MeV and E_d=14 MeV has more than the ALICE energies cross section.

Table 4.19. Show the numerical results of $\frac{d\sigma}{dE}$ both for ALICE and CEM03 programs. As can be seen in the table, the maximum $\frac{d\sigma}{dE}$ at CEM03 =1.315 mb/MeV while E_d =14 MeV. The maximum $\frac{d\sigma}{dE}$ at ALICE =0.6461 mb/MeV while E_d =12.5 MeV.

Table 4.19. Deuteron energy spectra for $p + {}_{79}Au^{197}$ reaction, $E_p=20$ MeV, Calculations have been made by ALICE and CEM03 programs

ALICE/ASH		CEM03	
E_d (MeV)	$d\sigma/dE$ (mb/MeV)	E_d (MeV)	$d\sigma/dE$ (mb/MeV)
0.5	0	5	0.1462
5.5	0.000005951	8	0.1462
6.5	0.001117	10	0.1462
7.5	0.01032	11	0.4385
8.5	0.05652	12	0.8769
9.5	0.1987	13	1.023
10.5	0.4192	14	1.315
11.5	0.5902		
12.5	0.6461		
13.5	0.5605		
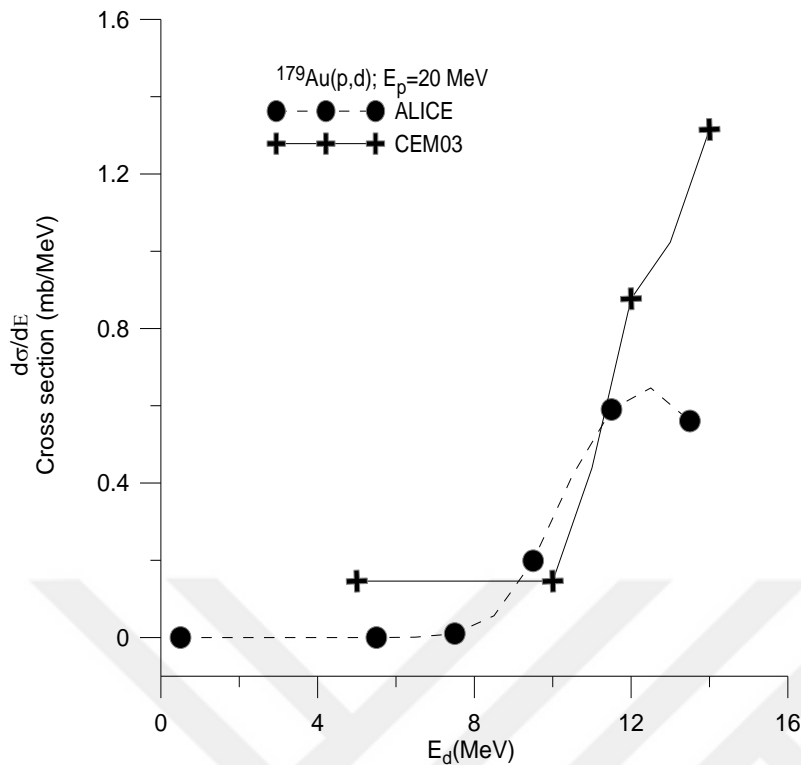
Figure 4.19. Energy spectra $^{d\sigma}/_{dE}$ of deuterons when bombarded $_{79}Au^{197}$ element by protons with 20 MeV energy

4.2.4. Alpha Energy Spectra (dσ/dE) for p + $_{79}Au^{197}$ Reaction at E_p=20 MeV

Figure 4.20. Shows a comparison of ALICE, CEM03, PCROSS and Experimental data results for the energy spectra ($\frac{d\sigma}{dE}$) of alphas when $_{79}Au^{197}$ element is bombarded by protons at 20 MeV. The figure shows the many difference energy spectra at each program. Consequently this figure shows the difference energy spectra at programs, therefore PCROSS at $E_{4_{He}}$=5.75 MeV unless $E_{4_{He}}$=14.05 MeV are more than the ALICE, CEM03 Experimental energies cross section, and another data's are near.

Table 4.20. Show the numerical results of $\frac{d\sigma}{dE}$ for each ALICE, CEM03, PCROSS and Experimental data. As can be seen in the table, the maximum $\frac{d\sigma}{dE}$ at PCROSS =8.60164 mb/MeV while $E_{4_{He}}$=7.85 MeV, maximum $\frac{d\sigma}{dE}$ at Experimental data =4.77 mb/MeV while $E_{4_{He}}$=15.09 MeV, ALICE/ASH =4.63 mb/MeV while $E_{4_{He}}$=16.5 MeV, and CEM03 =0.146 while $E_{4_{He}}$=22 MeV.

Table 4.20. Alpha energy spectra for p + $_{79}$Au^{197} reaction, E$_p$=20 MeV, Calculations have been made by ALICE, CEM03, PCROSS, and Experimental data at EXFOR

ALICE/ASH		CEM03		PCROSS		Experimental Data (Vop 1983)	
E_α (MeV)	$d\sigma/dE$ (mb/MeV)	E_α (MeV)	$d\sigma/dE$ (mb/MeV)	E_α (MeV)	$d\sigma/dE$ (mb/MeV)	E_α (MeV)	$d\sigma/dE$ (mb/MeV)
13.5	2.14	21	0.146	5.457	0	15.09	4.77
14.5	3.269	22	0.146	5.75	2.51437	15.62	4.37
15.5	3.993			6.05	4.57075	16.02	3.92
16.5	4.63			6.35	6.12033	16.22	3.1
17.5	0.1725			6.65	7.22719	16.8	3.09
18.5	0.3149			6.95	7.96197	16.95	3.02
19.5	0.5815			7.25	8.39415	17.2	2.55
20.5	0.9376			7.55	8.5882	17.54	2.37
				7.85	8.60164	17.86	2.52
				8.15	8.4922	18.19	1.82
				8.45	8.28357	18.54	1.1
				8.75	8.01611	18.79	1.02
				9.05	7.71491	18.94	0.6
				9.35	7.39878	19.43	0.21
				9.65	7.08139	19.67	0.23
				9.95	6.77227	19.97	0.5
				10.25	6.47058	20.34	0.16
				10.55	6.13993		
				10.85	5.79114		
				11.15	5.45196		
				11.45	5.11931		
				11.75	4.80171		
				12.05	4.50382		
				12.45	4.14043		
				12.85	3.81538		
				13.25	3.52541		
				13.65	3.26571		
				14.05	3.03103		
				14.45	2.81624		
				14.85	2.61673		
				15.25	2.42854		
				15.65	2.2484		
				16.05	2.07372		
				16.45	1.90251		
				16.85	1.73326		
				17.25	1.56493		
				17.65	1.39679		
				18.05	1.2284		
				18.45	1.05951		

				18.85	0.890048		
				19.25	0.720102		

Figure 4.20. Energy spectra $^{d\sigma}/_{dE}$ of alphas when bombarded $_{79}Au^{197}$ element by protons with 20 MeV energy

4.2.5. Neutron Energy Spectra (dσ/dE) for p + $_{79}Au^{197}$ Reaction at E_p=50 MeV

Figure 4.21. Shows a comparison of ALICE, CEM03 and PCROSS data results for the energy spectra $(\frac{d\sigma}{dE})$ of neutrons when $_{79}Au^{197}$ element is bombarded by protons at 50 MeV. The figure shows the less difference energy spectra at each data's. Because the difference between each data's is very low and they are close to each other, we can say the data collected by three programs are consistent to each other.

Table 4.21. Show the numerical results of $\frac{d\sigma}{dE}$ both for ALICE, CEM03 and PCROSS. As can be seen in the table, the maximum $\frac{d\sigma}{dE}$ at ALICE/ASH =2383 mb/MeV while E_n=0.5

MeV, maximum $\frac{d\sigma}{dE}$ at CEM03 =2168 mb/MeV while E_n=1 MeV, and PCROSS =1910.17

while E_n=0.65 MeV.

Table 4.21. Neutron energy spectra for p + $_{79}$Au^{197} reaction, E_p=50 MeV, Calculations have been made by ALICE, CEM03 and PCROSS programs

ALICE/ASH		CEM03		PCROSS	
E_n (MeV)	$d\sigma/dE$ (mb/MeV)	E_n (MeV)	$d\sigma/dE$ (mb/MeV)	E_n (MeV)	$d\sigma/dE$ (mb/MeV)
0.5	2383	1	2168	0.5	1901.39
1.5	1649	2	1813	0.65	1910.17
2.5	914.4	3	976.9	0.8	1885.69
3.5	505.4	4	520.6	0.95	1835.57
4.5	291	5	268.2	1.1	1768.08
5.5	176.8	6	154.1	1.25	1688.78
6.5	115.1	7	89.2	1.4	1603.45
7.5	81.39	8	68.66	1.55	1514.43
8.5	62.21	9	49.07	1.7	1423.99
9.5	50.44	10	35.19	1.85	1334.47
10.5	42.6	11	31.38	2	1246.79
11.5	37.05	12	31	2.15	1161.8
12.5	32.93	13	27.96	2.3	1080.38
13.5	29.78	14	27.01	2.45	1002.81
14.5	27.27	15	22.25	2.6	929.355
15.5	25.21	16	23.96	2.75	860.11
16.5	23.46	17	18.45	2.9	795.184
17.5	21.92	18	18.64	3.05	734.482
18.5	20.56	19	16.74	3.35	625.326
19.5	19.36	20	16.17	3.65	531.474
20.5	18.32	21	15.03	3.95	451.428
21.5	17.42	22	15.41	4.25	383.572
22.5	16.63	24	15.5	4.85	278.27
23.5	15.92	26	10.56	5.15	238.014
24.5	15.27	28	11.32	5.45	204.39
25.5	14.67	30	9.89	5.75	176.357
26.5	14.09	32	8.749	6.05	153.017
27.5	13.58	34	8.939	6.65	117.457
28.5	13.09	36	6.372	6.95	104.031
29.5	12.62	38	7.037	7.25	92.8582
30.5	12.18	40	7.608	7.85	75.7852
31.5	11.77	42	5.421	8.15	69.2913
32.5	11.32	44	5.991	8.45	63.8459
33.5	10.86	46	4.945	8.75	59.2641
34.5	10.43	48	4.375	9.05	55.3932

|					
35.5	10.01	50	0.7608	9.35	52.1073
36.5	9.552			9.65	49.3028
37.5	9.022			9.95	46.8946
38.5	8.498			10.25	44.8126
39.5	7.977			10.55	42.9994
40.5	7.441			10.85	41.4081
41.5	6.7			11.15	40
42.5	5.953			11.45	38.7436
43.5	5.2			11.75	37.613
44.5	4.283			12.05	36.5872
45.5	3.341			13.25	33.2294
46.5	2.265			14.05	31.4271
47.5	1.102			16.05	27.7345
				18.05	24.7053
				20.05	22.0868
				22.05	19.7719
				24.05	17.6973
				26.05	15.8171
				28.05	14.0953
				30.05	12.5023
				32.05	11.0137
				34.05	9.60838
				36.05	8.26814
				38.05	6.97677
				40.05	5.71946
				42.05	4.48235
				44.05	3.25202
				46.05	2.01512
				48.05	0.768532
				49.05	0.241059
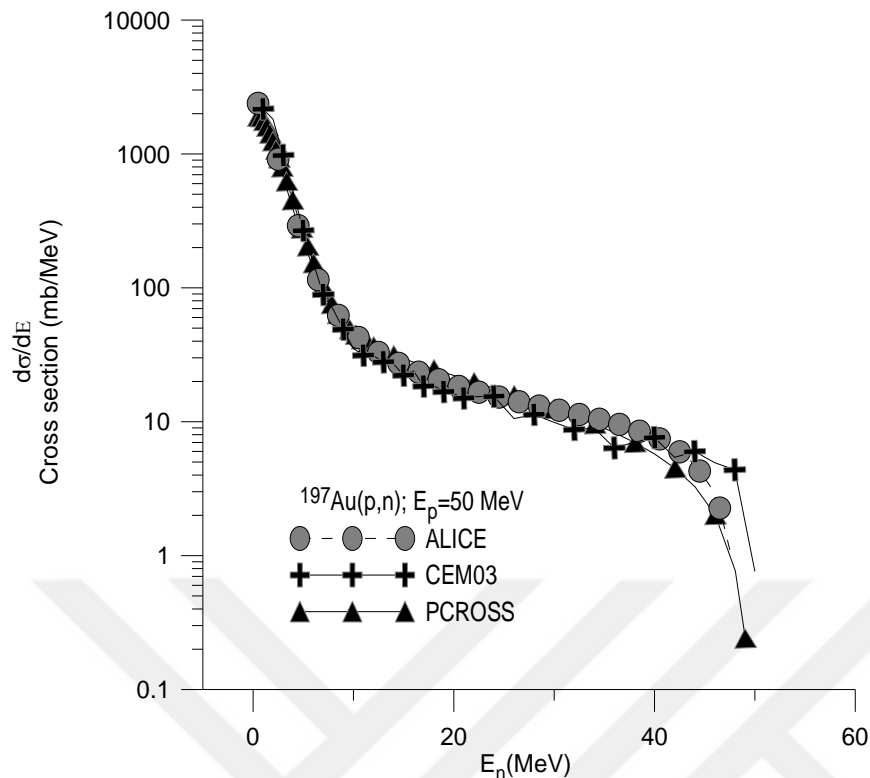
Figure 4.21. Energy spectra $\frac{d\sigma}{dE}$ of neutron when bombarded $_{79}Au^{197}$ element by protons with 50 MeV energy

4.2.6. Proton Energy Spectra (dσ/dE) for p + $_{79}Au^{197}$ Reaction at E_p=50 MeV

Figure 4.22. Shows a comparison of ALICE, CEM03 and PCROSS results for the energy spectra $(\frac{d\sigma}{dE})$ of protons when $_{79}Au^{197}$ element is bombarded by protons at 50 MeV. Consequently this figure shows the difference energy spectra at programs, therefore CEM03 at E_p=9 MeV unless E_p=14 MeV has more than the ALICE and PCROSS energies cross section, and ALICE at E_p=7.5 MeV unless E_p=49.5 MeV has more than the PCROSS.

Table 4.22. Show the numerical results of $\frac{d\sigma}{dE}$ each ALICE, CEM03 and PCROSS programs. As can be seen in the table, the maximum $\frac{d\sigma}{dE}$ at CEM03 =23.96 mb/MeV while E_p=20 MeV. The maximum $\frac{d\sigma}{dE}$ at ALICE/ASH =21.39 mb/MeV while E_p=19.5 MeV. And maximum $\frac{d\sigma}{dE}$ at PCROSS =6.99099 mb/MeV while E_p=18.5 MeV.

Table 4.22. Proton energy spectra for p + $_{79}$Au^{197} reaction, E$_p$=50 MeV, Calculations have been made by ALICE, CEM03 and PCROSS programs

ALICE/ASH		CEM03		PCROSS	
E_p (MeV)	$d\sigma/dE$ (mb/MeV)	E_p (MeV)	$d\sigma/dE$ (mb/MeV)	E_p (MeV)	$d\sigma/dE$ (mb/MeV)
0.5	0	8	1.902	6.7339	0
1.5	0	9	10.08	6.95	0.316962
2.5	0	10	13.69	7.25	0.647229
3.5	0	11	14.07	7.55	0.968354
4.5	0	12	18.64	7.85	1.26957
5.5	0.08994	13	16.36	8.15	1.54749
6.5	0.3987	14	19.59	8.45	1.80311
7.5	1.231	15	17.12	8.75	2.03982
8.5	2.97	16	21.87	9.05	2.26209
9.5	5.817	17	19.4	9.35	2.47462
10.5	9.347	18	20.54	9.65	2.68184
11.5	12.72	19	19.4	9.95	2.88765
12.5	15.48	20	23.96	10.25	3.09528
13.5	17.61	21	19.21	10.55	3.3073
14.5	19.2	22	16.93	10.85	3.5256
15.5	20.27	24	18.07	11.15	3.75152
16.5	20.91	26	16.74	11.45	3.98588
17.5	21.25	28	16.17	11.75	4.22911
18.5	21.38	30	16.17	12.05	4.48127
19.5	21.39	32	14.17	12.45	4.83102
20.5	21.28	34	13.31	12.85	5.19534
21.5	21.07	36	10.84	13.25	5.54012
22.5	20.8	38	12.93	13.65	5.83152
23.5	20.5	40	10.84	14.05	6.07776
24.5	20.22	42	8.369	14.45	6.28511
25.5	19.94	44	8.749	14.85	6.45845
26.5	19.68	46	6.276	15.25	6.60171
27.5	19.35	48	4.279	15.65	6.71818
28.5	18.99	50	2.473	16.05	6.81069
29.5	18.62			16.45	6.88168
30.5	18.2			16.85	6.93334
31.5	17.81			17.25	6.96763
32.5	17.46			17.65	6.98631
33.5	17.07			18.05	6.99099
34.5	16.61			18.45	6.9831
35.5	16.12			18.85	6.96398
36.5	15.61			19.25	6.93481
37.5	15.08			19.65	6.89668
38.5	14.34			20.05	6.85057

39.5	13.6			20.45	6.79736
40.5	12.85			20.85	6.73787
41.5	12.1			21.25	6.67282
42.5	11.1			21.65	6.60286
43.5	9.961			22.05	6.52859
44.5	8.792			24.05	6.1093
45.5	7.452			26.05	5.64248
46.5	5.958			28.05	5.1567
47.5	4.315			30.05	4.66769
48.5	2.501			32.05	4.18329
49.5	0.5356			34.05	3.70641
				36.05	3.23683
				38.05	2.77217
				40.05	2.30853
				42.05	1.84075
				44.05	1.36253
				46.05	0.866392
				48.05	0.343475
				49.05	0.068766
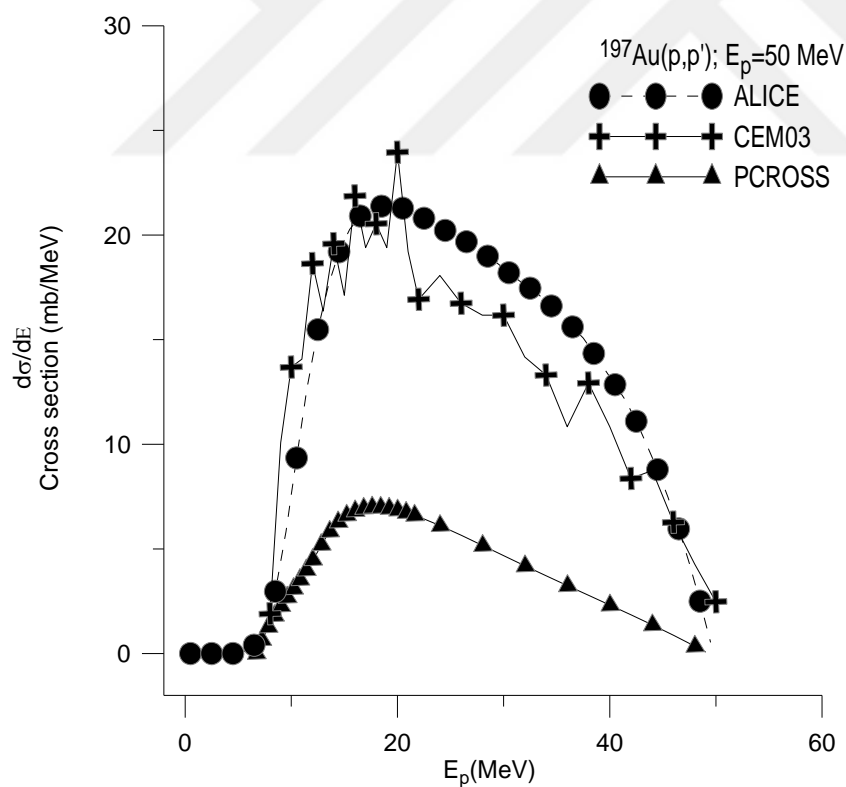
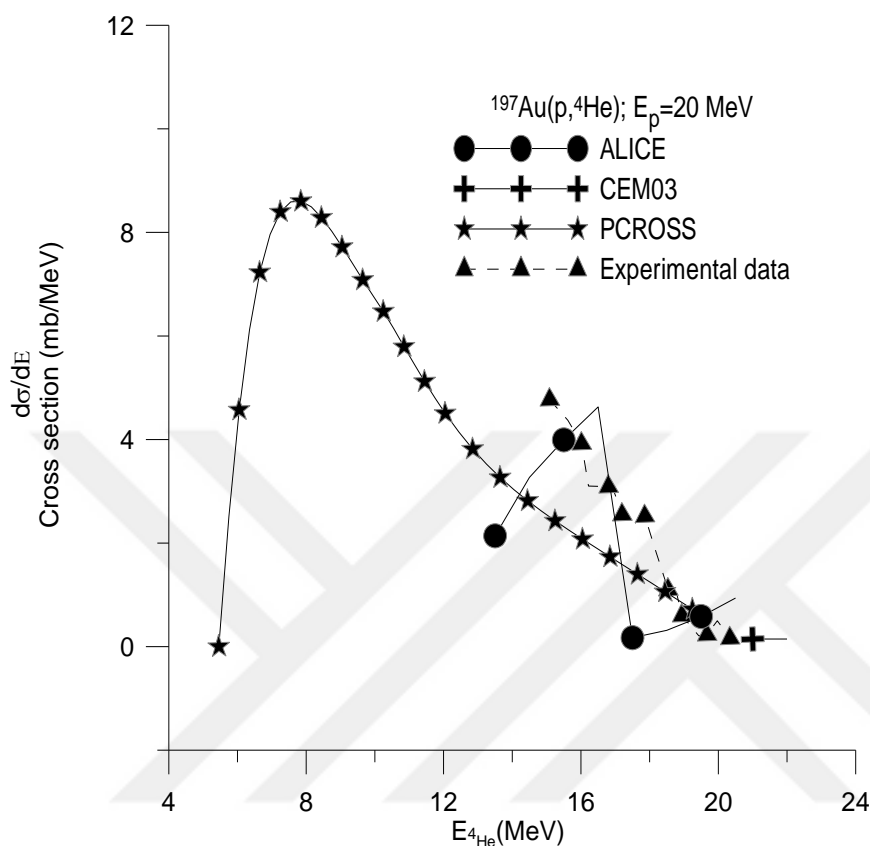
Figure 4.22. Energy spectra $^{d\sigma}/_{dE}$ of protons when bombarded $_{79}Au^{197}$ element by protons with 50 MeV energy

4.2.7. Deuteron Energy Spectra (dσ/dE) for p + $_{79}$Au^{197} Reaction at E$_p$=50 MeV

Figure 4.23. Shows a comparison both ALICE, CEM03 results for the energy spectra $(\frac{d\sigma}{dE})$ of deuterons when $_{79}$Au^{197} element is bombarded by protons at 50 MeV. The figure shows the many difference energy spectra at both programs, therefore CEM03 at E_d=3 MeV unless E_d=34 MeV has more than the ALICE energies cross section.

Table 4.23. Show the numerical results of $\frac{d\sigma}{dE}$ both for ALICE and CEM03 programs. As can be seen in the table, the maximum $\frac{d\sigma}{dE}$ at CEM03 =4.565 mb/MeV while E_d =18 MeV, and maximum $\frac{d\sigma}{dE}$ at ALICE =1.873 mb/MeV while E_d =38.5 MeV.

Table 4.23. Deuteron energy spectra for p + $_{79}$Au^{197} reaction, E$_p$=50 MeV, Calculations have been made by ALICE and CEM03 programs

ALICE/ASH		CEM03	
E$_d$ (MeV)	dσ/dE (mb/MeV)	E$_d$ (MeV)	dσ/dE (mb/MeV)
5.5	0.0004163	3	0.1902
6.5	0.004772	6	0.3804
7.5	0.02746	8	0.3804
8.5	0.1009	10	0.5706
9.5	0.2616	11	1.902
10.5	0.4962	12	3.424
11.5	0.7433	13	3.994
12.5	0.9631	14	3.614
13.5	1.145	15	3.424
14.5	1.289	16	3.804
15.5	1.398	17	4.184
16.5	1.476	18	4.565
17.5	1.534	19	2.853
18.5	1.584	20	2.663
19.5	1.618	21	3.424
20.5	1.646	22	3.043
21.5	1.672	24	2.663

22.5	1.688	26	3.138
23.5	1.697	28	4.375
24.5	1.7	30	1.997
25.5	1.698	32	1.712
26.5	1.692	34	1.807
27.5	1.682	36	1.236
28.5	1.671	38	1.046
29.5	1.657	40	1.902
30.5	1.642	42	1.236
31.5	1.628	44	2.092
32.5	1.614		
33.5	1.606		
34.5	1.606		
35.5	1.624		
36.5	1.668		
37.5	1.75		
38.5	1.873		
39.5	2.034		
40.5	2.014		
41.5	1.872		
42.5	1.671		
43.5	1.383		
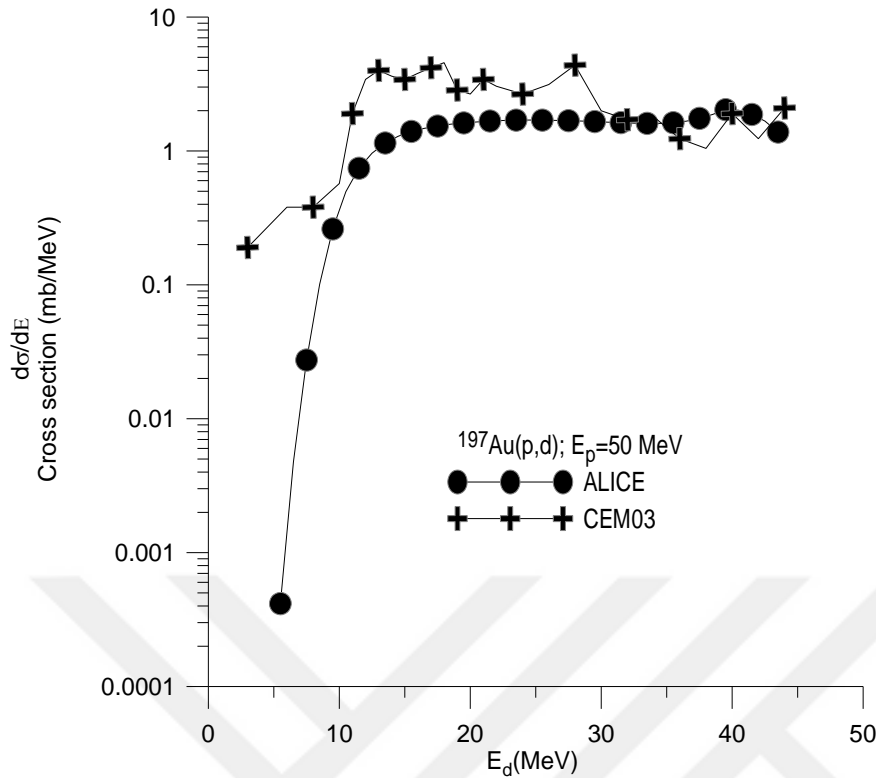
Figure 4.23. Energy spectra $^{d\sigma}/_{dE}$ of deuteron when bombarded $_{79}Au^{197}$ element by protons with 50 MeV energy

4.2.8. Alpha Energy Spectra (dσ/dE) for p + $_{79}Au^{197}$ Reaction at E_p=50 MeV

Figure 4.24. Shows a comparison both of ALICE, CEM03 programs for the energy spectra ($\frac{d\sigma}{dE}$) of alphas when $_{79}Au^{197}$ element is bombarded by protons at 50 MeV. The figure shows the many difference energy spectra at programs. Consequently this figure shows the difference energy spectra at programs, therefore CEM03 at points $E_{4_{He}}$=20 MeV, $E_{4_{He}}$=21 MeV and, $E_{4_{He}}$=22 MeV are more than the ALICE data's.

Table 4.24. Show the numerical results of $\frac{d\sigma}{dE}$ each as ALICE and CEM03 programs. As can be seen in the table, the maximum $\frac{d\sigma}{dE}$ at CEM03 =2.473 mb/MeV while $E_{4_{He}}$=20 MeV, and ALICE/ASH =1.4 while $E_{4_{He}}$=21.5 MeV.

Table 4.24. Alpha energy spectra for p + $_{79}$Au^{197} reaction, E$_p$=50 MeV, Calculations have been made by ALICE and CEM03 programs

ALICE/ASH		CEM03	
E$_\alpha$ (MeV)	dσ/dE (mb/MeV)	E$_\alpha$ (MeV)	dσ/dE (mb/MeV)
13.5	0.0233	19	0.5706
14.5	0.05992	20	2.473
15.5	0.1325	21	2.282
16.5	0.2598	22	2.092
17.5	0.4601	24	1.426
18.5	0.7388	26	1.426
19.5	1.055	28	1.522
20.5	1.303	30	0.5706
21.5	1.4	32	0.5706
22.5	1.374	34	0.4755
23.5	1.29	36	0.4755
24.5	1.208	38	0.3804
25.5	1.132	40	0.3804
26.5	1.058	42	0.2853
27.5	0.9873	44	0.2853
28.5	0.9175	50	0.0951
29.5	0.8487		
30.5	0.7813		
31.5	0.7156		
32.5	0.6524		
33.5	0.592		
34.5	0.5348		
36.5	0.4416		
37.5	0.4008		
38.5	0.3626		
39.5	0.327		
40.5	0.2939		
41.5	0.2631		
42.5	0.2344		
43.5	0.2078		
44.5	0.183		

| 45.5	0.1613		
46.5	0.1428		
48.5	0.1134		
50.5	0.08643		
52.5	0.06128		
54.5	0.03778		
56.5	0.01598		
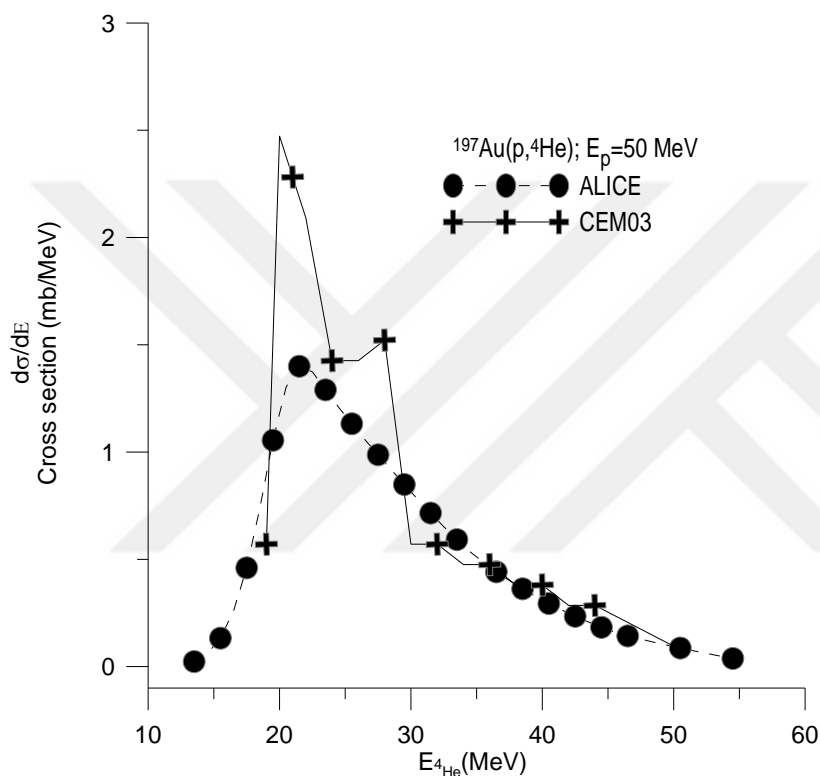
Figure 4.24. Energy spectra $^{d\sigma}/_{dE}$ of alphas when bombarded $_{79}Au^{197}$ element by protons with 50 MeV energy

4.2.9. Neutron Energy Spectra (dσ/dE) for p + $_{79}Au^{197}$ Reaction at E_p=190 MeV

Figure 4.25. Shows a comparison both of ALICE, CEM03 programs results for the energy spectra ($\frac{d\sigma}{dE}$) of neutrons when $_{79}Au^{197}$ element is bombarded by protons at 190 MeV. The figure shows the less difference energy spectra at each data's, therefore CEM03 at E_n=1 MeV unless E_n=80 MeV is more than the ALICE data's.

Table 4.25. Show the numerical results of $\frac{d\sigma}{dE}$ both for ALICE, CEM03. As can be seen in the table, the maximum $\frac{d\sigma}{dE}$ at CEM03 =2469 mb/MeV while E_n=2 MeV, maximum $\frac{d\sigma}{dE}$ at ALICE/ASH =1939 mb/MeV while E_n=0.5 MeV.

Table 4.25. Neutron energy spectra for p + $_{79}$Au^{197} reaction, E_p=190 MeV, Calculations have been made by ALICE and CEM03 programs

ALICE/ASH		CEM03	
E_n (MeV)	dσ/dE (mb/MeV)	E_n (MeV)	dσ/dE (mb/MeV)
0.5	1939	1	2364
1.5	1780	2	2469
2.5	1288	3	1591
3.5	896.1	4	1027
4.5	618.8	5	663.5
5.5	424.3	6	438.7
6.5	290	7	298.9
7.5	199.9	8	215.3
8.5	139.7	9	162.9
9.5	98.58	10	127.9
10.5	70.25	11	108.1
11.5	50.9	12	85.27
12.5	37.79	13	76.52
13.5	28.94	14	65.17
14.5	22.94	15	64.04
15.5	18.82	16	61.44
16.5	15.95	17	51.88
17.5	13.92	18	50.58
18.5	12.47	19	47.34
19.5	11.43	20	41.02
20.5	10.69	21	35.02
21.5	10.15	22	37.12
22.5	9.759	24	33.48
23.5	9.455	26	32.26
24.5	9.209	28	25.53
25.5	9.003	30	24.48
26.5	8.827	32	21.97
27.5	8.674	34	18.56
28.5	8.541	36	16.94
29.5	8.423	38	16.21
30.5	8.316	40	16.21
31.5	8.214	42	15.73
32.5	8.116	44	12.97
33.5	8.02	46	12.81

|			
34.5	7.926	48	9.808
35.5	7.836	50	9.646
36.5	7.75	52	9.484
37.5	7.666	54	9.808
38.5	7.586	56	7.538
39.5	7.507	58	7.295
40.5	7.428	60	7.782
41.5	7.351	62	7.782
42.5	7.274	64	7.457
43.5	7.199	66	8.673
44.5	7.125	68	5.917
45.5	7.054	70	5.755
46.5	6.984	72	5.917
47.5	6.916	74	5.026
48.5	6.849	76	6.079
49.5	6.783	78	6.404
50.5	6.718	80	5.107
51.5	6.655	82	6.728
52.5	6.592	84	4.377
53.5	6.531	86	4.62
54.5	6.471	88	4.377
55.5	6.413	90	3.972
56.5	6.356	92	4.215
57.5	6.3	94	3.972
58.5	6.245	96	4.296
59.5	6.191	98	4.377
60.5	6.139	100	3.81
61.5	6.088	102	4.053
85.5	5.171		
90.5	5.052		
95.5	4.971		
105.5	4.851		
110.5	4.809		
115.5	4.778		
120.5	4.758		
125.5	4.746		
130.5	4.742		
135.5	4.745		
140.5	4.754		
145.5	4.717		
160.5	3.594		
170.5	1.154		
171.5	0.6653		
172.5	0.1279		
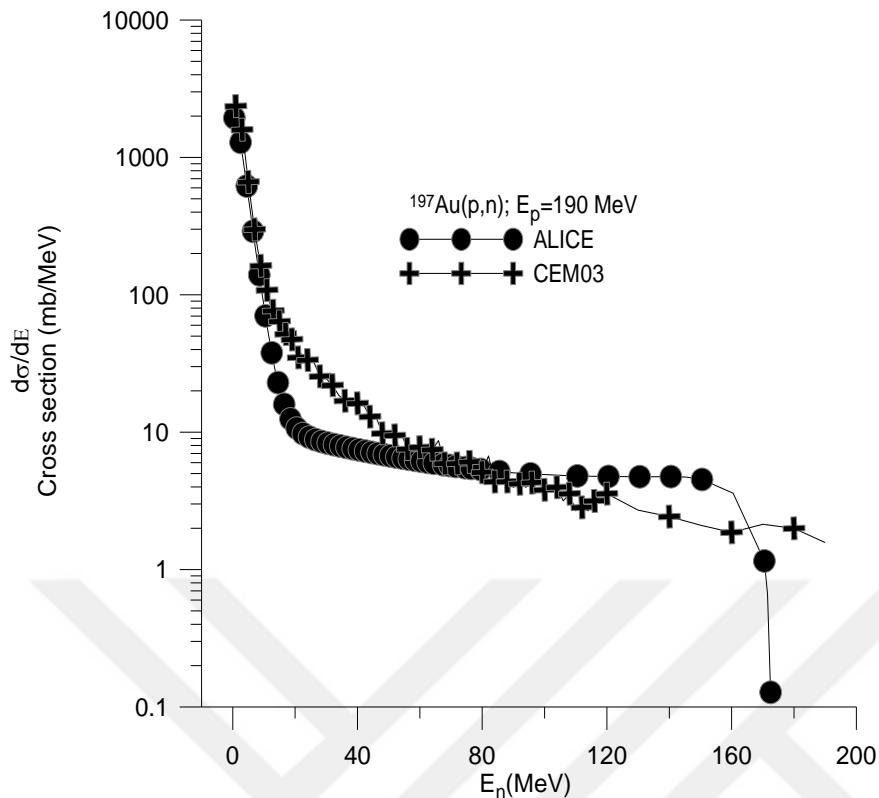
Figure 4.25. Energy spectra $d\sigma/dE$ of neutrons when bombarded $_{79}Au^{197}$ element by protons with 190 MeV energy

4.2.10. Proton Energy Spectra (dσ/dE) for p + $_{79}Au^{197}$ Reaction at E$_p$=190 MeV

Figure 4.26. Shows a comparison both of ALICE and CEM03 results for the energy spectra ($\frac{d\sigma}{dE}$) of protons when $_{79}Au^{197}$ element is bombarded by protons at 190 MeV. Consequently this figure shows the difference energy spectra at programs, therefore CEM03 at E_p=9 MeV unless E_p=40 MeV has more than the ALICE and but after this process is inversely.

Table 4.26. Show the numerical results of $\frac{d\sigma}{dE}$ both for ALICE and CEM03 programs. As can be seen in the table, the maximum $\frac{d\sigma}{dE}$ at CEM03 =64.85 mb/MeV while E_p=10 MeV. The maximum $\frac{d\sigma}{dE}$ at ALICE/ASH =17.64 mb/MeV while E_p=12.5 MeV.

Table 4.26. Proton energy spectra for p + $_{79}Au^{197}$ reaction, E_p=190 MeV, Calculations have been made by ALICE and CEM03 programs

ALICE/ASH		CEM03	
E_p (MeV)	dσ/dE (mb/MeV)	E_p (MeV)	dσ/dE (mb/MeV)
5.5	0.1728	5	0.4863
6.5	0.8707	6	0.3242
7.5	2.773	7	0.1621
8.5	6.317	8	6.16
9.5	10.95	9	59.33
10.5	15.03	10	64.85
11.5	17.22	11	58.04
12.5	17.64	12	49.28
13.5	17.09	13	39.23
14.5	16.15	14	37.61
15.5	15.14	15	32.42
16.5	14.21	16	25.94
17.5	13.46	17	23.99
18.5	12.9	18	24.8
19.5	12.53	19	22.21
20.5	12.27	20	19.29
21.5	12.1	21	20.43
22.5	12	22	19.29
23.5	11.94	24	19.86
24.5	11.94	26	17.1
25.5	11.97	28	15.81
26.5	12.01	30	14.19
27.5	12.04	32	15.81
28.5	12.06	34	13.62
29.5	12.06	36	14.67
30.5	12.05	38	12.08
31.5	12.06	40	13.05
32.5	12.09	42	10.94
33.5	12.12	44	10.46
34.5	12.14	46	9.97
35.5	12.14	48	8.997
36.5	12.12	50	8.754
37.5	12.09	52	9.565
38.5	12.04	54	7.376
39.5	12	56	8.349
40.5	11.97	58	7.538
41.5	11.94	60	8.106
42.5	11.91	62	5.917
43.5	11.88	64	7.7
44.5	11.84	66	5.431

|			
45.5	11.79	68	6.647
46.5	11.74	70	6.728
47.5	11.68	72	6.89
48.5	11.63	74	5.917
49.5	11.58	76	6.485
50.5	11.53	78	6.079
51.5	11.47	80	5.593
52.5	11.42	82	5.998
53.5	11.36	84	7.863
54.5	11.29	86	4.62
55.5	11.23	88	5.836
56.5	11.17	90	4.863
57.5	11.12	92	4.377
58.5	11.06	94	5.431
59.5	11.01	96	4.134
60.5	10.96	98	3.404
61.5	10.9	100	4.053
62.5	10.85	102	4.863
63.5	10.79	104	5.755
64.5	10.73	106	3.08
65.5	10.67	108	5.026
66.5	10.62	110	4.215
67.5	10.56	112	3.891
68.5	10.51	114	4.863
69.5	10.46	116	4.782
70.5	10.41	118	3.648
71.5	10.36	120	4.377
72.5	10.31	130	4.215
73.5	10.27	140	3.68
74.5	10.22	150	3.567
75.5	10.17	160	3.404
80.5	9.948	170	3.745
85.5	9.754	180	3.583
90.5	9.589	190	1.751
95.5	9.466		
100.5	9.365		
105.5	9.283		
110.5	9.22		
115.5	9.174		
120.5	9.144		
135.5	9.132		
160.5	7.192		
165.5	5.691		
170.5	3.197		
171.5	2.465		
172.5	1.606		
173.5	0.628		
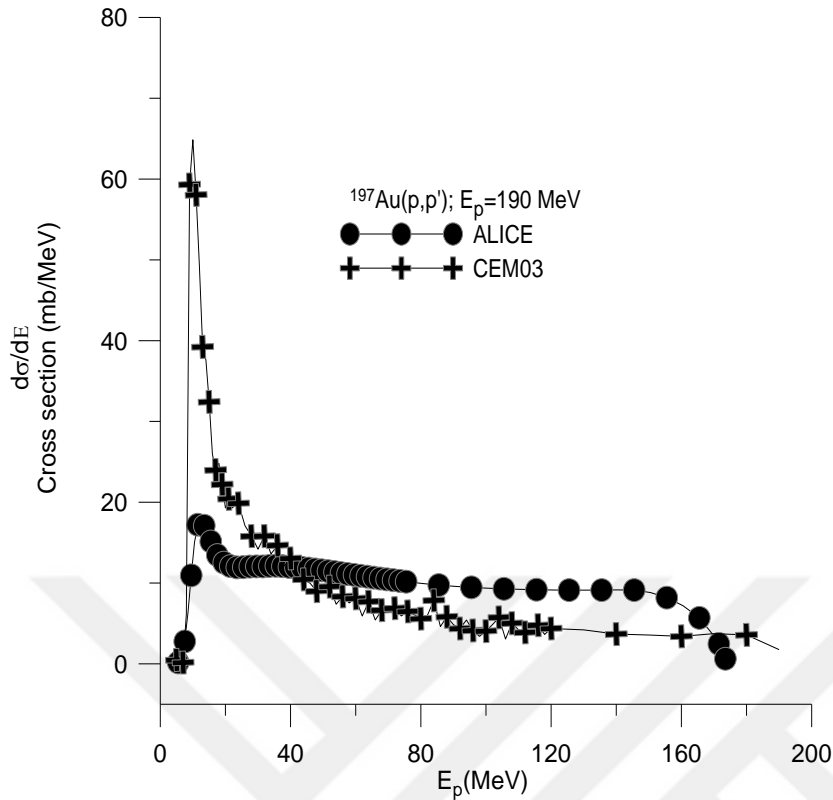
Figure 4.26. Energy spectra $\frac{d\sigma}{dE}$ of protons when bombarded $_{79}Au^{197}$ element by protons with 190 MeV energy

4.2.11. Deuteron Energy Spectra (dσ/dE) for p + $_{79}Au^{197}$ Reaction at E_p=190 MeV

Figure 4.27. Shows a comparison both ALICE, CEM03 results for the energy spectra $(\frac{d\sigma}{dE})$ of deuterons when $_{79}Au^{197}$ element is bombarded by protons at 190 MeV. The figure shows the many difference energy spectra at both programs, therefore CEM03 at E_d=6 MeV unless E_d=78 MeV has more than the ALICE energies cross section.

Table 4.27. Show the numerical results of $\frac{d\sigma}{dE}$ both for ALICE and CEM03 programs. As can be seen in the table, the maximum $\frac{d\sigma}{dE}$ at CEM03 =14.59 mb/MeV while E_d =11 MeV. The maximum $\frac{d\sigma}{dE}$ at ALICE =5.502 mb/MeV while E_d =11.5 MeV.

Table 4.27. Deuteron energy spectra for p + $_{79}Au^{197}$ reaction, E_p=190 MeV, Calculations have been made by ALICE and CEM03 programs

ALICE/ASH		CEM03	
E_d (MeV)	$d\sigma/dE$ (mb/MeV)	E_d (MeV)	$d\sigma/dE$ (mb/MeV)
5.5	0.003597	3	0.1621
6.5	0.04949	4	0.3242
7.5	0.3195	5	0.8106
8.5	1.202	6	1.297
9.5	2.881	7	1.135
10.5	4.625	8	4.215
11.5	5.502	9	8.916
12.5	5.445	10	11.67
13.5	4.849	11	14.59
14.5	4.061	12	12.81
15.5	3.283	13	12
16.5	2.605	14	12.64
17.5	2.054	15	13.94
18.5	1.628	16	12.16
19.5	1.304	17	10.54
20.5	1.064	18	8.592
21.5	0.8891	19	10.7
22.5	0.7622	20	9.727
23.5	0.6702	21	9.889
24.5	0.6033	22	8.916
25.5	0.5543	24	8.835
26.5	0.5178	26	7.619
27.5	0.4899	28	7.7
28.5	0.4678	30	7.214
29.5	0.4498	32	6.322
30.5	0.4344	34	4.782
31.5	0.4206	36	3.972
32.5	0.4081	38	4.053
33.5	0.3962	40	2.999
34.5	0.385	42	2.837
35.5	0.3741	44	2.675
36.5	0.3636	46	2.513
37.5	0.3535	48	2.107
38.5	0.3438	50	1.783
39.5	0.3345	52	1.297
40.5	0.3257	54	1.054
41.5	0.3175	56	1.135

42.5	0.31	58	1.135
43.5	0.3031	60	1.054
44.5	0.297	62	0.7295
45.5	0.2918	64	1.216
46.5	0.2874	66	0.7295
47.5	0.2841	68	0.4863
48.5	0.2817	70	0.08106
49.5	0.2804	72	0.2432
50.5	0.2802	74	0.4863
60.5	0.2945	76	0.4863
70.5	0.3116	78	0.3242
80.5	0.3221	80	0.2432
90.5	0.3277	84	0.08106
100.5	0.3297	86	0.1621
110.5	0.3289	88	0.1621
120.5	0.326	90	0.2432
130.5	0.3216	96	0.08106
140.5	0.3161	100	0.08106
150.5	0.3099	104	0.08106
160.5	0.5833	106	0.08106
167.5	2.35	114	0.08106
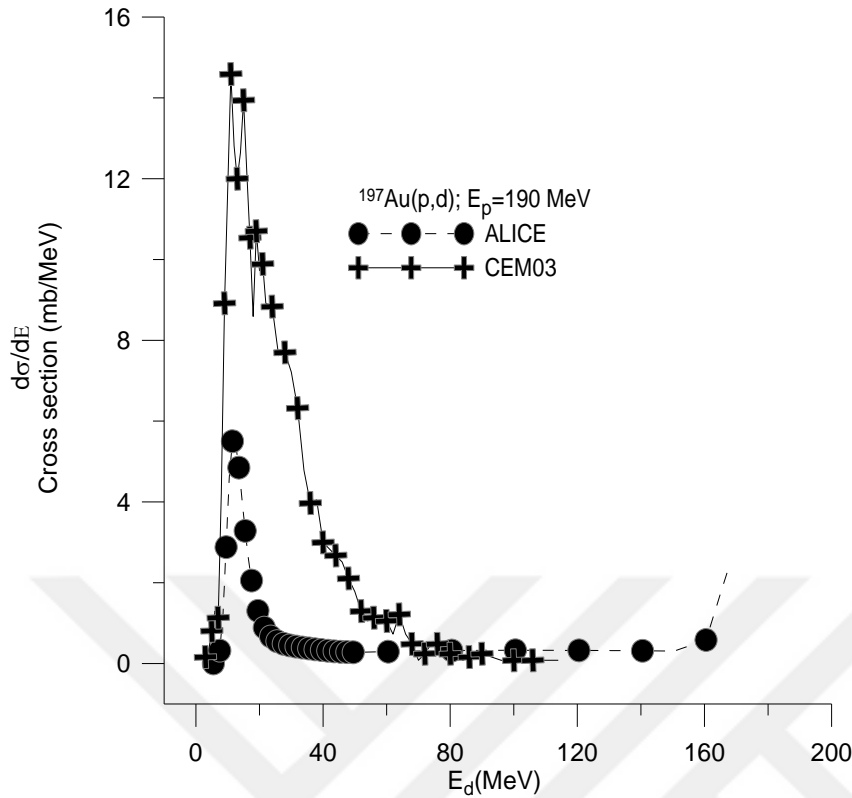
Figure 4.27. Energy spectra $d\sigma/dE$ of deuterons when bombarded $_{79}Au^{197}$ element by protons with 190 MeV energy

4.2.12. Alpha Energy Spectra (dσ/dE) for p + $_{79}Au^{197}$ Reaction at E_p=190 MeV

Figure 4.28. Shows a comparison both of ALICE, CEM03 programs for the energy spectra ($\frac{d\sigma}{dE}$) of alphas when $_{79}Au^{197}$ element is bombarded by protons at 190 MeV. This figure is show less difference energy spectra at programs. Consequently this figure shows the difference energy spectra at programs, therefore CEM03 some points are more than the ALICE data's.

Table 4.28. Show the numerical results of $\frac{d\sigma}{dE}$ each as ALICE and CEM03 programs. As can be seen in the table, the maximum $\frac{d\sigma}{dE}$ at CEM03 =25.45 mb/MeV while $E_{4_{He}}$=21 MeV, and ALICE/ASH =15.97 while $E_{4_{He}}$=21.5 MeV.

Table 4.28. Alpha energy spectra for p + $_{79}$Au^{197} reaction, E$_p$=190 MeV, Calculations have been made by ALICE and CEM03 programs

ALICE/ASH		CEM03	
E$_\alpha$ (MeV)	dσ/dE (mb/MeV)	E$_\alpha$ (MeV)	dσ/dE (mb/MeV)
13.5	0.1764	4	0.1621
14.5	0.3801	7	0.1621
15.5	0.8168	13	0.1621
16.5	1.723	17	0.1621
17.5	3.467	18	0.3242
18.5	6.431	19	7.944
19.5	10.46	20	21.56
20.5	14.21	21	25.45
21.5	15.97	22	19.94
22.5	15.48	24	13.37
23.5	13.62	26	7.7
24.5	11.33	28	4.377
26.5	7.227	30	2.27
27.5	5.696	32	1.459
28.5	4.501	34	1.459
29.5	3.588	36	1.216
30.5	2.897	38	1.702
32.5	1.981	40	1.297
33.5	1.68	42	0.9727
34.5	1.447	44	0.8106
35.5	1.272	46	0.4053
37.5	1.032	48	1.054
38.5	0.9431	50	0.6485
39.5	0.8675	52	0.6485
40.5	0.8016	54	0.6485
42.5	0.6898	56	0.4053
44.5	0.5954	58	0.2432
46.5	0.5266	60	0.2432
47.5	0.5074	62	0.08106
48.5	0.4888	64	0.4863
49.5	0.4705	66	0.7295
50.5	0.4514	68	0.3242

60.5	0.2882	70	0.4863
70.5	0.1699	72	0.1621
80.5	0.1109	74	0.2432
90.5	0.06533	76	0.4863
100.5	0.03602	78	0.2432
110.5	0.01882	80	0.2432
120.5	0.009353	82	0.2432
130.5	0.004419	84	0.08106
140.5	0.00197	86	0.08106
150.5	0.0008123	102	0.08106
160.5	0.0002963	104	0.08106
170.5	0.000008627		
180.5	0.000005722		
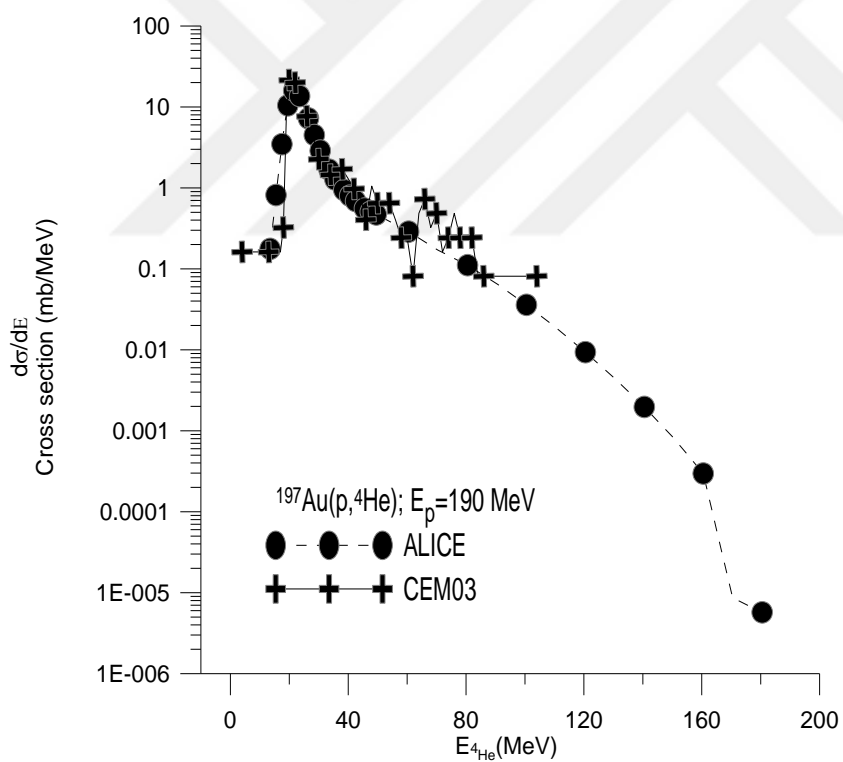
Figure 4.28. Energy spectra $\mathrm{d}\sigma/\mathrm{d}E$ of alphas when bombarded $_{79}\mathrm{Au}^{197}$ element by protons with 190 MeV energy

4.2.13. Neutron Energy Spectra (dσ/dE) for p + $_{79}$Au^{197} Reaction at E$_p$=290 MeV

Figure 4.29. Shows a comparison both of ALICE, CEM03 programs results for the energy spectra ($\frac{d\sigma}{dE}$) of neutrons when $_{79}$Au^{197} element is bombarded by protons at 290 MeV. The figure shows the less difference energy spectra at each data's, therefore CEM03 at E_n=1 MeV unless E_n=140 MeV is more than the ALICE data's.

Table 4.29. Show the numerical results of $\frac{d\sigma}{dE}$ both for ALICE, CEM03. As can be seen in the table, the maximum $\frac{d\sigma}{dE}$ at CEM03 =2596 mb/MeV while E_n=2 MeV, maximum $\frac{d\sigma}{dE}$ at ALICE/ASH =1338 mb/MeV while E_n=1.5 MeV.

Table 4.29. Neutron energy spectra for p + $_{79}$Au^{197} reaction, E$_p$=290 MeV, Calculations have been made by ALICE and CEM03 programs

ALICE/ASH		CEM03	
E$_n$ (MeV)	dσ/dE (mb/MeV)	E$_n$ (MeV)	dσ/dE (mb/MeV)
0.5	1263	1	2387
1.5	1338	2	2596
2.5	1102	3	1843
4.5	644	4	1261
6.5	348.3	5	852.5
8.5	186.5	6	584.1
10.5	99.93	7	402.3
12.5	53.92	8	298.5
14.5	30.38	9	233.1
16.5	18.14	10	181.6
18.5	11.61	11	146.9
20.5	8.153	12	129.3
22.5	6.342	13	98.79
24.5	5.368	14	92.9
26.5	4.824	15	82.2
27.5	4.649	16	70.57
28.5	4.518	17	67.77
29.5	4.42	18	57.07
30.5	4.344	19	55.06
31.5	4.285	20	51.49
32.5	4.236	21	51.96
33.5	4.194	22	47.61
34.5	4.159	24	42.26

35.5	4.129	26	37.69
36.5	4.102	28	32.8
37.5	4.078	30	30.4
38.5	4.057	32	28.38
39.5	4.036	34	23.96
40.5	4.016	36	21.56
41.5	3.996	38	20.55
42.5	3.975	40	20.24
43.5	3.955	42	17.91
44.5	3.936	44	17.14
45.5	3.916	46	14.81
46.5	3.897	48	11.86
47.5	3.878	50	13.11
48.5	3.859	52	11.48
49.5	3.84	54	10.24
50.5	3.82	56	12.1
51.5	3.8	58	11.63
52.5	3.78	60	9.693
53.5	3.76	62	11.17
54.5	3.741	64	8.763
55.5	3.721	66	8.995
56.5	3.701	68	8.763
57.5	3.681	70	8.065
58.5	3.661	72	8.065
59.5	3.641	74	7.134
60.5	3.621	76	6.204
61.5	3.601	78	6.669
62.5	3.581	80	7.444
63.5	3.561	82	6.281
64.5	3.541	84	6.281
65.5	3.521	86	6.204
66.5	3.502	88	5.196
67.5	3.482	90	5.118
68.5	3.462	92	5.738
69.5	3.443	94	5.428
70.5	3.423	96	5.661
71.5	3.404	98	3.49
72.5	3.384	100	4.808
73.5	3.365	102	4.498
74.5	3.346	104	4.265
75.5	3.327	106	3.645
76.5	3.308	108	2.947
77.5	3.289	110	4.73
78.5	3.27	112	4.032
79.5	3.252	114	3.102
80.5	3.233	116	3.722
90.5	3.06	118	3.024

100.5	2.934	120	3.645
110.5	2.816	130	3.04
120.5	2.71	140	3.195
130.5	2.616	150	2.404
140.5	2.535	160	2.714
150.5	2.466	170	2.218
160.5	2.41	180	1.892
170.5	2.364	190	1.846
180.5	2.328	200	1.846
190.5	2.301	210	1.877
200.5	2.282	220	1.52
210.5	2.27	230	1.38
220.5	2.264	240	1.535
230.5	2.263	250	1.349
240.5	2.265	260	1.551
250.5	2.234	270	1.411
260.5	1.89	280	1.21
270.5	1.065	290	0.4653
275.5	0.2813		
276.5	0.1162		
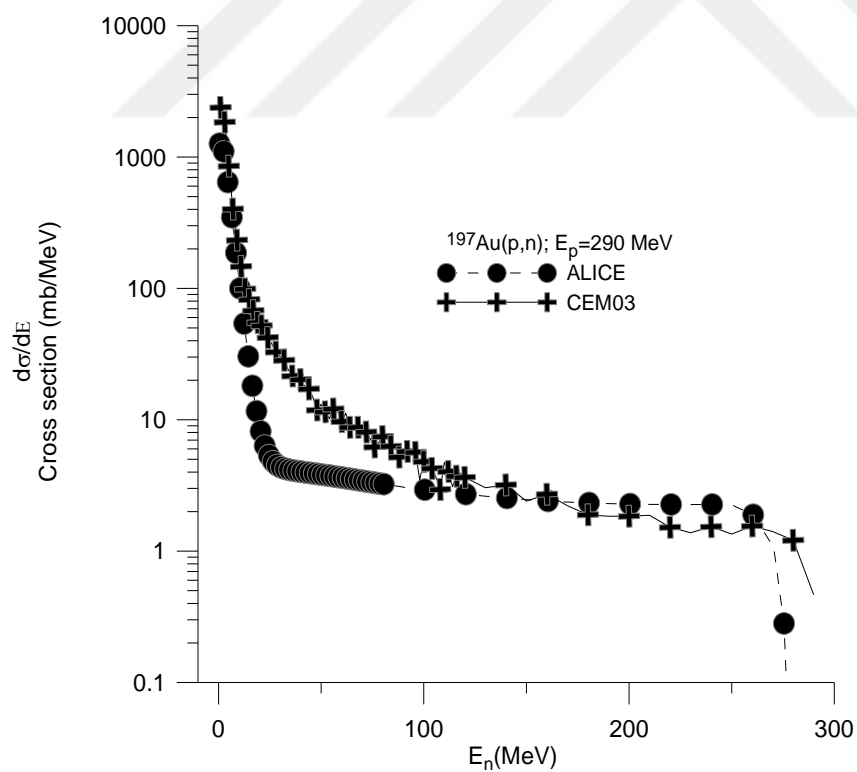
Figure 4.29. Energy spectra $d\sigma/dE$ of neutrons when bombarded $_{79}Au^{197}$ element by protons with 290 MeV energy

4.2.14. Proton Energy Spectra (dσ/dE) for p + $_{79}$Au^{197} Reaction at E$_p$=290 MeV

Figure 4.30. Shows a comparison both of ALICE and CEM03 results for the energy spectra ($\frac{d\sigma}{dE}$) of protons when $_{79}$Au^{197} element is bombarded by protons at 290 MeV. Consequently this figure shows the difference energy spectra at programs, therefore CEM03 at E_p=5 MeV, E_p=6 and E_p=8 MeV unless E_p=62 MeV has more than the ALICE data's.

Table 4.30. Show the numerical results of $\frac{d\sigma}{dE}$ both for ALICE and CEM03 programs. As can be seen in the table, the maximum $\frac{d\sigma}{dE}$ at CEM03 =96.93 mb/MeV while E_p=10 MeV. The maximum $\frac{d\sigma}{dE}$ at ALICE/ASH =21.65 mb/MeV while E_p=12.5 MeV.

Table 4.30. Proton energy spectra for p + $_{79}$Au^{197} reaction, E$_p$=290 MeV, Calculations have been made by ALICE, CEM03 programs

ALICE/ASH		CEM03	
E$_p$ (MeV)	dσ/dE (mb/MeV)	E$_p$ (MeV)	dσ/dE (mb/MeV)
5.5	0.1443	3	0.1551
6.5	0.8216	4	0.9305
7.5	2.862	5	0.7754
8.5	6.976	6	1.706
9.5	12.72	7	1.086
10.5	18.07	8	10.55
11.5	21.1	9	76.46
12.5	21.65	10	96.93
13.5	20.61	11	86.54
14.5	18.79	12	72.27
15.5	16.68	13	62.5
16.5	14.58	14	50.56
17.5	12.71	15	36.76
18.5	11.16	16	33.65
19.5	9.921	17	30.86
20.5	8.949	18	30.55
21.5	8.196	20	24.66
22.5	7.628	22	23.42
23.5	7.214	24	19.31
24.5	6.927	26	20.55
25.5	6.739	28	20.16
26.5	6.616	30	16.67

27.5	6.533	32	15.2
28.5	6.474	34	14.97
29.5	6.435	36	13.57
30.5	6.417	38	10.62
31.5	6.42	40	11.32
32.5	6.442	42	11.48
33.5	6.477	44	10.93
34.5	6.515	46	9.46
35.5	6.546	48	10
36.5	6.567	50	8.763
37.5	6.58	52	9.848
38.5	6.59	54	8.53
39.5	6.603	56	9.693
40.5	6.62	58	7.91
41.5	6.641	60	7.599
42.5	6.661	62	7.444
43.5	6.678	64	6.436
44.5	6.688	66	5.816
45.5	6.693	68	5.816
46.5	6.695	70	6.824
47.5	6.697	72	5.428
48.5	6.698	74	6.281
50.5	6.698	76	5.816
52.5	6.689	78	5.351
54.5	6.668	80	5.893
56.5	6.645	82	5.506
58.5	6.624	84	4.808
60.5	6.601	86	4.963
62.5	6.57	88	4.73
64.5	6.531	90	5.583
66.5	6.49	92	3.645
68.5	6.451	94	5.118
70.5	6.412	96	5.04
72.5	6.372	98	5.273
74.5	6.329	100	3.955
76.5	6.283	102	4.885
78.5	6.237	104	4.11
80.5	6.191	106	3.49
82.5	6.145	108	3.412
84.5	6.099	110	3.179
86.5	6.053	112	5.118
88.5	6.007	114	3.722
90.5	5.964	116	4.343
100.5	5.773	118	4.73
110.5	5.592	120	4.187
120.5	5.426	130	4.001
130.5	5.278	140	4.079

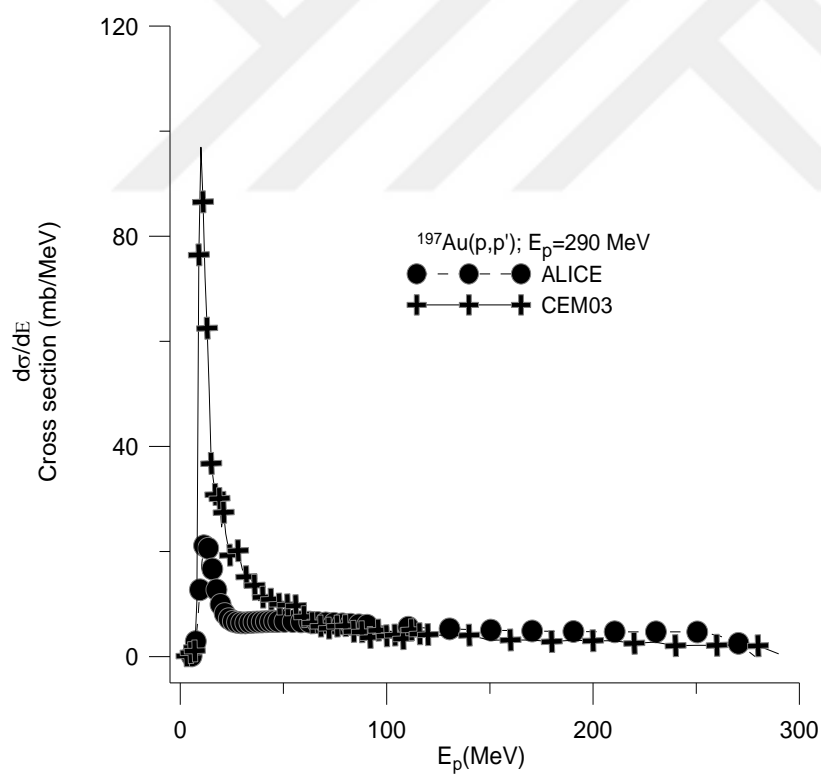| 140.5	5.149	150	3.117
150.5	5.039	160	3.164
160.5	4.948	170	3.148
170.5	4.874	180	2.869
180.5	4.816	190	3.102
190.5	4.772	200	3.024
200.5	4.741	210	3.024
210.5	4.722	220	2.543
220.5	4.713	230	2.745
230.5	4.711	240	2.078
240.5	4.716	250	2.14
250.5	4.687	260	2.156
260.5	4.059	270	2.233
270.5	2.515	280	2.063
278.5	0.02899	290	0.5273

Figure 4.30. Energy spectra $d\sigma/dE$ of protons when bombarded $_{79}Au^{197}$ element by protons with 290 MeV energy

4.2.15. Deuteron Energy Spectra (dσ/dE) for p + $_{79}$Au^{197} Reaction at E$_p$=290 MeV

Figure 4.31. Shows a comparison both ALICE, CEM03 results for the energy spectra ($\frac{d\sigma}{dE}$) of deuterons when $_{79}$Au^{197} element is bombarded by protons at 290 MeV. The figure shows the many difference energy spectra at both programs, therefore CEM03 at E_d=5 MeV unless E_d=270 MeV has more than the ALICE energies cross section.

Table 4.31. Show the numerical results of $\frac{d\sigma}{dE}$ both for ALICE and CEM03 programs. As can be seen in the table, the maximum $\frac{d\sigma}{dE}$ at CEM03 =96.93 mb/MeV while E_d =10 MeV. The maximum $\frac{d\sigma}{dE}$ at ALICE =10.65 mb/MeV while E_d =12.5 MeV.

Table 4.31. Deuteron energy spectra for p + $_{79}$Au^{197} reaction, E$_p$=290 MeV, Calculations have been made by ALICE and CEM03 programs

ALICE/ASH		CEM03	
E$_d$ (MeV)	dσ/dE (mb/MeV)	E$_d$ (MeV)	dσ/dE (mb/MeV)
5.5	0.004808	3	0.1551
6.5	0.07017	4	0.9305
7.5	0.4797	5	0.7754
8.5	1.909	6	1.706
9.5	4.832	7	1.086
10.5	8.181	8	10.55
11.5	10.24	9	76.46
12.5	10.65	10	96.93
13.5	9.924	11	86.54
14.5	8.659	12	72.27
15.5	7.247	13	62.5
16.5	5.904	14	50.56
17.5	4.726	15	36.76
18.5	3.739	16	33.65
19.5	2.935	18	30.55
20.5	2.295	20	24.66
21.5	1.792	21	27.45
22.5	1.402	22	23.42
23.5	1.1	24	19.31
24.5	0.8688	26	20.55
25.5	0.6917	28	20.16
26.5	0.5562	30	16.67
27.5	0.4526	32	15.2

28.5	0.3733	34	14.97
29.5	0.3122	36	13.57
30.5	0.265	38	10.62
31.5	0.2281	40	11.32
32.5	0.199	42	11.48
33.5	0.1757	44	10.93
34.5	0.1568	46	9.46
35.5	0.1413	48	10
36.5	0.1283	50	8.763
37.5	0.1172	52	9.848
38.5	0.1076	54	8.53
39.5	0.09919	56	9.693
40.5	0.09177	58	7.91
50.5	0.05386	60	7.599
60.5	0.05415	62	7.444
70.5	0.05875	64	6.436
80.5	0.06216	66	5.816
90.5	0.06461	68	5.816
100.5	0.06633	70	6.824
110.5	0.06743	72	5.428
120.5	0.06803	74	6.281
130.5	0.06822	76	5.816
140.5	0.0681	78	5.351
150.5	0.06772	80	5.893
160.5	0.06714	82	5.506
170.5	0.0664	84	4.808
180.5	0.06555	86	4.963
190.5	0.06462	88	4.73
200.5	0.06362	90	5.583
210.5	0.06259	92	3.645
220.5	0.06152	94	5.118
230.5	0.06045	96	5.04
240.5	0.05936	98	5.273
250.5	0.05829	100	3.955
260.5	0.06345	102	4.885
270.5	1.768	104	4.11
271.5	1.875	106	3.49
50.5	0.05386	108	3.412
60.5	0.05415	110	3.179
70.5	0.05875	112	5.118
80.5	0.06216	114	3.722
90.5	0.06461	116	4.343
100.5	0.06633	118	4.73
110.5	0.06743	120	4.187
120.5	0.06803	130	4.001
130.5	0.06822	140	4.079
140.5	0.0681	150	3.117

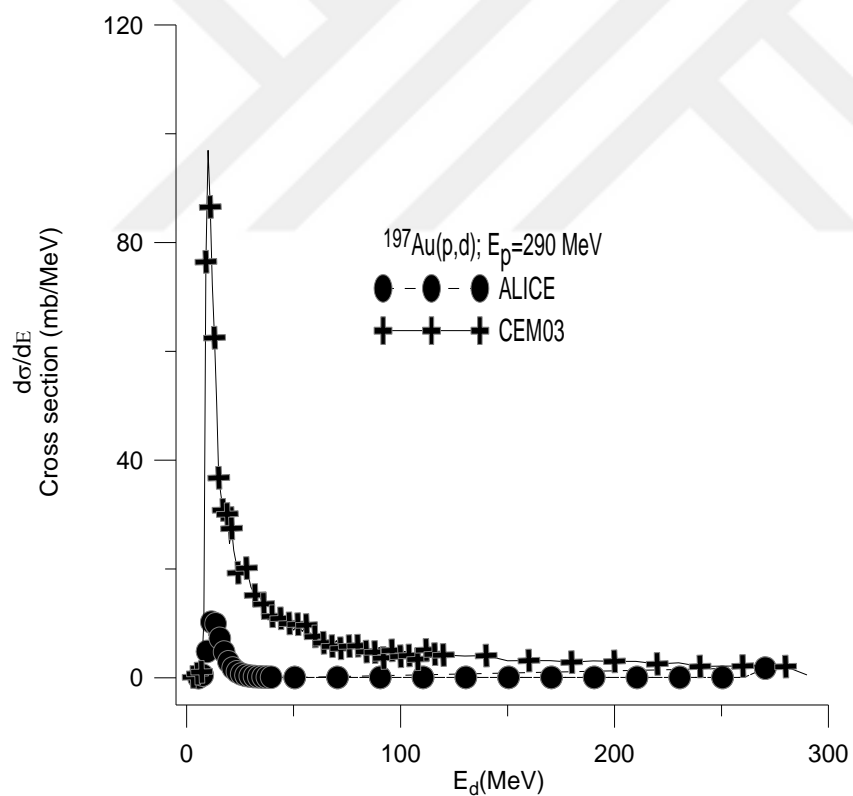|			
150.5	0.06772	160	3.164
160.5	0.06714	170	3.148
170.5	0.0664	180	2.869
180.5	0.06555	190	3.102
190.5	0.06462	200	3.024
200.5	0.06362	210	3.024
210.5	0.06259	220	2.543
220.5	0.06152	230	2.745
230.5	0.06045	240	2.078
240.5	0.05936	250	2.14
250.5	0.05829	260	2.156
260.5	0.06345	270	2.233
270.5	1.768	280	2.063
271.5	1.875	290	0.5273

Figure 4.31. Energy spectra $\frac{d\sigma}{dE}$ of deuterons when bombarded $_{79}\text{Au}^{197}$ element by protons with 290 MeV energy

4.2.16. Alpha Energy Spectra (dσ/dE) for p + $_{79}$Au^{197} Reaction at E$_p$=290 MeV

Figure 4.32. Shows a comparison both of ALICE, CEM03 programs for the energy spectra ($\frac{d\sigma}{dE}$) of alphas when $_{79}$Au^{197} element is bombarded by protons at 290 MeV. The figure shows the less difference energy spectra at programs. Consequently this figure shows the difference energy spectra at programs, when CEM03 some points are more than the ALICE data's.

Table 4.32. Show the numerical results of $\frac{d\sigma}{dE}$ each as ALICE and CEM03 programs. As can be seen in the table, the maximum $\frac{d\sigma}{dE}$ at CEM03 =35.21 mb/MeV while $E_{4_{He}}$=21 MeV, and ALICE/ASH =20.69 while $E_{4_{He}}$=22.5 MeV.

Table 4.32. Alpha energy spectra for p + $_{79}$Au^{197} reaction, E$_p$=290 MeV, Calculations have been made by ALICE and CEM03 programs

ALICE/ASH		CEM03	
E$_\alpha$ (MeV)	dσ/dE (mb/MeV)	E$_\alpha$ (MeV)	dσ/dE (mb/MeV)
13.5	0.1167	4	0.1551
14.5	0.2981	5	0.1551
15.5	0.7292	8	0.3102
16.5	1.687	13	0.1551
17.5	3.64	14	0.3102
18.5	7.149	15	0.1551
19.5	12.24	16	0.4653
20.5	17.42	17	0.3102
21.5	20.47	18	1.861
22.5	20.69	19	15.35
23.5	18.91	20	31.17
24.5	16.26	21	35.21
25.5	13.45	22	32.41
26.5	10.86	24	24.43
27.5	8.641	26	13.57
28.5	6.822	28	5.893
29.5	5.368	30	3.722
30.5	4.225	32	1.241
31.5	3.337	34	0.9305
32.5	2.652	36	0.9305
33.5	2.124	38	0.9305
34.5	1.718	40	0.4653

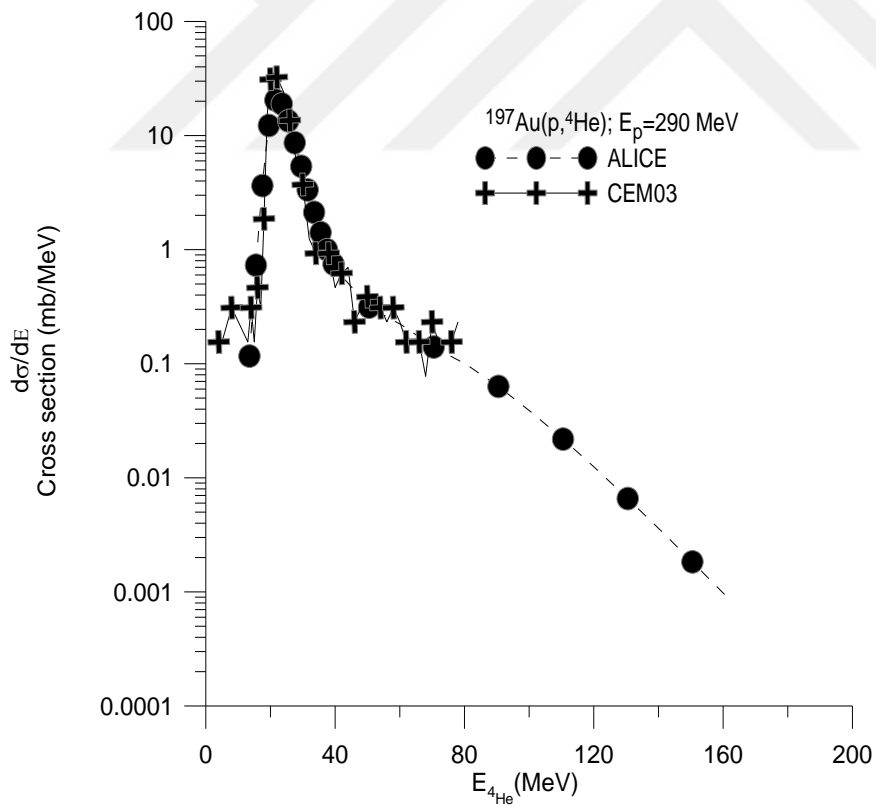| 35.5	1.41	42	0.6204
36.5	1.177	44	0.6979
38.5	0.8569	46	0.2326
40.5	0.6588	48	0.3102
50.5	0.3135	50	0.3877
60.5	0.2194	52	0.3877
70.5	0.1399	54	0.3102
80.5	0.09896	56	0.2326
90.5	0.06319	58	0.3102
100.5	0.03796	60	0.2326
110.5	0.02184	62	0.1551
120.5	0.01214	64	0.1551
130.5	0.006577	68	0.07754
140.5	0.003497	72	0.1551
150.5	0.001831	76	0.1551
160.5	0.000947	78	0.2326

Figure 4.32. Energy spectra $d\sigma/dE$ of alphas when bombarded $_{79}Au^{197}$ element by protons with 290 MeV energy

5. CONCLUSION

These results described calculation of energy spectra after the spallation to (n, p, d, α) particles, while using two elements such as ^{197}Au and ^{238}U target nuclei when bombarded incident proton energies between 20-290 MeV ranges. Then for this process we used three programs such as CEM03, ALICE/ASH, PCROSS, therefore working on these programs for producing destination results, when these results must be compared between them for the visibility of error ratio. After that conclusions, the results compared with another data when access in internet website (Nuclear Energy Agency data bank), while this data is a constant or original calculate, so it gives us the best results and approach between them.

If the results to be considered, there is a feeling of veracious calculation, because that calculations are very close together. Moreover those results have some errors, because some programs sometimes did not produce the output or result, and any programs have a special method. For example (PCROSS) program have some conditions when produce output, such as while interred the element information's must isotopes between as (39<A<220), therefore we can't work on uranium element. Also (ALICE/ASH) can't worked above (290 MeV), likewise that have a little data calculation in internet website; therefore that results have some obstacle in it.

Now we should describe the conclusion of reactions, when the number both figure and tables are the same, therefore just use the number of figure. About distribution the type of targets by this form: the (Figure 4.1) unless (Figure 4.16) were special with produce the energy spectra for uranium (^{238}U) target, and the (Figure 4.16) unless (Figure 4.32) were special with found of energy spectra for gold (^{179}Au) target.

About subdivisions of energy level for p + $_{92}$U^{238} target by this form: (Figure 4.1) unless (Figure 4.4) are special with bombarded this target by incident proton when energy (E$_p$=50 MeV), (Figure 4.5) unless (Figure 4.8) are energy (E$_p$=110 MeV), (Figure 4.9) unless (Figure 4.12) are energy (E$_p$=190 MeV), and (Figure 4.13) unless (Figure 4.16) are energy (E$_p$=290 MeV).

Also about distributed energy level for p + $_{79}$Au^{197} target by this form: (Figure 4.17) unless (Figure 4.20) are special with bombarded this target by incident proton when energy (E$_p$=20 MeV), (Figure 4.21) unless (Figure 4.24) are energy (E$_p$=50 MeV), (Figure 4.25) unless (Figure 4.28) are energy (E$_p$=190 MeV), and (Figure 4.29) unless (Figure 4.32) are energy (E$_p$=290 MeV). When each reaction has some particles are scattered do such as (p, n, d, α).

About uses programing data distributed for p + $_{92}$U^{238} target by this way: both calculates (Figure 4.2), (Figure 4.3), (Figure 4.5) unless (Figure 4.12), (Figure 4.14) and (Figure 4.15) are (ALICE/ASH, CEM03) programs used it. But (Figure 4.1), (Figure 4.3), (Figure 4.4), (Figure 4.13) and (Figure 4.16) are (ALICE/ASH, CEM03) programs and Experimental data from EXFOR used it.

Likewise about uses programing data distributed for p + $_{79}$Au^{197} target by this way: both calculates (Figure 4.19), (Figure 4.23) unless (Figure 4.32) are two programs used it such as (ALICE/ASH, CEM03). And (Figure 4.18), (Figure 4.21), (Figure 4.22) are three programs used it such as (ALICE/ASH, CEM03 and PCROSS). Also (Figure 4.17) and (Figure 4.20) are three programs and another one data used it such as (ALICE/ASH, CEM03, PCROSS) programs and Experimental data from EXFOR.

About compare that programs for p + $_{92}$U^{238} target by this way: both calculates (Figure 4.2), (Figure 4.3), (Figure 4.5), (Figure 4.6), (Figure 4.7), (Figure 4.9), (Figure 4.12), (Figure 4.13) and (Figure 4.16) the difference between programs are very low and they are close to each other, we can say the data collected by both programs are consistent to each other. But (Figure 4.1), (Figure 4.8), (Figure 4.10), (Figure 4.11), (Figure 4.14) and (Figure 4.15) the figure shows the many difference energy spectra at programs between them.

Also about uses programing data distributed for p + $_{79}$Au^{197} target by this way: both calculates (Figure 4.17), (Figure 4.21), (Figure 4.24), (Figure 4.25), (Figure 4.28), (Figure 4.29), (Figure 4.30) and (Figure 4.32) the difference between programs are very low and they are close to each other, we can say the data collected by both programs are consistent to each other. But (Figure 4.18), (Figure 4.19), (Figure 4.20), (Figure 4.22), (Figure 4.23), (Figure 4.26), (Figure 4.27) and (Figure 4.31) the figure shows the many difference energy spectra at programs between them.

REFERENCES

Abderrahim HA, Galambos J, Gohar Y, Henderson S, Lawrence G, McManamy T, Rimmer R (2010) Accelerator and target technology for accelerator driven transmutation and energy production. DOE white paper on ADS 1(1): 1-23

Barashenkov VS (1972) VD Toneev Interactions of High Energy Particles and Nuclei with Nuclei (in Russian) Atomizdat

Barashenkov VS, Gudima KK, Toneev VD (1969) JINR Communication P2-4066, Dubna 1968. Acta Physica Polinica 36: 415-432

Barros P, Pereira C, Veloso F, Lombardi Costa A, Da Silva CAM (2011) Fuel regeneration analysis of an accelerator driven system using the MCNPX 2.6.0 code

Bée M (1988) Quasielastic neutron scattering

Beers KM, Wong DT, Jackson AJ, Wang X, Pople JA, Hexemer A, Balsara NP (2014) Effect of Crystallization on Proton Transport in Model Polymer Electrolyte Membranes. Macromolecules 47(13): 4330-4336

Benlliure J (2006) Spallation reactions in applied and fundamental research. The Euroschool Lectures on Physics with Exotic Beams, Vol II Springer Berlin Heidelberg 191-238

Berggren KF, Matic A (2012) Science at the ESS: A brief outline

Blann M (1991) ALICE/ASH-91: Statistical model code system with fission competition. RSIC code package PSR-146

Blann M (1991) Code ALICE/ASH-91 PSR-146 Statistical Model Code System with Fission Competition Oak Ridge National Laboratory RSICC Peripheral Shielding Routine Collection Lawrence Livermore National Laboratory Livermore California and IAEA

Blann M, Vonach HK (1983) Global test of modified precompound decay models. Physical Review C 28(4): 1475

Blann M, Vonach HK (1983) Global test of modified precompound decay models. Physical Review C 28(4): 1475

Blann M, Mignerey A, Scobel W (1976) Equilibration processes in nuclear reactions nucleons to heavy ions. Nukleonika 21(4): 335-384

Bowman CD, Arthur ED, Lisowski PW, Lawrence GP, Jensen RJ, Anderson Capote R, Osório V, López R, Herrera E, Piris M (1991) Analysis of experimental data on neutron-induced reactions and development of code PCROSS for the calculation of differential pre-equilibrium emission spectra with modelling of level density function (No INDC (CUB)--004/L) International Atomic Energy Agency

Chao AW, Mess KH, Tigner M, Zimmermann F (Eds) (2013) Handbook of accelerator physics and engineering. World scientific

Chen R, Williams M (2011) US Patent Application 14: 240-185

Cho A (2008) Does Fermilab have a future. Science 320(5880): 1148-1151

Cline CK, Blann M (1971) The pre-equilibrium statistical model description of nuclear equilibration process and parameterization of model. Nuclear Physics A 172(2): 225-259

Conf.on Nucl. Data for Sci. and Technology Nice 2007 Volume 2(1085): 2007

Demirkol I (2003) The production neutron at design of energy amplifier in the collisions proton-heavy elements. Gazi University-ANKARA-Turkey- Institute of science-117

European Spallation Source. Construction Site Weekly Updates European spallation source se. Retrieved 17 July 2015

Gadioli E, Erba EG, Sona PG (1973) Intermediate-state decay rates in the exciton model. Nuclear Physics A 217(3): 589-610

Gudima KK, Mashnik SG, Toneev VD (1983) Cascade-exciton model of nuclear reactions. Nuclear Physics A 401(2): 329-361

Arnould H, Phys Lett B458: 167-180 Arnould H (1999) Neutron-Driven Nuclear Transmutation by Adiabatic Resonance Crossing CERN-SL-99-036 EET July 26 1999 and Report to the European Union DGXII EUR 19117 EN

Heilbron JL, Seidel RW (1989) Lawrence and his laboratory: a history of Lawrence Berkeley Laboratory (Vol 5) Univ of California Press

Heinze T, Hallonsten O, Heinecke S (2015) From Periphery to Center. HIST STUD NAT SCI 45(3): 447-492

Hill C, Hogan C, Holmes S, Kim YK, Lykken J, Quigg C, Yurkewicz K (2011) Fermilab - a plan for discovery. Frontiers A Journal of Women Studies 39

http://clinicalgate.com

http://h1.desy.de/

http://physics.tutorvista.com/modern-physics/fission.html#top

 http://www.dictionary.com/browse/cyclotron

http://www.ithec.org (http://indico.cern.ch/event/222140/timetable/#20131027)

http://www.jaea.go.jp/jaeri/english/ff/news1/high.html (Japan Atomic Energy Research Institute 2005)

http://www.science20.com

https://en.wikipedia.org/wiki/Subcritical_reactor#cite_note-2

https://www.oecd-nea.org

http://atomic.lindahall.org/what-is-an-atom-smasher.html

http://www.accelerators-for-society.org/prospects/index.php?id=10

IEEE Transactions on Nuclear Science Volume 30 issue (2): 1153 1983

Ishimoto S, Ishibashi K, Tenzou H, Sasa T (2002) Neutronics study on accelerator driven subcritical systems with thorium-based fuel for comparison between solid and molten-

salt-fuels. Nuclear Technology 138(3): 300-312

Engel LN (1992) Nuclear energy generation and waste transmutation using an accelerator-driven intense thermal neutron source. Nuclear Instruments and Methods in Physics Research Section A Accelerators Spectrometers Detectors and Associated Equipment 320(1-2): 336-367

Janes GS, Levy RH, Bethe HA, Feld BT (1966) New type of accelerator for heavy ions. Physical Review 145(3): 925

Jayanth SN (2016) KESHAV MEMORIAL INSTITUTE OF TECHNOLOGY

Kadi Y, Revol JP (2001 September) Design of an accelerator-driven system for the destruction of nuclear waste. In Lectures given at the Workshop on Hybrid Nuclear Systems for Energy Production Utilisation of Actinides Transmutation of Long-Lived Radioactive Waste Trieste (pp 3-7)

Kalos MH, Whitlock PA (2008) Monte carlo methods (Vol 1) John Wiley Sons

Katz JJ, Morss LR, Seaborg GT (1986) Summary and comparative aspects of actinide elements. In The chemistry of actinide elements (pp 1121-1195) Springer Netherlands

Khlophin R, Leningrad Report (Russia) number 17 1973

Krane KS, Halliday D (1988) Introductory nuclear physics (Vol 465) New York Wiley

Lawrence EO (1951) The evolution of cyclotron. Nobel Lecture

Mansur LK, Rowcliffe AF, Nanstad RK, Zinkle SJ, Corwin WR, Stoller RE (2004) Materials needs for fusion Generation IV fission reactors and spallation neutron sources–similarities and differences. Journal of Nuclear Materials 329: 166-172

Maschek W, Chen X, Delage F, Fernandez-Carretero A, Haas D, Boccaccini CM Wallenius J (2008) Accelerator driven systems for transmutation Fuel development, design and safety. Progress in Nuclear Energy 50(2): 333-340

Mashnik SG, Sierk AJ (2012) CEM03. 03 User Manual LANL Report LA-UR-12-01364

Mason TE, Abernathy D, Ankner J, Ekkebus A, Granroth G, Hagen M, Miller S (2005 June) The Spallation Neutron Source A powerful tool for materials research. In AIP Conference Proceedings (Vol 773 No 1, pp 21-25) AIP

McClain DE, Miller AC, Kalinich JF (2005) Status of Health Concerns about Military Use of Depleted Uranium and Surrogate Metals in Armor-Penetrating Munitions. ARMED FORCES RADIOBIOLOGY RESEARCH INST BETHESDA MD

McCracken G, Stott P (2012) Fusion the Energy of Universe. Academic Press

Medeiros-Romao L, Vandeplassche D (2012) Accelerator Driven Systems In Conf Proc Vol 1205201 No IPAC-2012-MOYAP01 pp 6-10

Meier MM, Amian WB, Goulding CA, Morgan GL, Moss CE (1992) Differential neutron production cross sections for 256-MeV protons. Nuclear science and engineering 110(3): 289-298 Nuclear Science and Engineering volume (110): 289 1992-03

Mishima K, Unesaki H, Misawa T, Tanigaki M, Mori Y, Shiroya S, Fukumoto S (2007) Research project on accelerator-driven subcritical system using FFAG accelerator and Kyoto University Critical Assembly. Journal of nuclear science and technology 44(3): 499-503

Murray R, Holbert KE (2014) Nuclear energy an introduction to the concepts systems and applications of nuclear processes. Elsevier

NA61/SHINE facility at the CERN SPS beams and detector system - NA61 Collaboration (Abgrall N *et al*) JINST 9 (2014) P06005 arXiv 1401 4699 [physics ins-det] CERN-PH-EP-2014-003

Nakahara Y (1983) Evaluation of computational models for fission and spallation reactions used in accelerator breeding and transmutation analysis code. Journal of Nuclear Science and Technology 20(6): 511-517

Nave CR (2012) Cyclotron Hyper physics Dept of Physics and Astronomy Georgia State University. Retrieved October 26 2014

NEA Nuclear Science Committee (2002) Accelerator-driven Systems (ADS) and Fast Reactor (FR) in Advanced Nuclear Cycles A Comparative Study. Nuclear Energy Agency Organization for Economic and Co-operation Development ISBN 92-64

Nifenecker H, Meplan O, David S (2003) Accelerator driven subcritical reactors. CRC Press

Parsons P (2014) The Periodic Table A Visual Guide to the Elements. Quercus

Progress WOP, Cemex C, Ferrovial GN, Fenosa MS, MiguelL H, Holcim ISS, Fenosa GN (2002) Activity report 2015

Rubbia C, Rubio JA (1996) A tentative programmed towards a full scale energy amplifier (No CERN-LHC-96-011-EET)

Rubbia C, Rubio JA, Buono S, Carminati F, Fiétier N, Galvez J, Revol JP (1995) Conceptual design of a fast neutron operated high power energy amplifier

Sarotto M, Castelliti D, Fernandez R, Lamberts D, Malambu E, Stankovskiy A, Mansani L (2013) The MYRRHA-FASTEF cores design for critical and sub-critical operational modes (EU FP7 Central Design Team project) Nuclear Engineering and Design 265: 184-200

Seaborg GT (1967) Public service and human contributions. Physics Today 20(10): 48-51

Shimomura O (2009) A Long History of Japanese Synchrotron Radiation Research

Sierk AJ (1986) Macroscopic model of rotating nuclei. Physical Review C 33(6): 2039

Smyth HD (1945) Atomic energy for military purposes. Reviews of Modern Physics 17(4): 351

Takahashi H, Rief H (1992 March) Concepts of accelerator based transmutation systems. In Proc of Specialists' Meeting on Accelerator-based Transmutation (pp 24-26)

Tomer C (2014) The World Wide Web

Witman S (2014) Ten things you might not know about particle accelerators. Symmetry Magazine Fermi National Accelerator Laboratory Retrieved 21

Kumar V, Kumawat H, Goel U, Barashenkov VS (2003) Neutron spallation source and the Dubna Cascade Code Pramana 60(3): 469-481

Sandberg JV (1982) Angular and energy distribution measurements of secondary hadron fluxes with multireaction spallation detectors at CERN SPS. Nuclear Instruments and Methods in Physics Research 200(2-3): 211-218

Vop NT, Ser YK, Volume 1983 issue 2(51): 57-1983

Yadernaya Fizika, volume 31 issue (3): 561-1980

CURRICULUM VITAE

Personal Identity

Name, Surname   : Soran Jalal Qadir
Nationality   : Iraq
Date and place of birth : 01 Jan, 1992 as Sulaymaniyah, Iraq
Marital Status   : Single
Telephone   : +964 750 127 02 20
E-mail   : Soran.h2009@yahoo.com

Educational Background

Degree	Place of Education	Date of Graduate	Department	Producer research
Bachelor's Degree	University of Sulaimani College of Education/Kalar Sulaimani, Kurdistan Region-Iraq	2013-2014	Physics	Global warming

Work Experience Year	Type of work	Stage	Place	Type of lessons teaching
2014-2018	Teacher and Civil servant	Basic School and Turkish company	Rania/ Sulaimani/ Iraq	Physic, Mathematical, Biology, Chemical, Educational and Technical device

Language Skills

Language	Understanding	writing	speaking
Kurdish (Mother language)	Excellent	Excellent	Excellent
English	Very good	Very good	Good
Arabic	Good	Very good	Good
Persian	Good	Very Good	Good
Turkish	Good	Good	Good